

THE EFFECT OF GROUP BEHAVIOR ON THE PULL-OUT
CAPACITY OF SOIL NAILS IN HIGH PLASTIC CLAY

A THESIS SUBMITTED TO
THE GRADUATE SCHOOL OF NATURAL AND APPLIED SCIENCES
OF
MIDDLE EAST TECHNICAL UNIVERSITY

BY

EBRU AKIŞ

IN PARTIAL FULFILLMENT OF THE REQUIREMENTS
FOR
THE DEGREE OF DOCTOR OF PHILOSOPHY
IN
CIVIL ENGINEERING

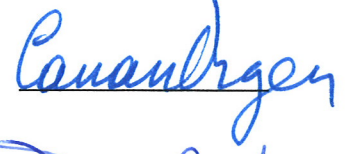
SEPTEMBER 2009

Approval of the thesis:

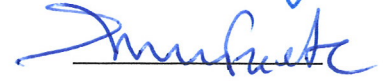
**THE EFFECT OF GROUP BEHAVIOR ON THE PULL-OUT
CAPACITY OF SOIL NAILS IN HIGH PLASTIC CLAY**

submitted by **EBRU AKIŞ** in partial fulfillment of the requirements for the degree of **Doctor of Philosophy in Civil Engineering Department, Middle East Technical University** by,

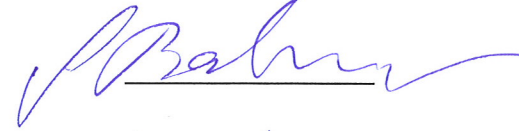
Prof. Dr. Canan Özgen
Dean, Graduate School of **Natural and Applied Sciences**



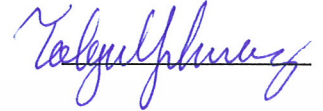
Prof. Dr. Güney Özcebe
Head of Department, **Civil Engineering**



Assoc. Prof. Dr. B. Sadık Bakır
Supervisor, **Civil Engineering Dept., METU**

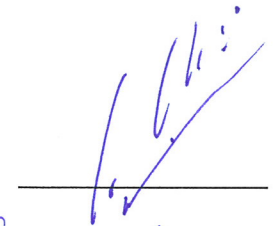


Asst. Prof. Dr. M. Tolga Yılmaz
Co-Supervisor, **Engineering Sciences Dept., METU**

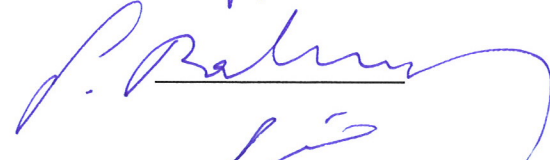


Examining Committee Members:

Prof. Dr. Erdal Çokça
Civil Engineering Dept., METU



Assoc. Prof. Dr. B. Sadık Bakır
Civil Engineering Dept., METU



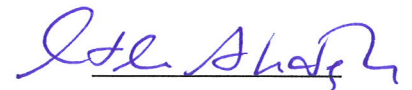
Assoc. Prof. Dr. Levent Tutluoğlu
Mine Engineering Dept., METU



Asst. Prof. Dr. Ayhan Gürbüz
Civil Engineering Dept., Atılım University



Dr. Mutlu Akdoğan
Geotechnical Engineer, Geoteknik Çözüm Proje




Date:

09/09/2009

I hereby declare that all information in this document has been obtained and presented in accordance with academic rules and ethical conduct. I also declare that, as required by these rules and conduct, I have fully cited and referenced all material and results that are not original to this work.

Name, Last Name: Ebru AKIŞ

Signature : 

ABSTRACT

THE EFFECT OF GROUP BEHAVIOR ON THE PULL-OUT CAPACITY OF SOIL NAILS IN HIGH PLASTIC CLAY

Akış, Ebru

Ph. D., Department of Civil Engineering

Supervisor : Assoc. Prof. Dr. B. Sadık Bakır

Co-Supervisor : Asst. Prof. Dr. M. Tolga Yılmaz

September 2009, 161 pages

Soil nailing technique is widely used in stabilizing roadway and tunnel portal cut excavations. The key parameter in the design of soil nail systems is the pull-out capacity. The pull-out capacity of the soil nails can be estimated from the studies involving similar soil conditions or can be estimated from the empirical formulas. Field verification tests are performed before the construction stage in order to confirm the parameter chosen in the design of soil nailing system. It is reported in the literature that, the pull-out resistance of a soil nail in sand should be reduced for the nails installed closer than a specific minimum distance, whereas no such requirement have been discussed for nail groups in clays.

In this study, the pull-out resistance of nails in high plastic clay are tested to investigate the influence of nail spacing in group applications. The laboratory set-up for the pull-out tests is composed of an aluminum model box (300mm (w) x 300mm (h) x 500 mm (l)), soil sample, reinforcements, pull-out device, overburden pressure applicator and monitoring device. A series of pull-out tests has been carried out on single nails and group of nails with spacings 2 and 6 times the diameter of a nail in order to observe the group effect on the pullout capacity of the nails. The nails are located into their positions during the placement of clay into the box.

Within the limitations of this study, it is observed that, there is a reduction in the pull-out capacity of the central nail in 2ϕ spaced group. The pull-out capacity of the central nail in nail group with 6ϕ spacing, is not affected from the neighboring nails. In all tests, the plots of pull-out load on nail versus nail displacement show that, the peak value of load is followed by a sharp reduction. The peak pull-out load is mobilized at first few millimeters of the nail displacements.

A 3D finite element program is used for numerical analyses of the experiments. The measured pull-out capacity of the soil nails are compared by the results of simulated forces obtained from these analyses. By and large, the agreement between the tests and the numerical analyses is observed to be satisfactory. The details of the numerical models are briefly presented in order to give insight into numerical modeling of soil nails in real applications.

Keywords: Soil nailing, pull-out capacity, nail group capacity, pull-out test, numerical analyses.

ÖZ

YÜKSEK PLASTİSİTELİ KİLLERDE GRUP DAVRANIŞININ ZEMİN ÇİVİLERİNİN SIYRILMA KAPASİTESİ ÜZERİNDEKİ ETKİSİ

Akış, Ebru

Doktora, İnşaat Mühendisliği Bölümü

Tez Yöneticisi : Doç. Dr. B. Sadık Bakır

Ortak Tez Yöneticisi : Yrd. Doç. Dr. M. Tolga Yılmaz

Eylül 2009, 161 sayfa

Zemin çivisi yol ve tünel portal yarmalarında yaygın olarak kullanılan bir tekniktir. Sıyırılma kapasitesi, zemin çivisi tasarımındaki en önemli parametre olarak tanımlanabilir. Çivinin sıyırılma kapasitesi benzer zemin özelliği gösteren önceki çalışmalardan ya da ampirik formüllerden belirlenebilir. Arazide yapıma başlamadan önce, tasarımda kullanılan sıyırılma kapasitesini kontrol etmek amacı ile arazi doğrulama testleri yapılır. Yapılan araştırmalarda, kumda her zemin çivisinin sıyırılma kapasitesinin, belirli mesafeden kısa olan aralıktaki çiviler için azaltılması gerektiği belirtilmekle birlikte, kil için böyle bir çalışma bulunmamaktadır.

Bu çalışmada, yüksek plastisiteli kil içindeki çivi gruplarında, çivi aralıklarının sıyırılma direncine etkisi incelenmiştir. Sıyırılma deneyleri için kurulan laboratuvar düzeneği, alüminyum model kutusu (330mm (g) x 330mm (y) x

500mm (u)), sıyırma cihazı, basınç göstergesi ve gözleme aletlerinden oluşmaktadır. Grup davranışın sıyırma kapasitesi üzerine etkisinin incelenmesi için tek çivi ile çivi çapının 2 ve 6 katı aralıklı paternlerde çivi gruplarında bir seri sıyırma deneyleri yapılmıştır. Çiviler, yerlerine zemin numunesinin yerleştirilmesi ve sıkıştırılması sırasında konumlandırılmıştır.

Bu çalışmanın kısıtlamaları içinde, 2Ø aralıklı yerleştirilen çivi grubunda yer alan ortadaki çivinin sıyırma kapasitesinde azalma gözlenmiştir. 6Ø aralıklı yerleştirilen çivi grubunda ise ortadaki çivi sıyırma kapasitesi çevre çivilerden etkilenmemiştir. Bütün deneylerden elde edilen sıyırma kapasitesi-çivi yer değiştirmesi grafiklerinde, yüksek sıyırma kapasitesine eriştikten sonra ani bir düşüş meydana geldiği görülmektedir. Yüksek sıyırma kapasitesi, çivi yer değiştirmesinin ilk milimetrelerinde mobilize olmaktadır.

Deneylerin sayısal analizleri için 3 boyutlu sonlu elemanlar programı kullanılmıştır. Çivilerin ölçülen sıyırma kapasiteleri, analizler sonucunda hesaplanan sıyırma kapasiteleri ile karşılaştırılmıştır. Genellikle, deney ve sayısal analiz sonuçları arasındaki tutarlılık tatmin edicidir. Sayısal modellemelerin detayları, gerçek uygulamalardaki zemin çivisi modellemelerinin kavranması için kısaca sunulmuştur.

Anahtar Kelimeler: zemin çivisi, sıyırma kapasitesi, grup kapasitesi, sıyırma testi, sayısal analiz.

to all my family

ACKNOWLEDGEMENTS

I would like to express sincere thanks to my supervisor Assoc. Prof. Dr. B. Sadık Bakır for his support, comments and guidance throughout this study. I would like to thank to my co-supervisor Asst. Prof. Dr. M.Tolga Yılmaz for his useful comments, advices and support.

I would like to express my gratitude to Asst. Prof. Dr. Tolga Akış for his patience, understanding, technical and financial supports during this study.

I would like to thank my organization KGM, General Directorate of Turkish Highways. I am especially grateful to my president, director, colleagues and technicians working in the laboratories of the Technical Research Department of General Directorate of Highways for their patience, valuable ideas, encouragement, extraordinary amount of time and efforts during this study. Hüseyin Pekardan, Şenda Sarıalioğlu, Metin Bulat and Günay Öztürk are acknowledged for their great contributions in the test set-up and support during the tests.

I would like to thank to Sarp Dinçer and Uğur Kurd from TDG, and Asst. Prof. Dr. Erdem Canbay for their support in measuring and recording the data during experiments.

A special acknowledgement is given to my son, Deniz Akış, for his great patience during my study.

The most grateful thanks and deep gratitude to my parents, my sister, mother-in-love and father-in-love for their love and support.

TABLE OF CONTENTS

ABSTRACT.....	iv
ÖZ.....	vi
ACKNOWLEDGMENTS.....	ix
TABLE OF CONTENTS.....	x
LIST OF TABLES.....	xiii
LIST OF FIGURES.....	xvi
LIST OF SYMBOLS.....	xxvi
CHAPTERS	
1 INTRODUCTION AND LITERATURE REVIEW.....	1
1.1 Introduction.....	1
1.2 Literature Review.....	4
1.2.1 History and Development of Soil Nailing.....	4
1.2.2 Fundamental Mechanisms of Soil Nail Behavior.....	7
1.2.2.1 Soil Nailing System.....	8
1.2.2.2 Development of Loads in Soil Nails.....	10
1.2.2.3 Role of Bending and Shear Resistance.....	14
1.2.2.4 Role of Facing.....	15
1.2.3 Potential Failure Modes of Soil Nailed Structures.....	15
1.2.4 Pull-Out Resistance of Soil Nails.....	17
1.2.5 Research on Shear Resistance of Soil-Nail Interface.....	18
1.2.5.1 Pull-Out Tests.....	18
1.2.5.2 Direct Shear Tests.....	33
1.2.5.3 Centrifuge Tests.....	35
2 EXPERIMENTAL STUDY.....	37

2.1 Physical Characteristics of Soil Sample.....	37
2.2 Determination of the Soil Sample Preparation Technique.....	40
3 DETAILS OF PULL-OUT TESTS.....	49
3.1 Introduction.....	49
3.2 Details of Test Set-Up.....	49
3.2.1 Model Box.....	53
3.2.2 Pull-Out Device.....	54
3.2.3 Application of Overburden Pressure.....	57
3.2.4 Measuring Equipment.....	58
3.3 Soil Sample Preparation.....	59
3.4 Soil Nails.....	60
3.5 Placement of Soil Sample.....	62
3.6 Pull-Out Test Procedure.....	66
4 RESULTS OF THE PULL-OUT TESTS.....	72
4.1 Nail Spacing and Nail Layout.....	72
4.2 Pull-Out Tests.....	73
5 NUMERICAL ANALYSES.....	85
5.1 Introduction.....	85
5.2 Modelling the Pull-Out Tests.....	86
5.2.1 Dimensions of the Model.....	86
5.2.2 Boundary Conditions	86
5.2.3 Soil Parameters.....	87
5.2.4 Modelling of Soil Nails.....	91
5.2.5 Finite Element Mesh.....	93
5.2.6 Calculation Stages.....	96
5.3 Results of the Numerical Analyses.....	97
5.4 Comparison of the Deformed Mesh and the Experiments.....	104
5.5 A Parametric Study.....	105
6 SUMMARY, DISCUSSION AND CONCLUSION.....	108
6.1 Summary.....	108

6.2 Discussion.....	109
6.3 Conclusions.....	113
6.4 Recommendation for the Future Studies.....	113
REFERENCES.....	115
APPENDICES	
A. HYDROMETER TEST RESULTS.....	124
B. DETERMINATION OF SOIL PARAMETERS.....	125
C. INPUT AND OUTPUT DATA OF PLAXIS 3D FOUNDATION	
SOFTWARE.....	135
VITA.....	160

LIST OF TABLES

TABLES

Table 1.1 The estimated bond strength of the soil nails in soil and rock (Phear et al, 2005).....	21
Table 1.2 Summary of the pull-out capacity model tests in literature.....	22
Table 2.1 Sieve analyses results.....	38
Table 2.2 Hydrometer test results.....	39
Table 2.3 Atterberg limits of the soil sample.....	40
Table 2.4 Optimum water content and maximum dry unit weight of the soil sample.....	43
Table 2.5 Confining pressures (σ_3) used in the tests.....	44
Table 2.6 Shear strength parameters determined from tri-axial UU tests.....	45
Table 2.7 Shear strength parameters of clay sample prepared with static compactor using tri-axial compression tests (UU).....	48
Table 3.1 The displacement-rates and the box dimensions in various pull-out tests.....	56

Table 4.1 Strength parameters of the soil samples used in pull-out tests.....	74
Table 4.2 Maximum measured pull-out loads during the tests.....	75
Table 4.3 Measured pull-out loads and the corresponding strength parameters measured for each test.....	77
Table 5.1 The soil parameters employed in numerical analyses.....	90
Table 5.2 Skin resistance data used in the analyses.....	92
Table 5.3 Pull-out loads calculated by PLAXIS 3D FOUNDATION with different mesh densities.....	96
Table 5.4 Comparison of the maximum pull-out loads measured during tests and calculated from numerical analyses.....	103
Table 5.5 Summary of the results of the parametric study.....	106
Table 6.1 The comparison of the pull-out capacity measured and calculated according to Cartier et al. (1983).....	112
Table B.1 Shear strength parameters of test T3.....	130
Table B.2 Shear strength parameters of test T4.....	130
Table B.3 Shear strength parameters of test T5.....	131
Table B.4 Shear strength parameters of test T6.....	132
Table B.5 Shear strength parameters of test T8.....	132
Table B.6 Shear strength parameters of test T9.....	133

Table B.7 Shear strength parameters of test T10.....	134
Table B.8 Shear strength parameters of test T12.....	134

LIST OF FIGURES

FIGURES

Figure 1.1 Main applications of soil nailing (Mitchell et al., 1987).....	2
Figure 1.2 Main components of a typical soil nail (Phear et al., 2005)....	2
Figure 1.3 The principles of NATM (FHWA, 1993).....	5
Figure 1.4 The section through the first soil-nailed wall in the world (FHWA, 1993).....	6
Figure 1.5 Schematic diagram of a soil nailed slope (Phear et al., 2005).	9
Figure 1.6 Soil nail stress transfer mechanism (FHWA, 2003).....	10
Figure 1.7 Simplified distribution of nail tensile force (FHWA, 2003).....	11
Figure 1.8 Idealized development of deformation and tensile load in soil nails (Phear et al., 2005).....	13
Figure 1.9 Nail bending and shear failure (FHWA, 2003).....	14
Figure 1.10 External failure modes (FHWA, 2003).....	16
Figure 1.11 Internal failure modes (FHWA, 2003).....	16
Figure 1.12 Facing failure modes (FHWA, 2003).....	17
Figure 1.13 The laboratory nailing apparatus (Morris, 1999).....	23

Figure 1.14 The laboratory nailing apparatus (Chu et al., 2005).....	24
Figure 1.15 The pull-out test results of the soil nails in different degree of saturation under a stress of 300 kPa (Chu et al., 2005).....	25
Figure 1.16 The pull-out test results of the soil nails under different overburden pressures (Chu et al., 2005).....	25
Figure 1.17 Test apparatus used by Junaideen et al. (2004).....	26
Figure 1.18 Load displacement curves of different bars (Junaideen et al., 2004).....	27
Figure 1.19 Variation of pull-out resistance with overburden pressure (Pradhan et al., 2006).....	28
Figure 1.20 Pull-out box and instrumentation (Su et al., 2008).....	29
Figure 1.21 Variation of the pull-out resistance with displacement under different overburden pressures (Su et al., 2008).....	30
Figure 1.22 Comparison of measured and calculated pull-out resistance of the soil nails under different overburden pressures (Su et al., 2008)...	30
Figure 1.23 Pull-out apparatus (Chai, 2005).....	31
Figure 1.24 A schematic view of the pull-out apparatus (Hong et al., 2003).....	32
Figure 1.25 Pull-out forces versus displacement of double nail tests (Hong et al., 2003).....	33
Figure 1.26 View of the large size direct shear box test apparatus developed by Chu et al. (2005).....	34

Figure 1.27.a The 7 m diameter centrifuge (Morgan, 2002).....	36
Figure 1.27.b The assembled model of Morgan (2002).....	36
Figure 2.1 Collection of the soil sample.....	38
Figure 2.2 Grain size distribution.....	39
Figure 2.3 Compaction curve of the soil sample obtained by the Standard Proctor Compaction Test.....	42
Figure 2.4 Compaction curve of the soil sample obtained by the Dynamic Compaction Test.....	42
Figure 2.5 Mohr-Coulomb failure envelope for specimens used in set-A tri-axial UU tests.....	44
Figure 2.6 Mohr-Coulomb failure envelope for specimens used in set-B tri-axial UU tests.....	45
Figure 2.7 Results of tri-axial tests (UU) (soil sample (Set 1) prepared by static pressure).....	47
Figure 2.8 Results of tri-axial tests (UU) (soil sample (Set 2) prepared by static pressure).....	47
Figure 3.1 The set-up for single nail pull-out tests.....	50
Figure 3.2 The drawing of set-up for single nail pull-out tests.....	51
Figure 3.3 The details of the model box, piston and the testing machine.....	52
Figure 3.4 Details of the nails mounted on the stationary steel plate.....	52

Figure 3.5 A view of model box dimensions of 300 mm width, 300 mm height, 500 mm length.....	54
Figure 3.6 The details of the overburden pressure applicator.....	57
Figure 3.7 Measurement and monitoring devices used in the experiments.....	58
Figure 3.8 Adding water to the sample in order to obtain the optimum water content.....	59
Figure 3.9 Mixing and molding of the sample.....	60
Figure 3.10 An application of soil nails on a road cut.....	61
Figure 3.11 Pull-out test details of single nail and group nails.....	61
Figure 3.12 Details of the compaction process of the soil sample.....	63
Figure 3.13 The sequences of thicknesses of soil layers placed in model box.....	64
Figure 3.14 Compaction of clay.....	65
Figure 3.15 Measurement of compaction.....	65
Figure 3.16 The placement of the model box.....	66
Figure 3.17 Application of the overburden pressure.....	67
Figure 3.18 Connection details of the load-cell, single nail and the plate.	68
Figure 3.19 Connection details of 2Ø spaced soil nails.....	68
Figure 3.20 Connection details of 6Ø spaced soil nails.....	69

Figure 3.21 Measuring devices	70
Figure 3.22 Details of the pull-out tests.....	71
Figure 4.1 Pull-out response of central nail in test T3.....	78
Figure 4.2 Pull-out response of central nail in test T6.....	78
Figure 4.3 Pull-out response of central nail in test T12.....	79
Figure 4.4 Pull-out response of central nail in test T9.....	79
Figure 4.5 Pull-out response of central nail in test T10.....	80
Figure 4.6 Pull-out response of central nail in test T4.....	80
Figure 4.7 Pull-out response of central nail in test T5.....	81
Figure 4.8 Pull-out response of central nail in test T8.....	81
Figure 4.9 Pull-out responses of single nails.....	82
Figure 4.10 Pull-out responses of nails in groups with 2Ø spacing.....	82
Figure 4.11 Pull-out responses of nails in groups with 6Ø spacing.....	83
Figure 4.12 Comparison of the results of the pull-out tests with single nails, 2Ø and 6Ø nail spacing	83
Figure 4.13 Maximum pull-out capacity of the nails tested.....	84
Figure 5.1 Boundary conditions of the model.....	87
Figure 5.2 The general presentation of the p-q diagrams (Craig, 1986)...	88
Figure 5.3 Finite-element used for soil modeling.....	93

Figure 5.4 The plan view of the coarse mesh.....	94
Figure 5.5 The plan view of the medium mesh.....	94
Figure 5.6 The plan view of the fine mesh.....	95
Figure 5.7 Deformed mesh of Test 6 (Single Nail).....	97
Figure 5.8 Deformed mesh of Test 12(Single Nail).....	98
Figure 5.9 Deformed mesh of Test 9 (2Ø spaced group).....	98
Figure 5.10 Deformed mesh of Test 10 (2Ø spaced group).....	99
Figure 5.11 Deformed mesh of Test 4 (6Ø spaced group).....	99
Figure 5.12 Deformed mesh of Test 5 (6Ø spaced group).....	100
Figure 5.13 Deformed mesh of Test 8 (6Ø spaced group).....	100
Figure 5.14 Axial force on the single nail tests (T12 and T6).....	101
Figure 5.15 Axial force on the central nail in 2Ø spaced nail groups (T9 and T10).....	101
Figure 5.16 Axial force on the central nail in 6Ø spaced nail groups (T4, T5 and T8)	102
Figure 5.17 Comparison of the deformed mesh of the numerical analyses and the photograph taken during the experiment T10.....	104
Figure 5.18 Comparison of the deformed mesh of the numerical analyses and the photograph taken during the experiment T8.....	105

Figure 5.19 Reduction in the pull-out capacity of group nails with respect to single nail capacity.....	107
Figure B.1 Stress-strain diagram of tri-axial test T3.....	125
Figure B.2 Stress-strain diagram of tri-axial test T4.....	126
Figure B.3 Stress-strain diagram of tri-axial test T5.....	126
Figure B.4 Stress-strain diagram of tri-axial test T6.....	127
Figure B.5 Stress-strain diagram of tri-axial test T8.....	127
Figure B.6 Stress-strain diagram of tri-axial test T9.....	128
Figure B.7 Stress-strain diagram of tri-axial test T10.....	128
Figure B.8 Stress-strain diagram of tri-axial test T12.....	129
Figure B.9 The results of tri-axial test T3.....	129
Figure B.10 The results of tri-axial test T4.....	130
Figure B.11 The results of tri-axial test T5.....	131
Figure B.12 The results of tri-axial test T6.....	131
Figure B.13 The results of tri-axial test T8.....	132
Figure B.14 The results of tri-axial test T9.....	133
Figure B.15 The results of tri-axial test T10.....	133
Figure B.16 The results of tri-axial test T12.....	134
Figure C.1.a Input data of single nail (T3).....	135

Figure C.1.b Input data of single nail (T3).....	136
Figure C.1.c Input data of single nail (T3).....	136
Figure C.1.d Input data of single nail (T3).....	137
Figure C.1.e Input data of single nail (T3).....	137
Figure C.1.f Output data of single nail (T3).....	138
Figure C.2.a Input data of single nail (T6).....	138
Figure C.2.b Input data of single nail (T6).....	139
Figure C.2.c Input data of single nail (T6).....	139
Figure C.2.d Input data of single nail (T6).....	140
Figure C.2.e Input data of single nail (T6).....	140
Figure C.2.f Output data of single nail (T6).....	141
Figure C.3.a Input data of single nail (T12).....	141
Figure C.3.b Input data of single nail (T12).....	142
Figure C.3.c Input data of single nail (T12).....	142
Figure C.3.d Input data of single nail (T12).....	143
Figure C.3.e Input data of single nail (T12).....	143
Figure C.3.f Output data of single nail (T12).....	144
Figure C.4.a Input data of 2Ø spaced nail group (T9).....	144
Figure C.4.b Input data of 2Ø spaced nail group (T9).....	145

Figure C.4.c Input data of 2Ø spaced nail group (T9).....	145
Figure C.4.d Input data of 2Ø spaced nail group (T9).....	146
Figure C.4.e Input data of 2Ø spaced nail group (T9).....	146
Figure C.4.f Output data of 2Ø spaced nail group (T9).....	147
Figure C.5.a Input data of 2Ø spaced nail group (T10).....	147
Figure C.5.b Input data of 2Ø spaced nail group (T10).....	148
Figure C.5.c Input data of 2Ø spaced nail group (T10).....	148
Figure C.5.d Input data of 2Ø spaced nail group (T10).....	149
Figure C.5.e Input data of 2Ø spaced nail group (T10).....	149
Figure C.5.f Output data of 2Ø spaced nail group (T10).....	150
Figure C.6.a Input data of 6Ø spaced nail group (T4).....	150
Figure C.6.b Input data of 6Ø spaced nail group (T4).....	151
Figure C.6.c Input data of 6Ø spaced nail group (T4).....	151
Figure C.6.d Input data of 6Ø spaced nail group (T4).....	152
Figure C.6.e Input data of 6Ø spaced nail group (T4).....	152
Figure C.6.f Output data of 6Ø spaced nail group (T4).....	153
Figure C.7.a Input data of 6Ø spaced nail group (T5).....	153
Figure C.7.b Input data of 6Ø spaced nail group (T5).....	154
Figure C.7.c Input data of 6Ø spaced nail group (T5).....	154

Figure C.7.d Input data of 6Ø spaced nail group (T5).....	155
Figure C.7.e Input data of 6Ø spaced nail group (T5).....	155
Figure C.7.f Output data of 6Ø spaced nail group (T5).....	156
Figure C.8.a Input data of 6Ø spaced nail group (T8).....	156
Figure C.8.b Input data of 6Ø spaced nail group (T8).....	157
Figure C.8.c Input data of 6Ø spaced nail group (T8).....	157
Figure C.8.d Input data of 6Ø spaced nail group (T8).....	158
Figure C.8.e Input data of 6Ø spaced nail group (T8).....	158
Figure C.8.f Output data of 6Ø spaced nail group (T8).....	159

LIST OF SYMBOLS

a	Intercept of p-q diagrams
c	Cohesion
D	Nail diameter
E	Young's Modulus
f_b	Bond coefficient
g	Acceleration due to the earth gravity
K_o	Coefficient of the earth pressure
L	Length of the nail
L_a	Length
LL	Liquid limit
P	Pull-out force per meter of buried length of the nail
P_L	Limit pressure
p_o	Earth pressure
PL	Plastic Limit
q	Mobilized shear stress along the grout-nail interface

Q_u	Pull-out capacity per unit length
R_P	Pull-out capacity of the nail
R_T	Tensile capacity of the nail
R_F	Facing capacity
T	Tensile force
T	Pull-out force
T_{max}	Equivalent local skin resistance
α	Inclination angle of p-q diagrams
γ	Density
μ	Poisson's ratio
ψ	Dilatancy
σ'_r	Average normal effective stress on soil-nail interface
σ'_v	Theoretical vertical stress at the mid-depth of the nail
σ_3	Confining pressure
\emptyset	Angle of internal friction
θ	Perimeter of the reinforcing nail
τ_{ult}	Ultimate bond stress

CHAPTER 1

INTRODUCTION AND LITERATURE REVIEW

1.1 INTRODUCTION

Soil nail retaining walls are generally used as an alternative to other retaining systems such as tieback soldier piles and conventional retaining walls where geometry or adjacent property constraints do not permit unsupported permanent cut excavations. They are widely used in highway and roadway cut excavations, widening under existing bridge ends, tunnel portal cut stabilizations, and repair and reconstruction of existing retaining structures (FHWA, 1998). The applications of the soil nailing method for retaining structures and for slope stabilization are shown in Figure 1.1.

Soil nailing is a technique that reinforces the natural soil or fill material by the insertion of passive bars. These bars can be described as slender and tension carrying elements made of metallic or polymeric material. They can be inserted to the soil using displacement technique or installed into pre-drilled hole and then grouted, or drilled or grouted simultaneously. Soil nails are attached to a hard, flexible or soft facing at the surface of the slope. The main components of a typical soil nail are shown in Figure 1.2 (Phear et al., 2005).

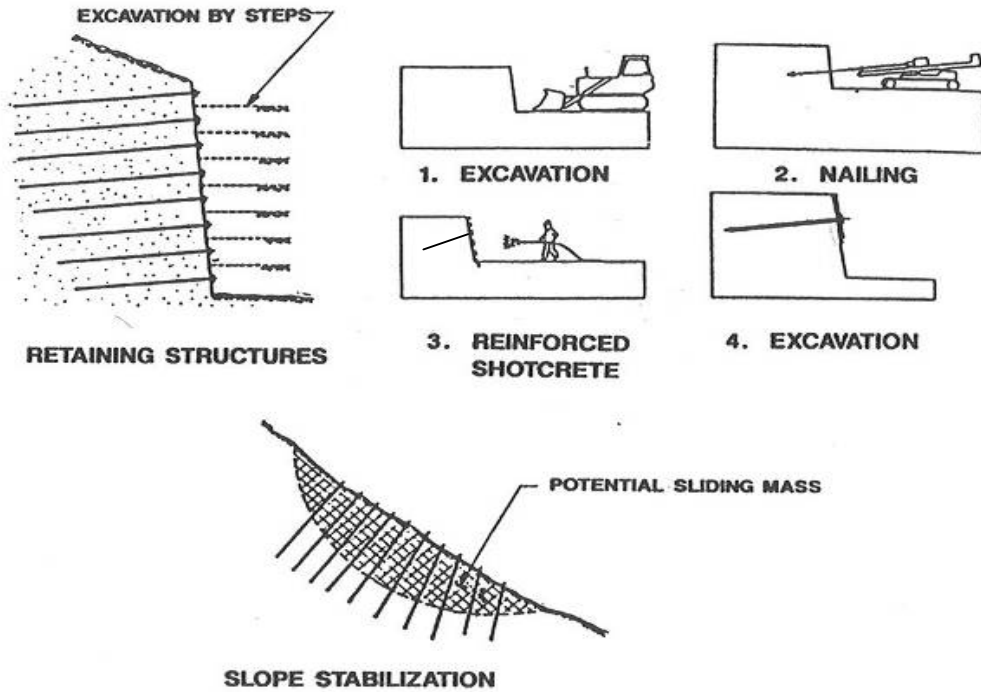


Figure 1.1 Main applications of soil nailing (Mitchell et al., 1987)

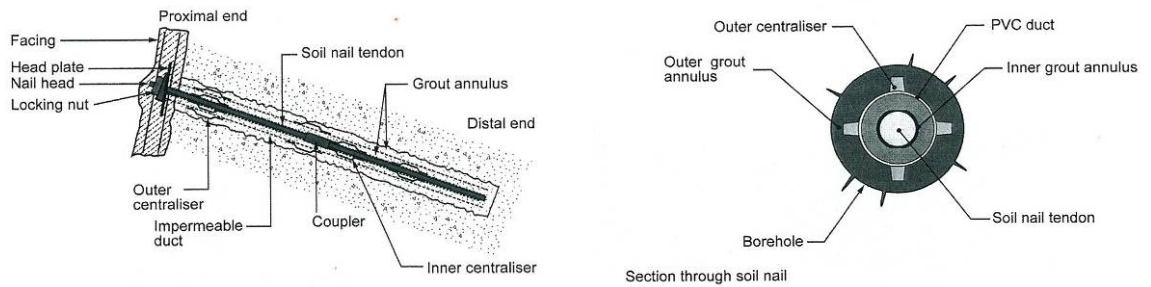


Figure 1.2 Main components of a typical soil nail (Phear et al., 2005)

In the stability analyses of the soil nailing technique, limit equilibrium methods are commonly used to estimate the factor of safety of the slope. In

the limit equilibrium analyses factor of safety of the slope against sliding failure is calculated from the global force and/or moment equilibrium such that the contribution of the soil nails to stability is considered in terms of pull-out resistance of the nails. Several potential failure surfaces are evaluated until the most critical surface is obtained (Junaideen et al., 2004, FHWA, 2003).

The main concern of the soil nail design is the pull-out resistance or bond strength of the nails. The pullout capacity of a soil nail estimated in the analyses is affected by the spacing between nails, the size and length of the nail and the ultimate strength of bond between the nail and the soil. There is no universally agreed method in order to determine the ultimate bond strength, and the designs are based on the values estimated from empirical studies on in-situ tests and on experience in similar applications. On the other hand, the pull-out capacity of the soil nails can be affected from the interaction zones of neighboring soil nails. The pull-out resistance of the soil nails in sand may be less than the determined capacity due to this fact. In order to overcome this problem, some modifications should be made on the pull-out capacity of the nail to avoid overestimation of nail pull-out resistance (Hong et al., 2003).

The objective of this research is to investigate the effect of group behavior on the pull-out capacity of the soil nails with different spacings in high plastic clay. The study consists of six chapters. Chapter 1 introduces the theoretical background of the soil nailing and the methodology of the study. Chapter 2 presents the physical characteristics of the soil sample used in the experiments and summarizes the work done for the determination of the soil sample preparation technique. In Chapter 3, the physical model used for

pull-out tests are presented, the details of the soil sample preparation method and placement technique are explained and the procedure for a series of pull-out tests performed with a single nail and a group of nails is described. In Chapter 4, the test results for single and groups of soil nails with different spacing are presented. The establishment of a three dimensional numerical (finite element) model for simulation of the physical models is explained in Chapter 5. Results of the numerical analyses corresponding to each test are presented and a parametric study investigating the effect of group behavior on the central nail is also introduced in this chapter. Finally, in Chapter 6, the discussion of results, the summary of major conclusions and the future work suggested after this study are presented.

1.2 LITERATURE REVIEW

1.2.1 HISTORY AND DEVELOPMENT OF SOIL NAILING

The roots of the soil nailing are in the former techniques of rock bolting, multi-anchorage systems and reinforced earth techniques. Soil nailing is an extension of rock bolting of the New Australian Tunneling Method (NATM) that is developed by Rabcewicz (1964). In this method, a flexible support system which is formed from reinforced shotcrete and rock bolting is used to support underground excavations. The flexible system reinforces the ground all around the gallery, such that an appreciable reduction in cost of final lining is achieved. The principles of New Australian Tunneling Method (NATM) are shown in Figure 1.3 (FHWA, 1993, 1998).

In North America, the first documented soil-nail application was for temporary excavation support in Vancouver, in the early 1970s. In Europe (Spain 1972, France 1972/73 and Germany 1976) the earliest reported works involving soil nails were for retaining wall constructions on highway or railroad cuts or temporary supports for excavations in the same period (FHWA, 1998). Among them, the first reported soil-nailed wall in the world was built at Versailles in France by a French contractor between 1972 and 1973, in joint venture with the specialist contractor Soletanche. This application was a part of a railway widening project. 18 m high 70° cut slope in Fontainebleau sand was reinforced with closely spaced, 4 m and 6 m long grouted nails (FHWA, 1993, 1998). The section through this soil-nailed wall is shown in Figure 1.4.

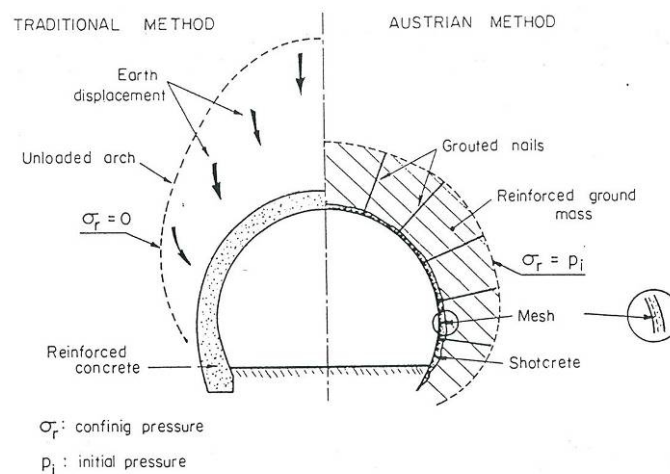


Figure 1.3 The principles of NATM (FHWA, 1993)

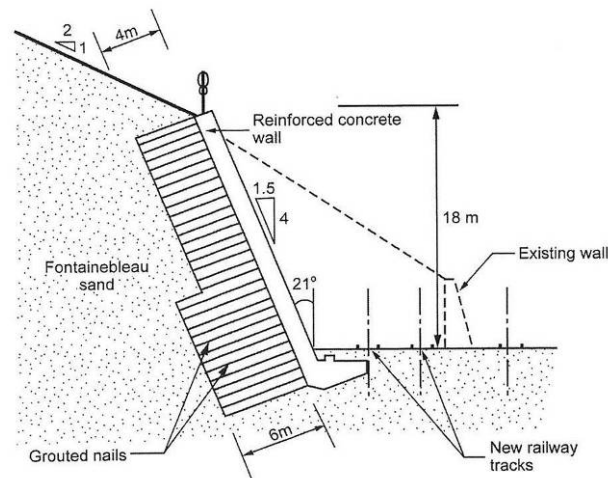


Figure 1.4 The section through the first soil-nailed wall in the world (FHWA, 1993)

Following these applications, the first major research program was undertaken in Germany (Gassler et al., 1981). A fund of approximately \$2,300,000 was used by the University of Karlsruhe and the contractor Bauer between 1975 and 1981. In this program full-scale testing of a variety of experimental wall configurations were investigated and the analysis procedures were developed. After that, by considering the increasing use of soil nailing and lack of defensible design methodology, France started their own experimental program, namely Clouterre, in 1986. French government accepted 21 individual private and public participants to cooperate in Clouterre with a budget in the order of \$5,000,000. Three large-scale experiments in Fontainebleau sand fill were done and six in-service structures were monitored (FHWA, 1998).

The first document of U.S. Department of Transportation and Federal Highway Administration (FHWA) on the soil nailing was prepared by Elias and Juran (1991) and published by FHWA's Office of Research and Development in order to disseminate soil nailing technique as a retaining system in highway projects. In 1992, FHWA organized technical tours to France, Germany and England to learn the current European state-of-the-practice in soil nail wall technology and to update the information on the soil nail wall performance, design approach and computer programs as well as construction specifications, corrosion protection details and contracting practices. At the end of these technical tours two studies were published: (1) FHWA International Scanning Tour for Geotechnology (1993a), and (2) English translation of the French Practice Summary on Soil Nailing (1993b). In 1994, Soil Nailing Inspector's Manual and Demonstration Project (FHWA, 1994) were issued by FHWA. The work on "Manual for Design and Construction Monitoring of Soil Nail Walls" was carried by Byrne et al. (1998) and published by FHWA in 1998. The update to Design Manual (FHWA, 1998) was done in 2003 (FHWA, 2003) concerning the recent trends in design methods, construction contracting and construction monitoring.

1.2.2 FUNDAMENTAL MECHANISMS OF SOIL NAIL BEHAVIOUR

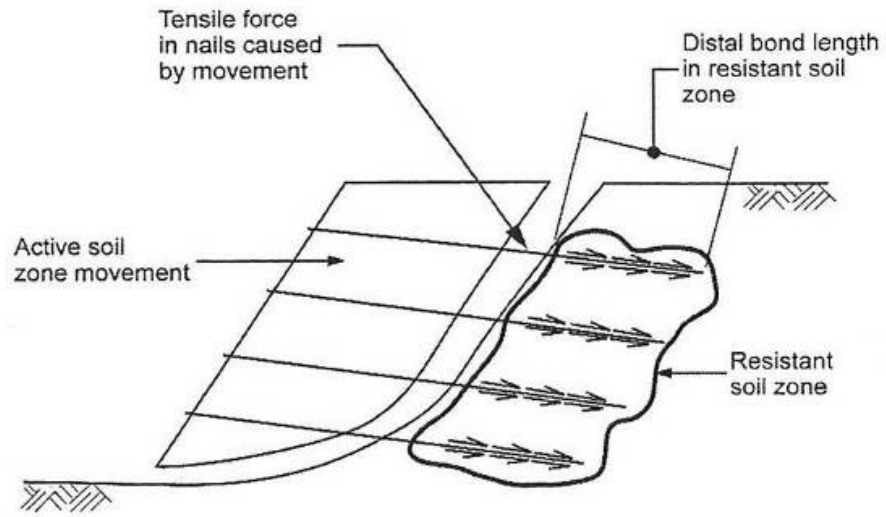
In the soil nailing system, the development of loads in soil nails, the bending and shear resistance of the nails and the facing of the soil nailed slopes can be called as the fundamental mechanisms of the soil nail behavior (Phear et al., 2005). These fundamental mechanisms are further explained in the following part.

1.2.2.1 SOIL NAILING SYSTEM

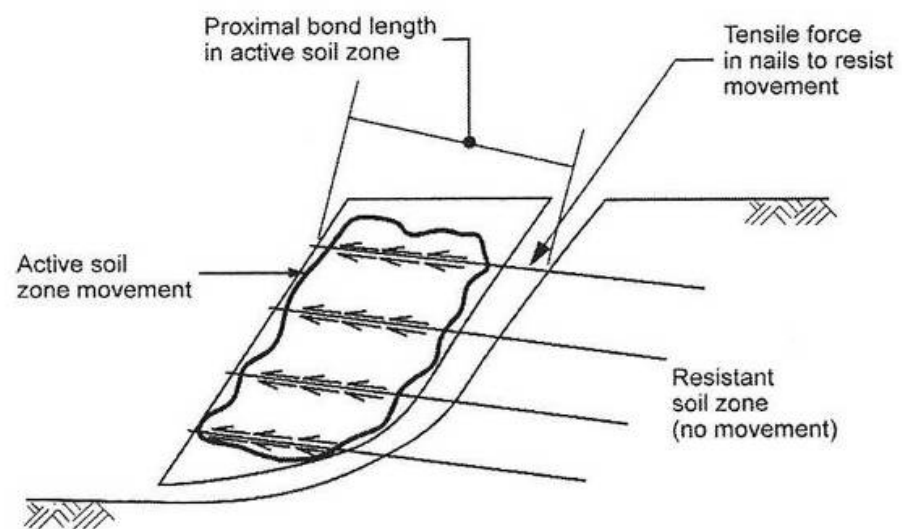
The soil block reinforced by the nails is capable of resisting both internal nail forces that form due to relative movements and local material failures and destabilizing external loads such as earth pressure, surcharge and live load. The resistance is supplied by the mobilization of the shear stresses at the soil-nail interface.

The soil nailed slope can be separated into two zones namely the active and passive zones by considering the internal stability (Figure 1.5). The zone located in front of the potential failure plane is called the active zone. Within this region, the skin friction stresses on the soil nails are directed outward. In the passive (resistant) zone, on the other hand, the skin friction stresses, directed inward, resisting the reinforcement being pulled out.

By considering the mechanism of the soil nail behavior mentioned above, the internal stability failure can occur firstly, due to the rupture of the soil nail due to the exceeding of the tensile capacity of the nail. Secondly, for the grouted nails, the grout nail interface bond capacity can be reached. Finally, the bond capacity of the soil/nail interface in the active or passive zone can be reached. Among the mentioned parameters, the prediction of the capacity of the soil nail interface is one of the most critical parameter (Phear et al., 2005).



Bond in resistant soil zone



Bond in active soil zone

Note: Arrows represent direction of tensile stress

Figure 1.5 Schematic diagram of a soil nailed slope (Phear et al., 2005)

1.2.2.2 DEVELOPMENT OF LOADS IN SOIL NAILS

As discussed previously, there are two zones as active and passive, in soil nail systems. In the active zone, the stresses along the nail-ground interface are transferred laterally towards the excavation face. The resisting stresses acting in opposite direction to the direction of expansion formed in passive zone. The tensile forces begin at the end of nail and reach to a maximum at the mid-length and decrease to a value at nail head. Variation of the tensile force (T) and the mobilized shear stress along the grout-nail interface (q) is shown in Figure 1.6 (FHWA, 2003).

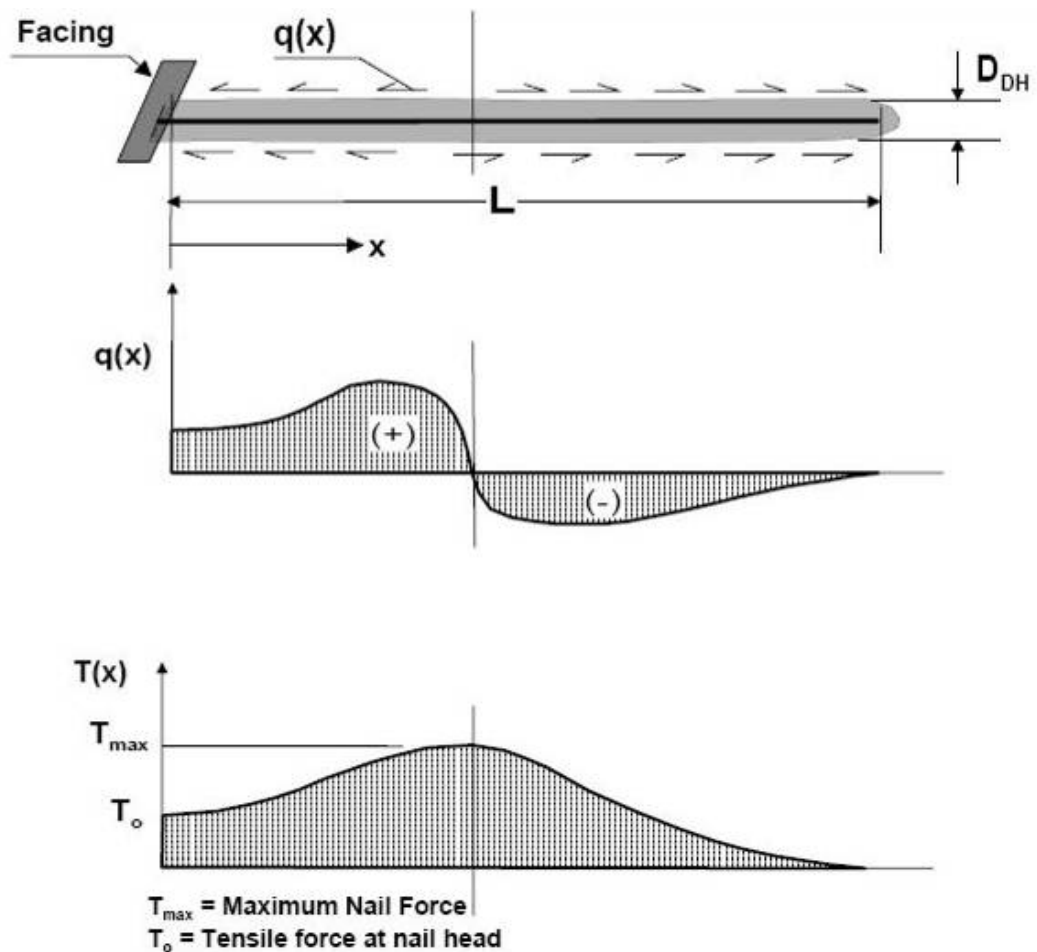
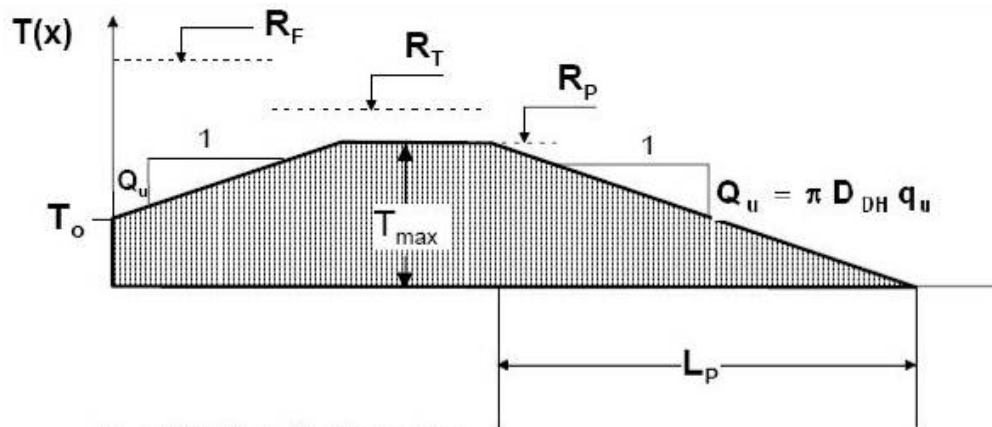


Figure 1.6 Soil nail stress transfer mechanism (FHWA, 2003)

For design purposes, the tensile force distribution can be simplified as shown in Figure 1.7. The tensile forces in the nail start at zero at the end of the nail, increase at a constant slope that is defined as the pull-out capacity per unit length (Q_u), reach to a maximum (T_{max}), and then decrease at the rate Q_u to a value at the nail head (T_o). Maximum tension in the nail is limited by the pull-out capacity (R_p), the tensile capacity (R_T) or the facing capacity (R_F) (FHWA, 2003).



R_T = Nail Tensile Capacity

R_F = Facing Capacity

R_p = Pullout Capacity

Q_u, q_u = Ultimate load transfer rate and bond strength

$T_o \sim 0.6-1.0 T_{max}$

- 1) $R_p < R_T < R_F$ (pullout controls, shown in example above)
- 2) $R_T < R_p < R_F$ (tensile failure controls)
- 3) $R_F < R_p$ or R_T (facing failure may control depending on T_o/T_{max})

Figure 1.7 Simplified distribution of nail tensile force (FHWA, 2003)

In the field applications, the reinforcement of the slope with the soil nails is realized by cutting the slope in successive phases. As the successive excavations are in progress, the soil nailed wall is subjected to lateral extension and settlement. As a result of these relatively small deformations, the tensile strength of the steel reinforcement is mobilized through the friction at the interfaces: the stresses on nails are not prominent during the installation of top rows of nails, because the soil displacements are rather limited. However, the displacements increase considerably through the successive stages of excavation, which consequently augment stresses acting on nails. The deformations and the tensile loads corresponding to each excavation step are shown in Figure 1.8 (FHWA 1993b, Phear et al., 2005).

Note: This figure ignores any load generated at the nail head

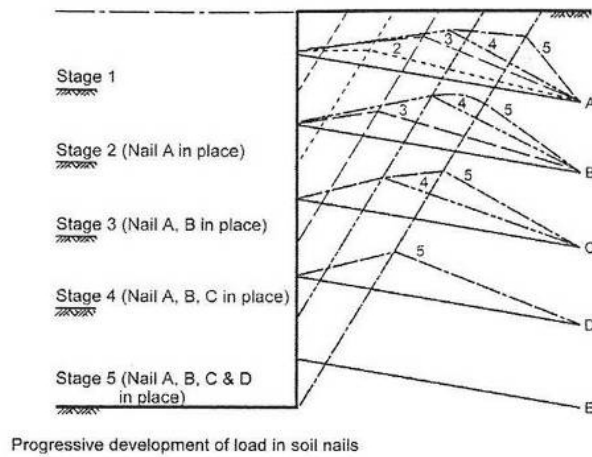
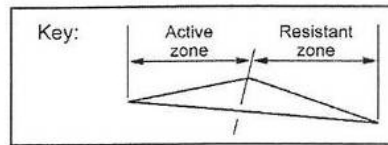
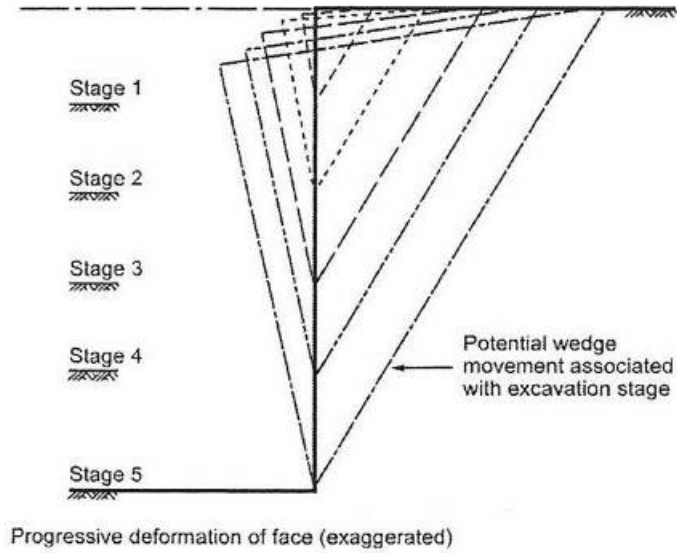


Figure 1.8 Idealized development of deformation and tensile load in soil nails (Phear et al., 2005).

1.2.2.3 ROLE OF BENDING AND SHEAR RESISTANCE

Due to the working mechanism of the nails, they are subjected mainly to the tensile forces, but considering the movement along the potential failure surface, nails may be subjected to the shear forces and bending moments simultaneously (Elias et al., 1991). The nail bending and shear failure is schematically shown in Figure 1.9. Researches focusing on the contribution of bending stiffness of soil nails is available in literature. Pedley et al. (1990) and Jewell et al. (1992) stated that the bending/shear resistance compared with the tensile resistance will only be of secondary importance and such effects can be neglected for practical purposes. Therefore, due to this relatively small contribution, the shear and bending strengths of the soil nails may be disregarded according to FHWA (2003).

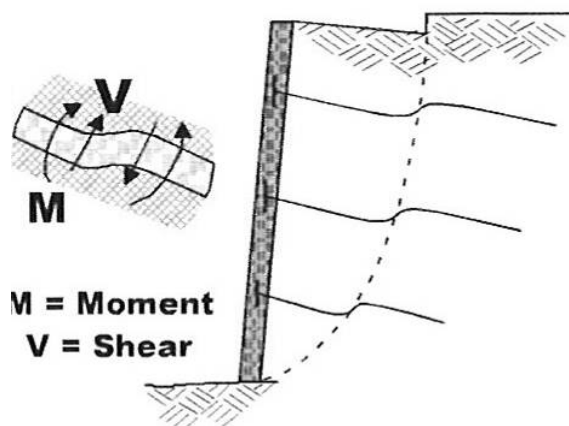


Figure 1.9 Nail bending and shear failure (FHWA, 2003)

1.2.2.4 ROLE OF FACING

Stabilization of an existing slope with soil nails is performed by means of the head plates or facing. Clouterre (FHWA,1993b) stated that the facing behaves like a slab that is subjected to tension (T_o) of the nails at the head and to earth pressure p_o between the nails. The facing system may be hard, flexible or soft. The transferred proportion of the bond stresses developed along the nail to the facing depends on the type and stiffness of facing (Phear et al., 2005).

1.2.3 POTENTIAL FAILURE MODES OF SOIL NAILED STRUCTURES

There are three types of potential failure conditions in the soil nailed structures, classified as external, internal and facing failure modes (FHWA, 2003).

In the external failure mode, the potential failure surface develops behind the reach of nails. The soil reinforced by nails is treated as a block and the failure may be like that of any retaining structure. For a soil nail wall the external failure modes are defined as the global, sliding, and bearing failure modes. These external types of failures are shown in Figure 1.10.



Figure 1.10 External failure modes (FHWA, 2003)

The internal failure modes occur inside the reinforced zone and refer to the failure in the load transfer mechanism between the soil, the nail and the grout. Depending on various factors such as the nail tensile strength, length and bond strength, different failure modes can be encountered. Nail pull-out failure, slippage of the bar-grout interface, tensile failure of the nail, bending and shear failure of the nail are the typical internal failure modes and they are schematically shown in Figure 1.11.

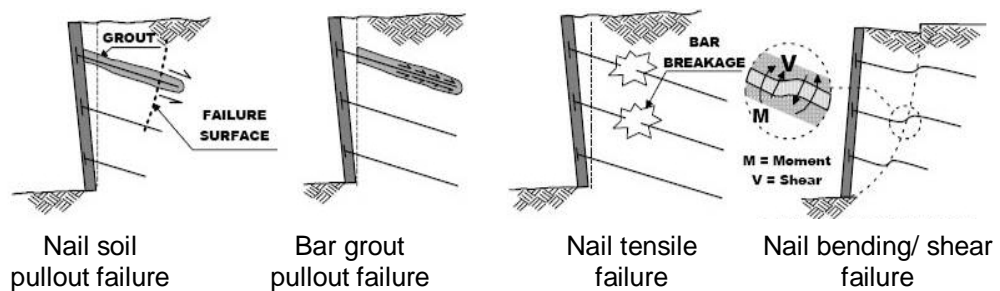


Figure 1.11 Internal failure modes (FHWA, 2003)

Flexure, punching shear and head-stud tensile failures are classified as the facing failure modes. If the excessive bending is beyond the facing's flexural capacity, flexural failure mode occurs (Figure 1.12.a). Also, punching shear failure may occur in the facing around the nails (Figure 1.12.b), and the headed studs may fail in tension as well (Figure 1.12.c).

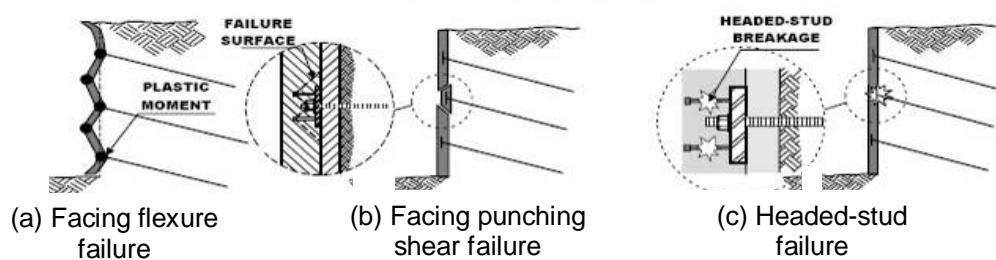


Figure 1.12 Facing failure modes (FHWA, 2003)

1.2.4 PULL-OUT RESISTANCE OF SOIL NAILS

Up to now, the general information about the soil nailing technique is presented. As mentioned before, the soil interface capacity is one of the most difficult parameters to predict in the soil nail wall design. The sufficient pull-out resistance of a soil nail is of fundamental importance for a soil-nailed slope. The ultimate pull-out resistance of a soil nail is a function of soil conditions, nail dimensions, nail surface conditions and methods of nail installation (Phear et al., 2005). In the following part, the studies on factors that affect pull out resistance of nails are presented.

1.2.5 RESEARCH ON SHEAR RESISTANCE OF SOIL-NAIL INTERFACE

The pull-out resistance of a nail is difficult to estimate with high accuracy due to the uncertainties about the soil-nail interaction behavior during pull-out (Franzen, 1998). In literature, field and laboratory pull-out tests, direct shear box tests and centrifuge tests are employed in order to investigate the behavior of soil nails. In the following section, the studies on the pull-out resistance of the soil nails carried out by different researchers are presented.

1.2.5.1 PULL-OUT TESTS

As stated previously, the pull-out resistance of the soil nails is of key importance in the design. In order to estimate the pull-out resistance, several researchers studied the relationship between the pull-out resistance and the overburden pressure both for the driven and grouted nails. The earliest study on this subject was made by Shen et al. (1981). They assumed that the maximum bond stress is governed by the Coulomb failure criterion. Later, Jewell (1990) presented the following equation for the correlation of pull-out resistance with the shear strength of soil and overburden pressure:

$$T = \pi D L_a \sigma'_r f_b \tan \phi' \quad (1.1)$$

Here, T is the pull-out force, D is the nail diameter, L_a is the anchorage length, σ'_r is the average normal effective stress on soil-nail interface, f_b is the bond coefficient (1.0 for a fully rough interface and 0.2-0.4 for a smooth interface), and ϕ' is the effective angle of internal friction for soil.

Another study was carried on the pull-out resistance of driven nails in granular soil by Cartier et al. (1983). They correlated the pull-out resistance with the vertical stress and the apparent coefficient of friction (μ^*) as

$$P = \theta c' + 2 D \sigma'_v \mu^* \quad (1.2)$$

where, P is the pullout force per meter of buried length of the nail, θ is the perimeter of the reinforcing nail, c' is the cohesion of the soil, D is the width of the equivalent flat reinforcement strip/ nail drillhole diameter, and σ'_v is the theoretical vertical stress at the mid-depth of the reinforcing nail. This relation has been adopted by the practicing engineers in Hong Kong (Powell et al., 1990) and in other countries for grouted nails.

Pull-out capacity of nails is also affected by the soil dilation. Gassler (1983,1992) stated that the shear resistance depends on the dilatancy in the shear zone between the nail and the soil rather than the overburden pressure and the angle of internal friction in medium-dense or dense soils. Additionally, he concluded that, during the construction of nails, the initial stress conditions are changed due to the drilling method. As a result of several tests carried on silty sand, Guilloux et al. (1982) and Cartier et al. (1983) stated that the maximum shear stress mobilized is not dependent on depth. Due to the mobilized shear stress, the soil surrounding the reinforcement tends to dilate and the other parts of the soil restrain this dilation. As a result of this behavior, the normal stresses on the nail increase. They concluded that, the dilative tendency decreases with depth,

but the pull-out resistance is not sensitive to depth, since the effect of dilation on pull-out capacity is compensated by the increase of overburden pressure.

As stated previously, the pull-out resistance that is to be used in the design can be obtained from the previous pull-out test results. In order to do this, a databank consisting of the ultimate pull-out stress considering the soil type and installation technique is firstly formed by Elias and Juran (1991). The estimated bond strengths of the soil nails in soil and rock obtained in this study and in the studies performed by FHWA are presented in Table 1.1.

Another empirical correlation is obtained from a series of large number of pull-out tests (FHWA, 2003) as

$$\tau_{ult} = 14 P_L (6 - P_L) \quad (1.3)$$

In this equation, P_L is the limit pressure obtained from pressuremeter tests in unit of MPa, and τ_{ult} is the ultimate bond stress in unit of kPa.

Table 1.1 The estimated bond strength of the soil nails in soil and rock
(Phear et al., 2005)

Construction method	Soil type	Ultimate bond stress (kN/m ²)	Source
Augered	Loess	25-75	2
	Soft clay	20-30	1
	Stiff to hard clay	40-60	1
	Clayey silt	40-100	1
	Calcareous sandy clay	90-140	1
	Silty sand fill	15-20	1
Open hole	Non-plastic silt	20-30	2
	Medium-dense sand and silty sand/sandy silt	50-75	2
	Dense silty sand and gravel	80-100	2
	Very dense silty sand and gravel	120-240	2
	Stiff clay	40-60	2
	Stiff clayey silt	40-100	2
	Stiff sandy clay	50-100	3
Rotary-drilled	Marl/limestone	300-400	1
	Soft dolomite	400-600	1
	Weathered sandstone	200-300	1
	Weathered shale	100-150	1
	Weathered schist	100-175	1
	Basalt	500-600	1
	Silty sand	100-150	1
	Silt	60-75	1
Driven casing	Dense sand/gravel	180-210	3
	Sandy colluvium	70-150	3
	Clayey colluvium	40-75	1
Jet-grouted	Sand	380	1
	Sand/gravel	700	1

Sources

- 1 Elias and Juran (1991)
- 2 FHWA (1998 and 2003) **installed using tremie and low-pressure grouting**
- 3 Suggested values for preliminary design - values from original FHWA (1998), which have been reduced based on authors' experience.

Research was also conducted on the pull-out tests by considering the effect of soil type, nail type, nail surface roughness and installation techniques. The summary of models employed for testing pull-out resistance of nails is presented in Table 1.2. These studies show that there is no unique method or widely accepted test procedure for the determination of pull-out capacity of soil nails. Moreover, there is no consensus on the relationship between the overburden pressure and the pull-out capacity of the soil nails.

Table 1.2 Summary of the pull-out capacity model tests in literature

Author	Year	Dimensions of the box (mm)	Nail type	Soil Type	Investigated Factors
Morris	1999	428x463x450	Single, grouted nail	Stiff clayey soil	Overburden, nail type, loading rate
Hong et al.	2003	600x800x400	Double, driven nail	Dry sand	Roughness of the nails, group efficiency
Junaideen et al.	2004	2000x1600x1400	Single, driven nail	Completely decomposed granite	Roughness of the nails, overburden pressure
Chu et al.	2005	700x560x605	Single, grouted nail	Completely decomposed granite	Saturation ratio, overburden pressure
Pradhan et al.	2006	2000x1600x1400	Single, grouted nail	Completely decomposed granite	Overburden pressure
Su et al.	2008	1000x600x830	Single, grouted nail	Completely decomposed granite	Overburden pressure

Morris (1999) investigated the bond resistance of drilled and grouted soil nails in stiff clay soil (coal measure shale). A 428 mm by 463 mm by 450 mm tank was used for soil fill. Then, a 50 mm diameter hole drilled in which a 10 mm diameter reinforcement bar was grouted. The apparatus used in the pull-out tests is shown in Figure 1.13. The pull-out resistance of the nails is investigated for different overburden pressure values (varied from 50 to 200 kPa) for different rates of loading (3.2 to 60 mm/min). Morris (1999) stated that, the loading rate has a significant effect on the pull-out resistance. The highest peak values in pull-out resistance were measured during the fastest pull-out tests. On the other hand, for a given in-situ stresses, the bond resistance of nails towards the end of tests was similar regardless of pull-out displacement rate. He found that the shape of shear curves obtained from medium and slow pull-out rate tests were very similar. Additionally, he concluded that, both the peak and post peak bond resistance of nails increased with in-situ stress.

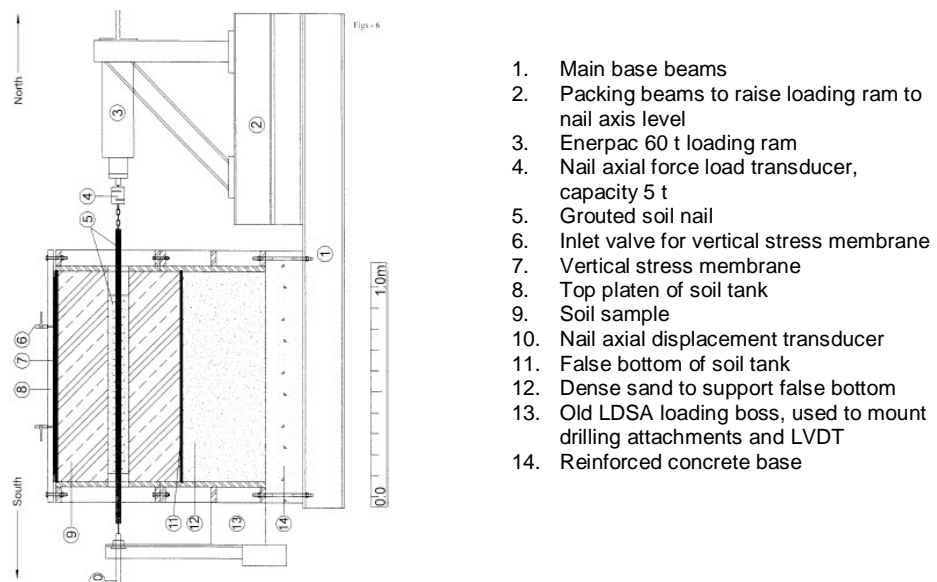


Figure 1.13 The laboratory nailing apparatus (Morris, 1999)

Chu et al. (2005) performed a series of laboratory pull-out tests with a cement grouted nail in a completely decomposed granite soil. They used a test box with dimensions 700 mm long, 560 mm wide and 605 mm high. The sketches of the pull-out test apparatus are shown in Figure 1.14. The effect of the degree of saturation of the soil sample on the pullout resistance and the variation of pull-out resistance under different overburden pressures were investigated. The results indicate that the load-displacement curves for pull-out tests exhibit a significant peak and post peak shear strength behavior (Figure 1.15). The variation of pull-out capacity with overburden pressure is shown in Figure 1.16.

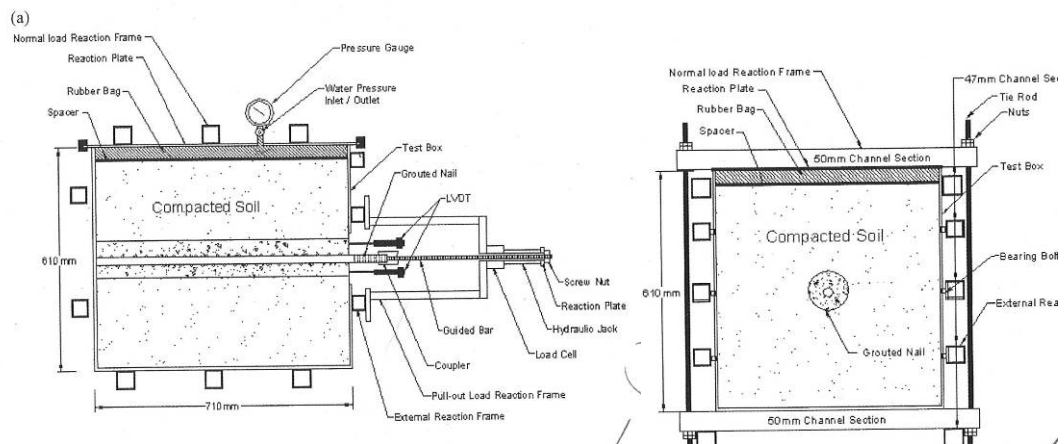


Figure 1.14 The laboratory nailing apparatus (Chu et al., 2005)

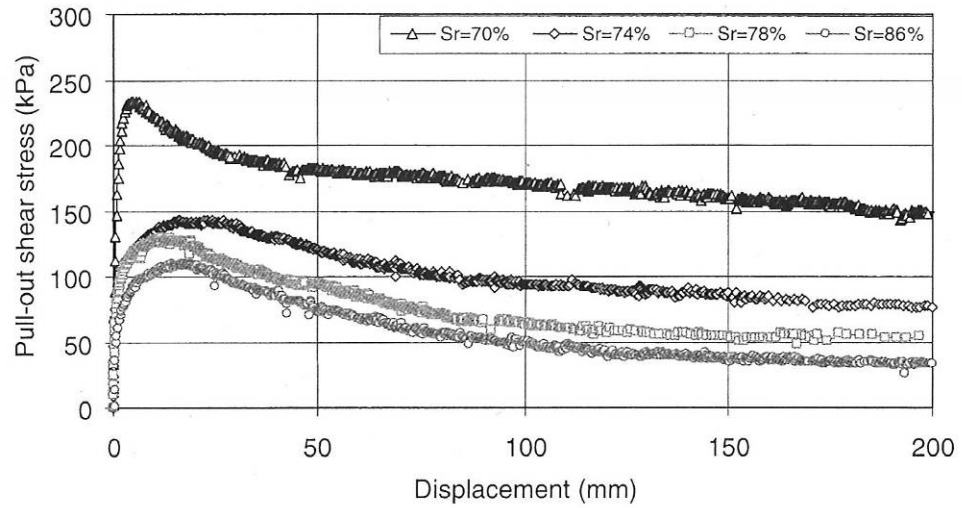


Figure 1.15 The pull-out test results of the soil nails in different degree of saturation under a stress of 300 kPa (Chu et al., 2005)

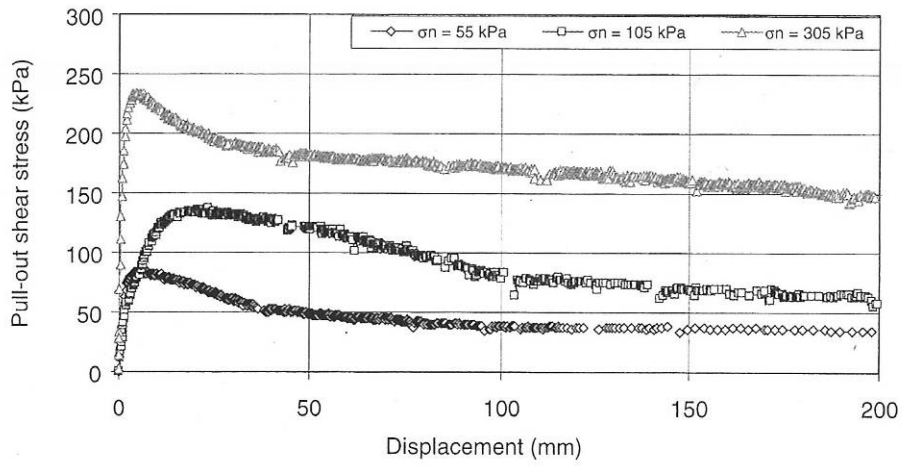


Figure 1.16 The pull-out test results of the soil nails under different overburden pressures (Chu et al., 2005).

Junaideen et al. (2004), stated that there was no consensus on the methods used to estimate pullout resistance and they concluded that, the pull-out tests used by designers and researchers are the best and simplest tests available. In their study, a large box (2m long x 1.6 m wide x 1.4 m high) was used to model the pull-out resistance of the 25 mm diameter, 1.8 m long ($L/D=72$) ribbed, knurled and smooth bar nails located inside the completely decomposed granite. The test apparatus is shown in Figure 1.17. The tests were carried out for different bars under different overburden pressures. As a result of these tests it was reported that, the ribs have a significant influence on the pull-out resistance. Additionally, as obtained from the pull-out load-displacement curves, the peak pull-out forces are mobilized at a few millimeters of nail displacements and the distinct peak values followed by a sharp reduction. Some of the results obtained from this study are shown in Figure 1.18.

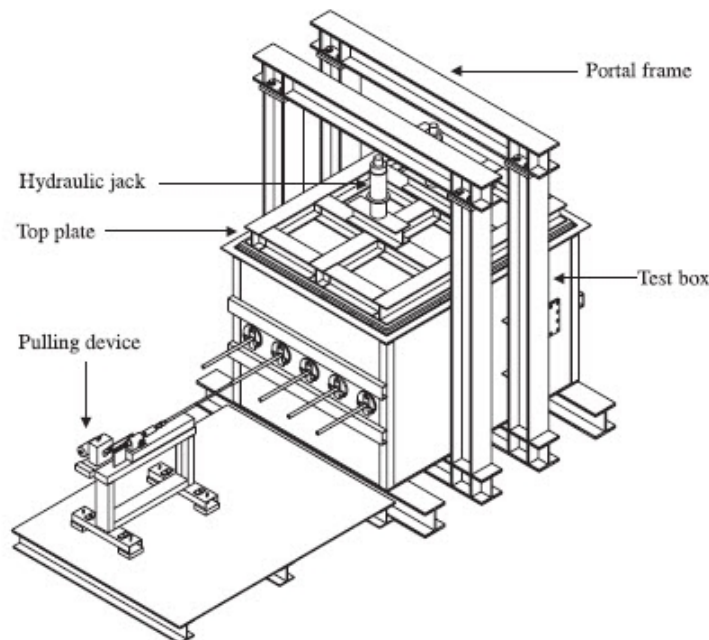


Figure 1.17 Test apparatus used by Junaideen et al. (2004)

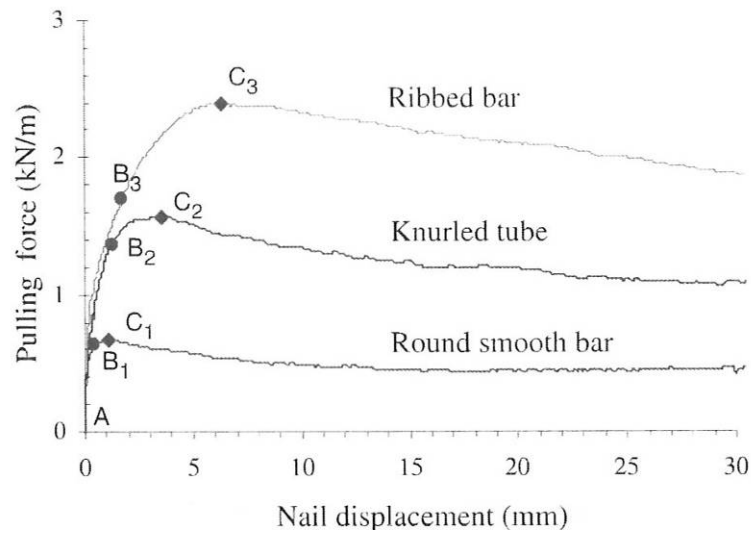


Figure 1.18 Load displacement curves of different bars (Junaideen et al., 2004)

Pradhan et al. (2006) carried out pull-out tests to determine the pull-out behavior of grouted nail in loose sandy fills material (completely decomposed granite). The sand tank used in tests is similar to that used by Junaideen et al. (2004). They stated that the pull-out resistance of the soil nails is correlated with overburden pressure. Since the tests are performed in loosely compacted fill, the effect of dilatancy could be neglected. Due to this reason, the pull-out resistance is expected to be increased with depth conversely to dense sand which shows significant dilation during shearing (Figure 1.19).

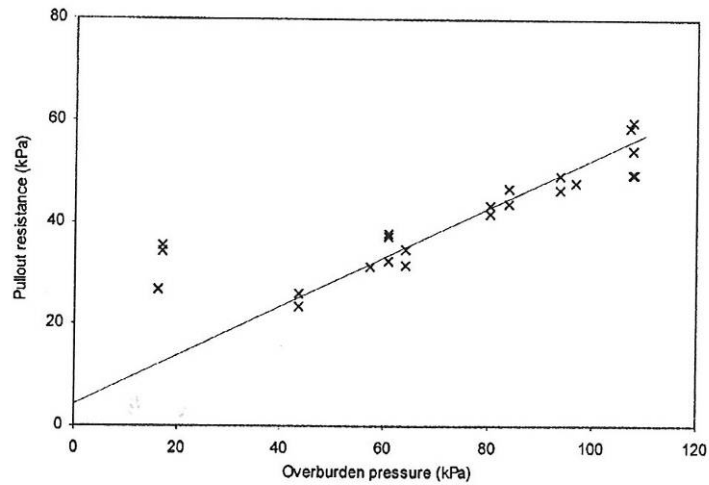


Figure 1.19 Variation of pull-out resistance with overburden pressure
(Pradhan et al., 2006)

In order to examine the influence of the overburden pressure on the bond resistance of the grouted soil nail in completely decomposed granite, Su et al. (2008) performed a series of pull-out tests by using 1000 mm by 600 mm by 830 mm model box. The pull-out box and the instrumentation are shown in Figure 1.20. It is concluded that the installation process of soil nail induced significant vertical stress changes in soil around the soil nails and that the soil nail pull-out shear resistance is independent of the overburden pressure. This is in agreement with Guilox et al. (1982) and Cartier et al. (1983). But on the other hand, the findings are not in agreement with the results of studies performed by Chue et al. (2005), Junaideen et al. (2004), and Pradhan et al. (2006). The relationship between the pull-out resistance and displacement of this study is shown in Figure 1.21. Additionally, numerical simulations of the physical model were performed through 3D finite-element

analyses. The comparison of the measured and simulated pull-out shear stress versus displacement plots are presented in Figure 1.22.

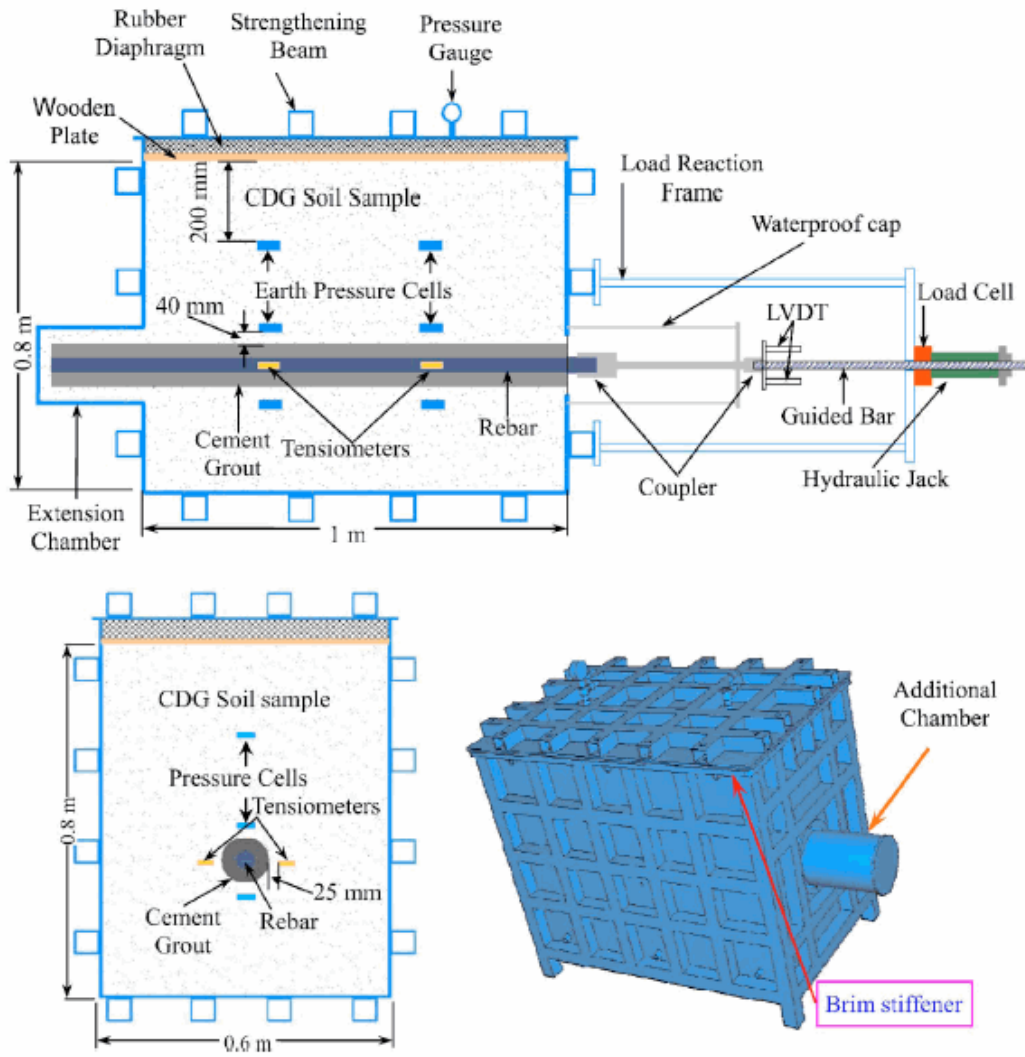


Figure 1.20 Pull-out box and instrumentation (Su et al. 2008)

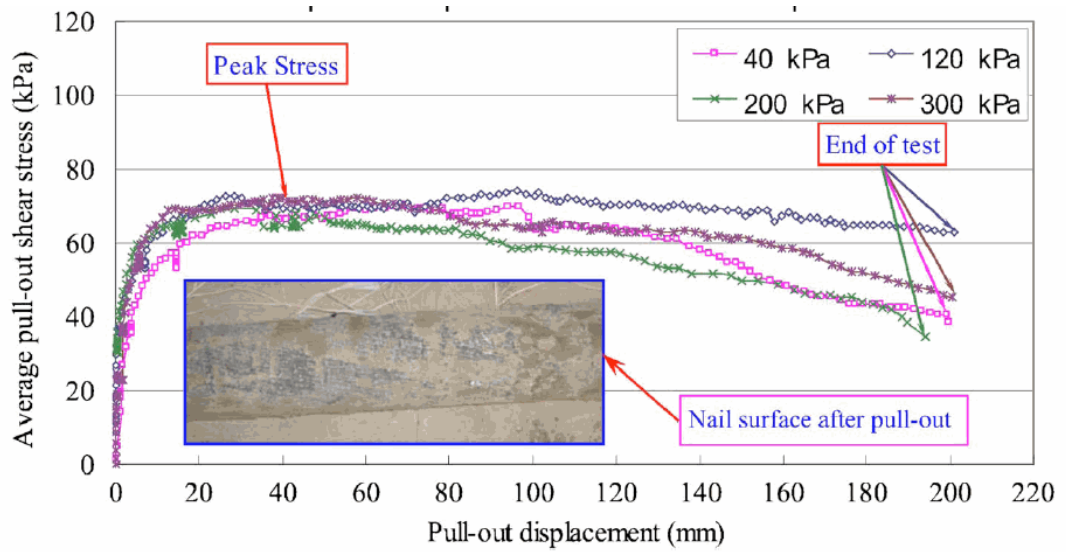


Figure 1.21 Variation of the pull-out resistance with displacement under different overburden pressures (Su et al., 2008)

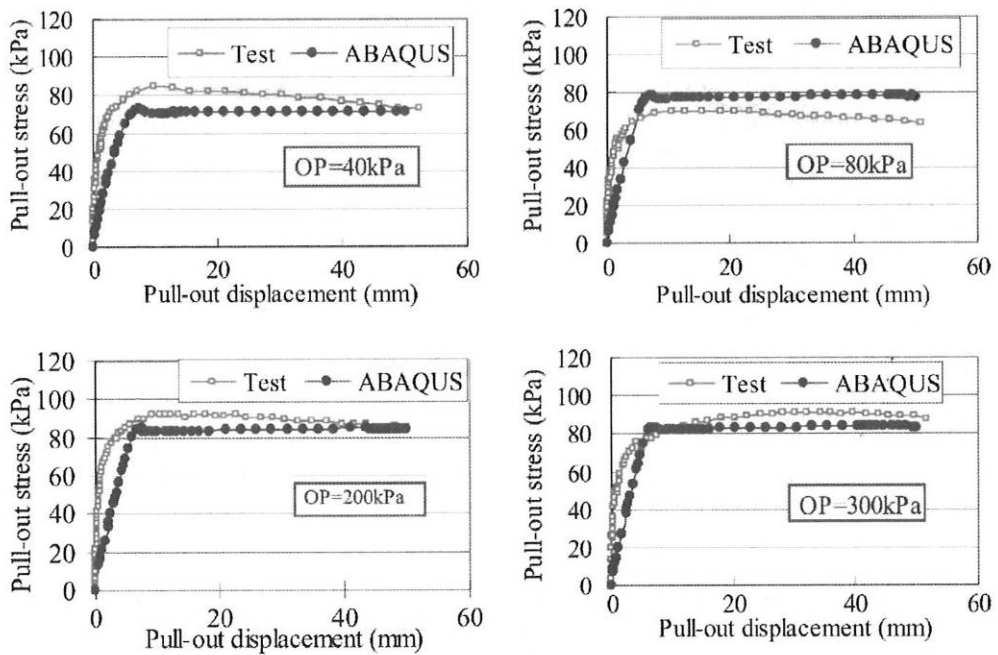


Figure 1.22 Comparison of measured and calculated pull-out resistance of the soil nails under different overburden pressures (Su et al. 2008)

In another study by Chai et al. (2005), the earth sewing technique, a combined technology of chemical grouting and soil nailing, is investigated. Unsaturated sandy clay is used and a 3 mm diameter bolt is located in a 7 mm drill hole. The pull-out apparatus is shown in Figure 1.23. The relationship between the maximum pull-out force and the water content is investigated and it is stated that the water content influences the ultimate bond stress of nails through shear strength parameters. Pull out capacity of the soil nails decrease with increasing water content.

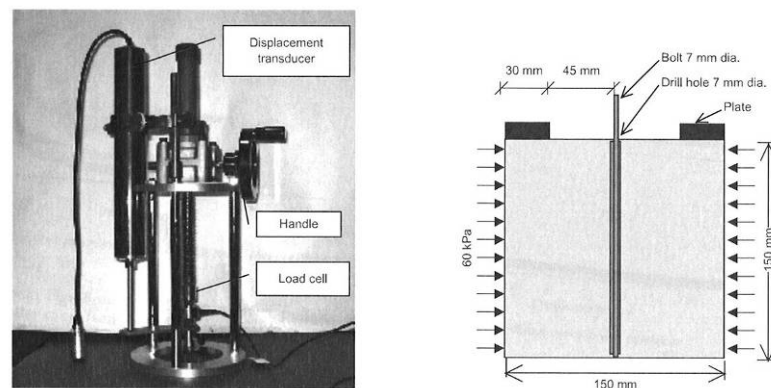


Figure 1.23 Pull-out apparatus (Chai, 2005)

All the studies presented above investigated the influence of factors relating to the soil characteristics, type of nail on the pull-out capacity of a single nail behavior under different overburden pressures. Different from them, Hong et al. (2003) studied the pull-out resistance of single and double nails in a 600 mm long, 800 mm wide x 400 mm high model sandbox with dry sand. A schematic view of the pull-out apparatus is shown in Figure 1.24. The pull-out resistance of the driven nails is investigated for the variations in the

surface roughness, the ratio of nail length to nail diameter (10-50), the overburden pressure and the distance between two nails. They found that the apparent friction coefficient at the soil-nail interface is dependent upon the nail surface roughness. In their study, the group efficiency is defined as the ratio of the average pull-out force from the double nail test to that from a single nail test. The nail efficiency of the two nails placed horizontally with different spacings were investigated during the pulling out the nails simultaneously. The test results showed that the pull-out force increases with increasing spacing until a limit is reached. The results of the tests corresponding to pull-out force versus displacement of double nail tests are given in Figure 1.25 for different roughness and spacing of the soil nails. Consequently, Hong et al. (2003) concluded that when the pull-out resistance of a nail obtained from a pull-out test is used as the basis for a group nail design, the pull-out resistance of each soil nail should be reduced for the nails installed closer than minimum required distance.

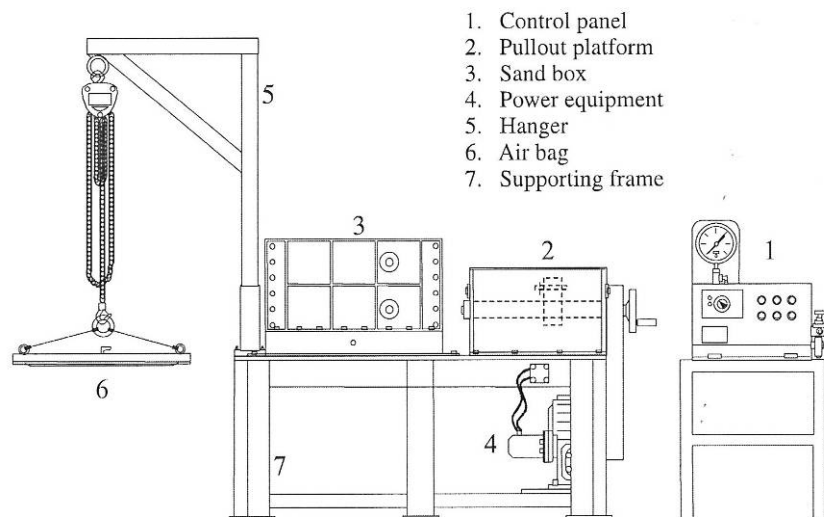


Figure 1.24 A schematic view of the pull-out apparatus (Hong et al., 2003)

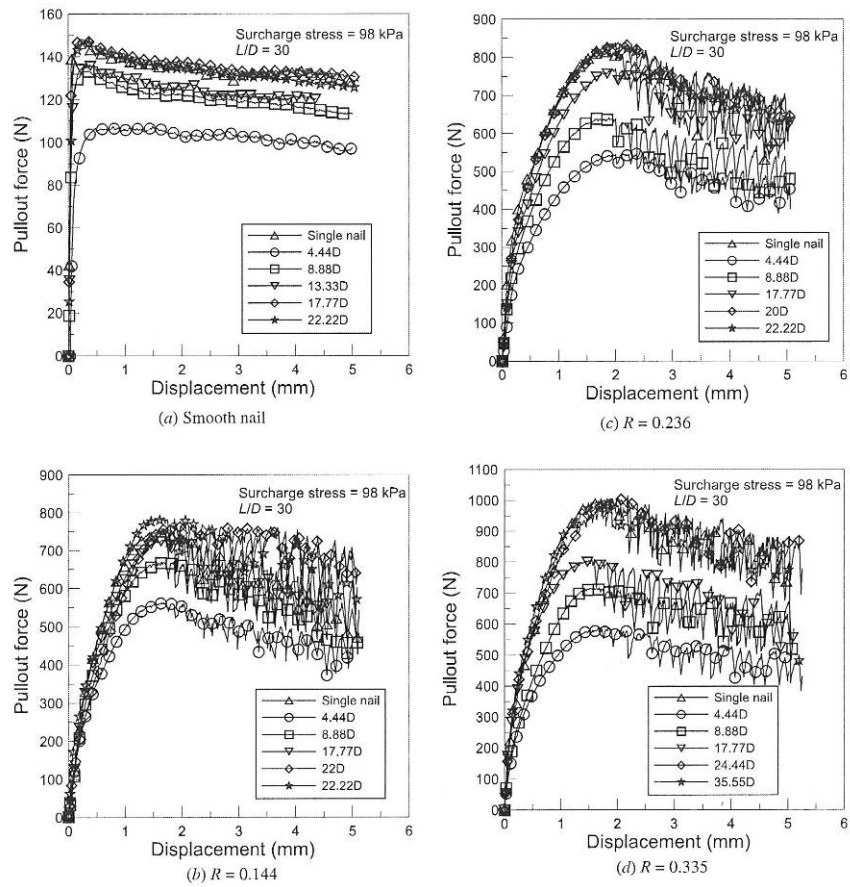


Figure 1.25 Pull-out forces versus displacement of double nail tests (Hong et al., 2003)

1.2.5.2 DIRECT SHEAR TESTS

The pull-out friction, which is an important design parameter of reinforced soil structures, can be identified by direct shear tests as well as the pullout tests. Compared to the results of the pull-out tests, the direct shear tests

yield much smaller values. In some cases, the pull-out test result may be up to 13 times greater than the direct shear test results. This phenomenon results from the dilatancy of soil under shear and also depends on the roughness of the reinforcement (Ingold, 1982; O'Rourke et al., 1990). Wang et al. (2002) developed a mechanical model to relate the sand dilatancy to soil reinforcement interface friction so that the coefficient of pull-out friction can be related to the direct shear friction coefficient. Chu et al. (2005) used a large size direct shear apparatus (Figure 1.26) to investigate the shear stress-displacement relationship for a better understanding of the difference between interface shear stress tests and laboratory pull-out tests of grouted nails in completely decomposed granite. They concluded that the shear stress-displacement relationship of the soil-grout interface observed in the interface shear tests is significantly different from that observed in the pull-out test models.

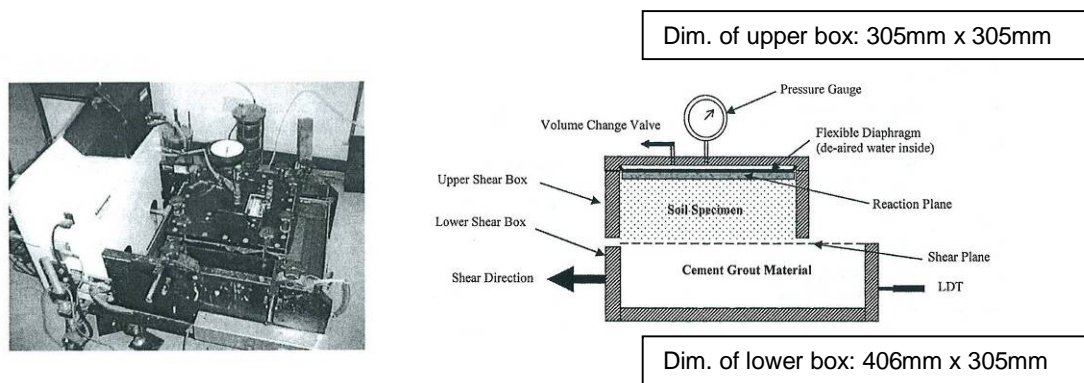


Figure 1.26 View of the large size direct shear box test apparatus developed by Chu et al. (2005)

1.2.5.3 CENTRIFUGE TESTS

In the centrifuge modeling, the stress state that exists in a full-scale prototype is created by using a reduced scale model. This is done by subjecting the model components to an enhanced body force, which is provided by a centripetal acceleration of magnitude ng , where g is the acceleration due to the Earth gravity (i.e. 9.81 m/s^2) (Ng et al.).

Centrifuge modeling was used firstly by Sheen et al. (1982) in soil nailed structures to identify the possible failure mechanism for stability. A model box (420 x 200 x 250 mm) with silty sand compacted in layers was used with a grouted piano wire to model the nails in the model. The model was accelerated up to failure of the 150 mm cut at accelerations of 30g to 40g. The line of the failure is obtained by the photographs taken during failure. In another study performed by Bolton et al. (1990) kaolin was used. The aim of their study was to monitor the loads in the nails as excavation took place and the effect of increased pore pressures on the stability of the system. They concluded that as a result of the inundation of water, the failure plane was similar to that reported by Shen et al. (1982). Additionally, they reported the variation of the load on the nails. Another investigation about the failure of the soil nailed walls was performed by Tei (1993) to investigate the effect of nail roughness, inclination and the facing stiffness. He stated that the increasing nail length and surface roughness reduce the displacements. Frydman et al. (1994) modeled the soil nail walls in clayey sand and investigated the pull-out loads in their experimental set-up. Moreover, the behavior of soil nailed wall in sand during excavation and surcharge loading was investigated by several researchers such as Gammage (1997) and Aminfar (1998). Further studies were conducted to investigate the variation of axial loads and bending moments on the soil nails by considering the

parameters such as slope angle, reinforcement density, effect of drainage and the changes in effective stress. Among them, Morgan (2002) used a 7 m diameter centrifuge in his assembled model (Figure 1.27).



Figure 1.27.a The 7 m diameter centrifuge (Morgan, 2002)



Figure 1.27.b The assembled model of Morgan (2002)

CHAPTER 2

EXPERIMENTAL STUDY

In this chapter, the physical characteristics of the soil sample which is used in the experiments are presented first. Then, the work carried out for the determination of the soil sample preparation technique is given.

2.1 PHYSICAL CHARACTERISTICS OF SOIL SAMPLE

In this study, Ankara Clay is used in the experiments. Material was taken from a building foundation excavation between 4.0-5.0 m depths, located at Çukurambar, Ankara (Figure 2.1). Nearly 3 m³ of clay is obtained from this site and transported to the Technical Research Department of the General Directorate of Highways, where sieve analysis and hydrometer test are performed on it. In Table 2.1, the result of the sieve analysis are given and the corresponding grain size distribution is shown in Figure 2.2. Table 2.2 shows the results obtained by the hydrometer test. The details of the hydrometer test is given in Appendix A. In addition, Atterberg limits of the soil sample are determined and the results are presented in Table 2.3. Based on the result of these tests, the soil sample was classified as high plastic clay (CH) according to the Unified Soil Classification System (Wagner, 1957).



Figure 2.1 Collection of the soil sample

Table 2.1 Sieve analyses results

Sieve No	Sieve Spacing (mm)	Total Passing (%)
4	4.750	100
10	2.000	99
20	0.840	94
40	0.425	91
100	0.149	85
200	0.075	82

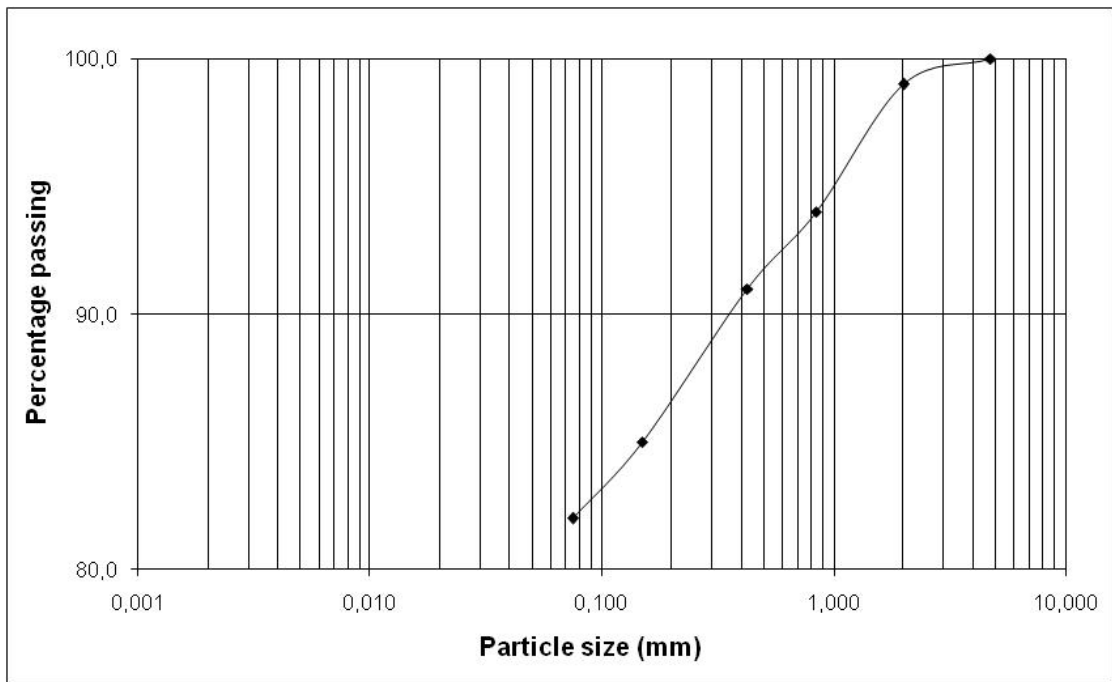


Figure 2.2 Grain size distribution

Table 2.2 Hydrometer test results

Gravel (>2 mm) (%)	1.0
Coarse Sand (2-0.42mm) (%)	6.3
Fine Sand (0.42-0.075m) (%)	10.1
Silt (0.075-0.002mm) (%)	28.9
Clay (0.002-0.001mm) (%)	7.6
Colloidal Clay (<0.002mm) (%)	46.1

Table 2.3 Atterberg limits of the soil sample

Liquid Limit (%)	69
Plastic Limit (%)	26
Plasticity Index (LL-PL) (%)	43

2.2 DETERMINATION OF THE SOIL SAMPLE PREPARATION TECHNIQUE

In the design of the experiments, different patterns of soil nails are considered. The shear strength parameters of the soil have a great effect on the pull-out capacity of soil nails. Accordingly, to be able to compare the results of different tests, the soil sample used in each case should have similar characteristics. On the other hand, the compaction of cohesive soils with smaller water content is difficult and the obtained samples have smaller density with greater void ratio. With increasing water content (upto a certain limit) the cohesion decreases and the sliding between particles increases which results in better compaction of soil sample. If the water content becomes greater than a certain limit, water and voids separate the particles and the maximum dry unit weight becomes smaller. Considering these facts, in order to have similar soil properties for each test, it is decided to place the soil sample at its optimum water content and maximum dry density.

For each soil, there is a unique water content that makes dry unit weight maximum. The optimum water content and maximum dry density of the soil is determined by evaluating the results of several tests. In the Standard Proctor Technique, the soil sample is compacted into a 4" diameter mold. In

the compaction, 3 layers are formed by using a 2.49 kg hammer. 25 blows are performed for each layer. The compacted soil is removed from the mold, and the water content and the dry unit weight are determined. This experiment is repeated for at least five soil samples having different water contents and the results are plotted such that the dry unit weight and water content are y- and x-axes, respectively. The maximum dry density and the corresponding water content are determined from the plot as shown in Figure 2.3. In the Dynamic Compaction Test, the same procedure is followed as mentioned in the Standard Proctor Test. Only the compaction technique is different. The soil is compacted into the mold in 3 layers and for each layer dynamic impact is applied for 60 seconds. The soil sample of which maximum dry density and optimum water content to be determined is prepared with the help of two tests namely, the Standard Proctor and Dynamic Compaction Tests (Demirel et al. 2003, KTŞ 2006). In Figures 2.3 and 2.4, the compaction curves obtained by the Standard Proctor Compaction and Dynamic Proctor Compaction tests are given, respectively. In Table 2.4, the optimum water content and maximum dry unit weight of the soil sample obtained by these tests are presented.

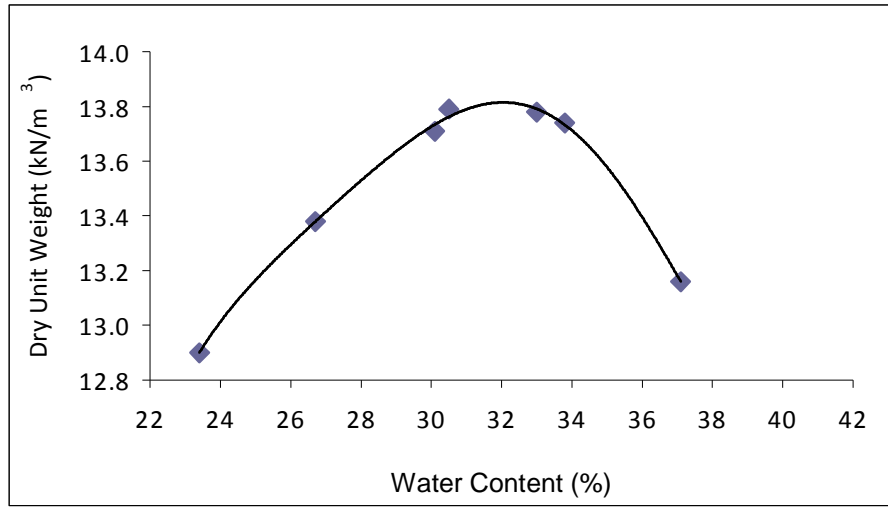


Figure 2.3. Compaction curve of the soil sample obtained by the Standard Proctor Compaction Test

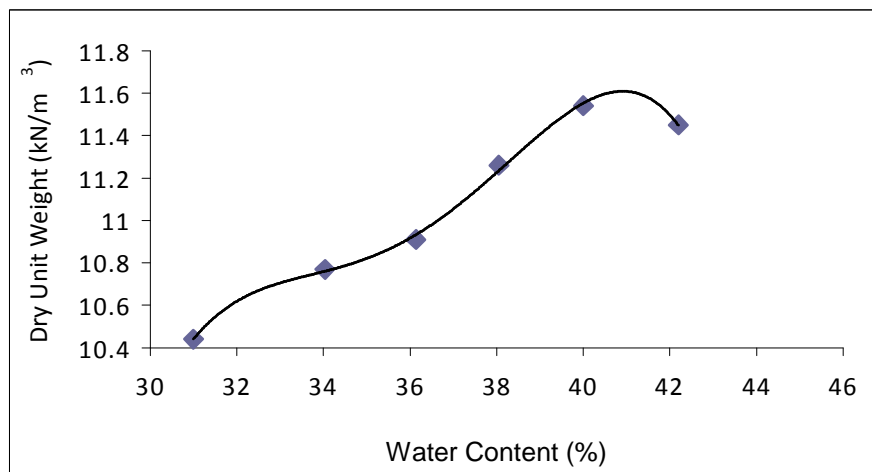


Figure 2.4 Compaction curve of the soil sample obtained by the Dynamic Compaction Test

Table 2.4 Optimum water content and maximum dry unit weight of the soil sample

Type of Compaction	Maximum Dry Unit Weight (kN/m ³)	Optimum Water Content (%)
Standard	13.84	31.8
Dynamic	11.56	40.0

For the determination of shear strength parameters and the overburden pressure that will be applied during the pull-out tests, tri-axial compression tests (UU) are performed in accordance with TS 1900-2. The mechanical behavior of the soil sample is investigated under different confining pressures. Soil samples located inside the cylindrical mold at optimum water contents obtained from both Dynamic Compaction and Standard Proctor Compaction Tests are used in undrained-unconsolidated (UU) tri-axial compression test. In Table 2.5, the confining pressures, (σ_3) used in tri-axial compression tests are given for both Standard Proctor Compaction and Dynamic Compaction Tests. In addition, in Figures 2.5 and 2.6 the result of tri-axial tests prepared by Standard Proctor Compaction and Dynamic Compaction Tests are presented for the values given in Table 2.6.

Table 2.5 Confining pressures (σ_3) used in the tests

Set	Compaction Technique	Confining Pressures Used in Triaxial Tests (kN/m ²)
A	Standard Proctor Compaction Test	25; 50; 100; 200; 300
B	Dynamic Compaction Test	50; 100; 200

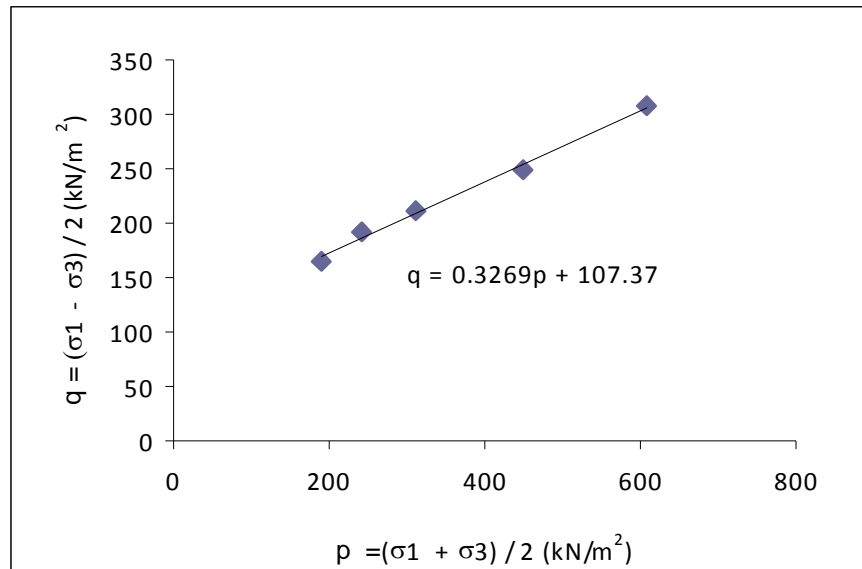


Figure 2.5 Mohr-Coulomb failure envelope for specimens used in set-A tri-axial UU tests

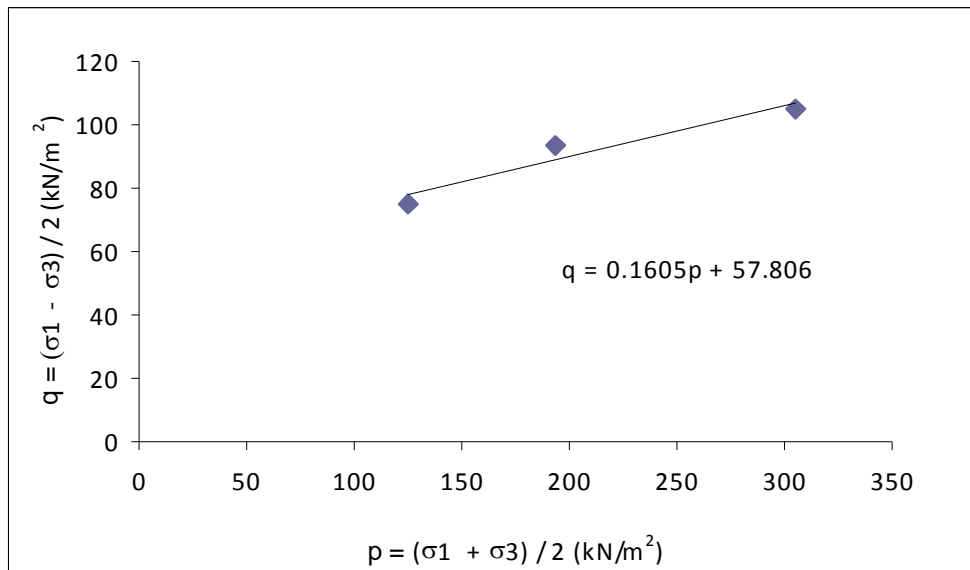


Figure 2.6 Mohr-Coulomb failure envelope for specimens used in set-B tri-axial UU tests

Table 2.6 Shear strength parameters determined from tri-axial UU tests

Compaction Technique	Confining pressure (σ_3 kN/m ²)	Tan α	a	c (kPa) { $c=a/\cos\phi$ }	ϕ ($^\circ$) { $\phi=\sin^{-1}(\tan\alpha)$ }
Standard Proctor Test	25; 50; 100; 200; 300	0,326	107.3	114	19
Dynamic Compaction	50; 100;200	0,160	57.8	59	9

In view of the results of the tri-axial tests, it is concluded that the compaction technique to be used in all experiments can be assessed using the Standard Proctor Test as the cohesion obtained is greater.

As a result of the work carried out during the compaction of clay, it is observed that, due to the size of the soil sample, it is not possible to use standard proctor technique to obtain similar characteristics for each layer in the model box. In addition, the time required is relatively long, which can affect the soil properties during the compaction. In order to overcome this difficulty, the clay is compacted in cylindrical molds by using static compactor to gain time and speed. The clay sample is located inside a cylindrical mold first. During this process, to obtain the target density, the volume of the cylinder and the volume of the soil sample that is compacted should be determined for each compaction layer. Hence, the layer thickness and the amount of material that should be placed inside the mold can be calculated. The samples from two different sets (Set 1 and Set 2) of cylindrical molds are taken in order to determine the shear strength parameters of the compacted soil.

For the comparison of shear strength parameters, undrained–unconsolidated tri-axial compression tests with 50, 100 and 200 kN/m² cell pressures, are performed for each sample. The Mohr-Coulomb failure envelope obtained after these tests are shown in Figures 2.7 and 2.8. The shear strength parameters are summarized in Table 2.7.

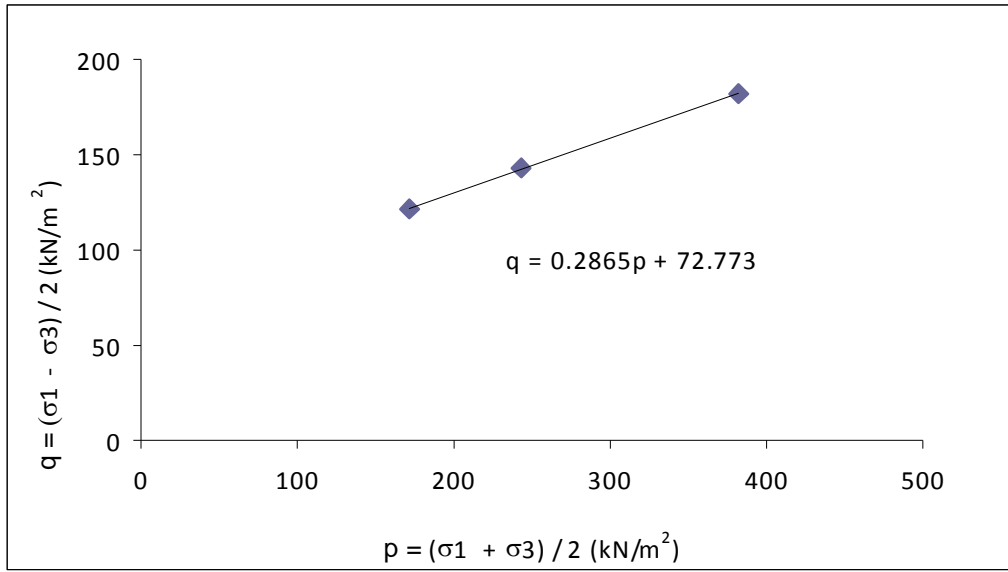


Figure 2.7 Results of tri-axial tests (UU) (soil sample (Set 1) prepared by static pressure)

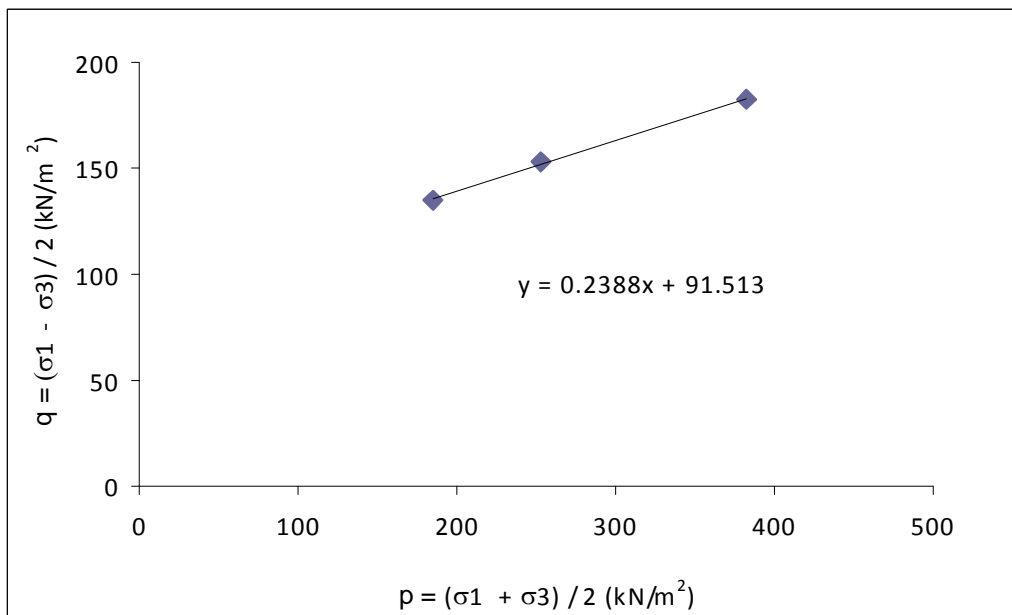


Figure 2.8 Results of tri-axial tests (UU) (soil sample (Set 2) prepared by static pressure)

Table 2.7 Shear strength parameters of clay sample prepared with static compactor using tri-axial compression tests (UU)

	Compaction Technique	$\tan \alpha$	a	c (kPa) { $c=a/\cos\phi$ }	ϕ ($^{\circ}$) { $\phi=\sin^{-1}(\tan\alpha)$ }
Sample Set 1	static pressure	0,286	72.7	76	17
Sample Set 2	static pressure	0,238	91.5	94	14

CHAPTER 3

DETAILS OF PULL-OUT TESTS

3.1 INTRODUCTION

In this chapter, the test set-up used in the pull-out tests is presented first. Then, the details of soil sample preparation and placement are given. Finally, the procedure for the pull-out tests is explained.

3.2 DETAILS OF TEST SET-UP

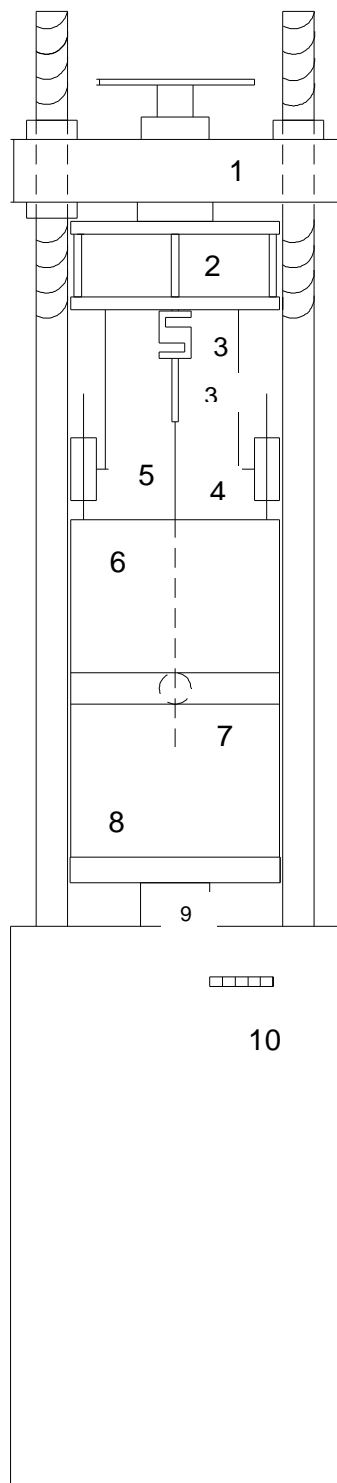
The set-up for the pull-out tests is composed of an aluminum sample box, a pull-out device, an overburden pressure applicator, and measuring equipments (two linear variable differential transformers, LVDT's, a load-cell and a monitoring device). The picture and the sketch of the set-up is shown in Figures 3.1 and 3.2.

The model box with the pre-buried nails is located in the pull-out device and it is fixed to the cap of the piston of the loading machine by using steel bars. The details of the system are shown in Figure 3.3. The nails are mounted on a steel plate, which is the stationary part of the set-up (Figure 3.4). During

the pull-out test, the piston located at lower part is moved downwards with a constant speed.



Figure 3.1 The set-up for single nail pull-out tests.



- 1 Stationary part of the frame
- 2 Steel plates to mount the nails to the stationary part
- 3 Load-cell
- 4 LDVT's
- 5 Soil nail
- 6 Model box
- 7 Specially designed frame to apply overburden pressure
- 8 Steel cap of the piston
- 9 Piston
- 10 Press machine

Figure 3.2 The drawing of set-up for single nail pull-out tests

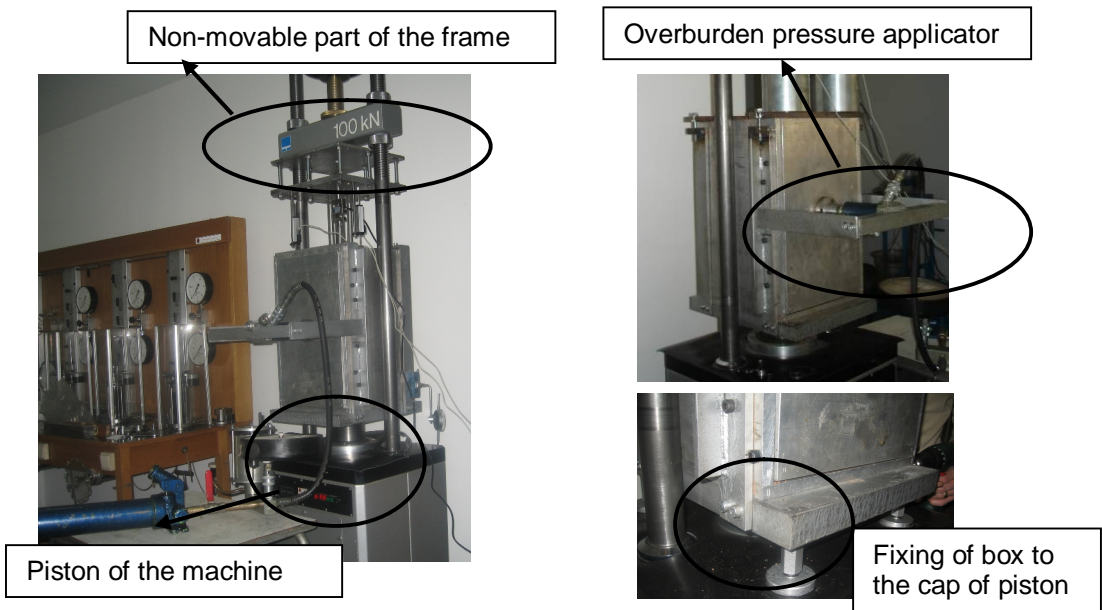


Figure 3.3 Details of the model box, piston and the testing machine

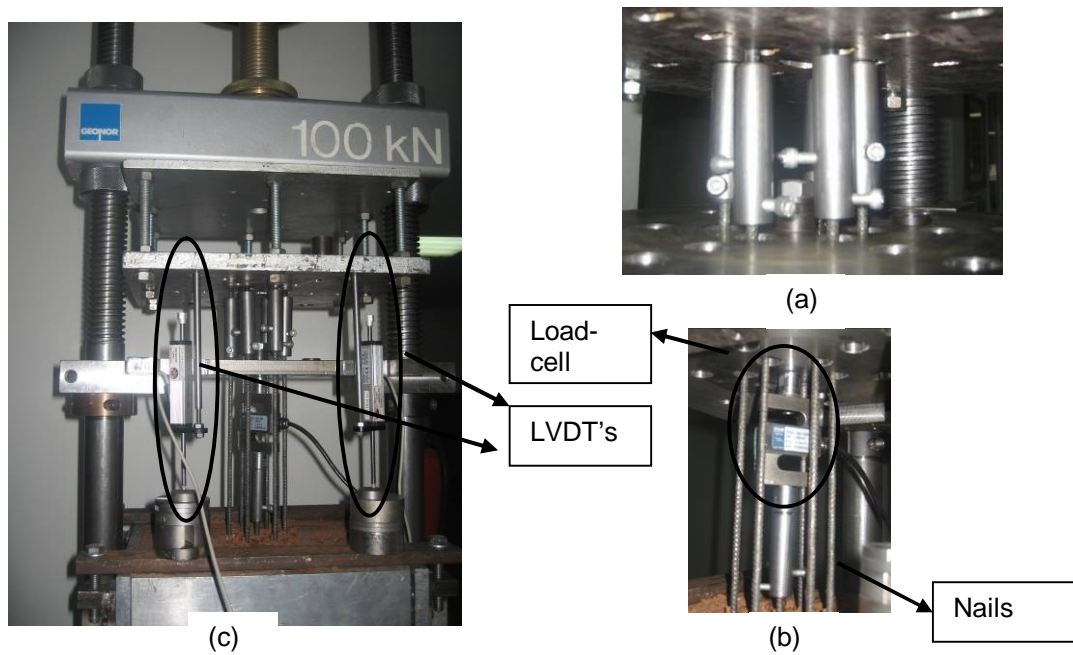


Figure 3.4 Details of the nails mounted on the stationary steel plate (a) LVDT's, (b) Non movable part of the frame, (c) Load-cell and nails

3.2.1 MODEL BOX

The model box is made of 15 mm thick aluminum plates joined by steel bolts. The box is strengthened with two steel rings in order to resist the vertical load applied during the compaction of the clay through the box. The model box is manufactured in the laboratory of the Technical Research Department of General Directorate of Highways. In the front face of the box, seven holes are opened for nail installation during the compaction phase.

Because of the difficulty of preparing large amounts of clay sample and to minimize the possible effects of boundary conditions on the test results, the decision on the dimensions of the model box is important. Hong and Chen (2000) recommended that, in order to avoid the boundary effects, the shortest distance between the nail and the box boundary should be at least 20 times the nail diameter. On the other hand, Nicholson (1986) stated that the nail spacing ranging between 6 and 10 times the nail diameter was common in the United States, whereas nail spacing as high as 15 times the nail diameter was used in Europe (Hong et. al 2003). Based on the information available in literature, the distance between the side wall and the central nail is determined to be at least twenty five times the nail diameter and the box dimension is chosen as 300 mm (width) x 300 mm (height).

As presented in Chapter 1, the nail aspect ratio (L/D) varied between 10 and 80 in the previous studies. The nail aspect ratio is chosen as 60 in the experiments and the length of the box is fixed as 500 mm. In Figure 3.5, a view of the model box is given.

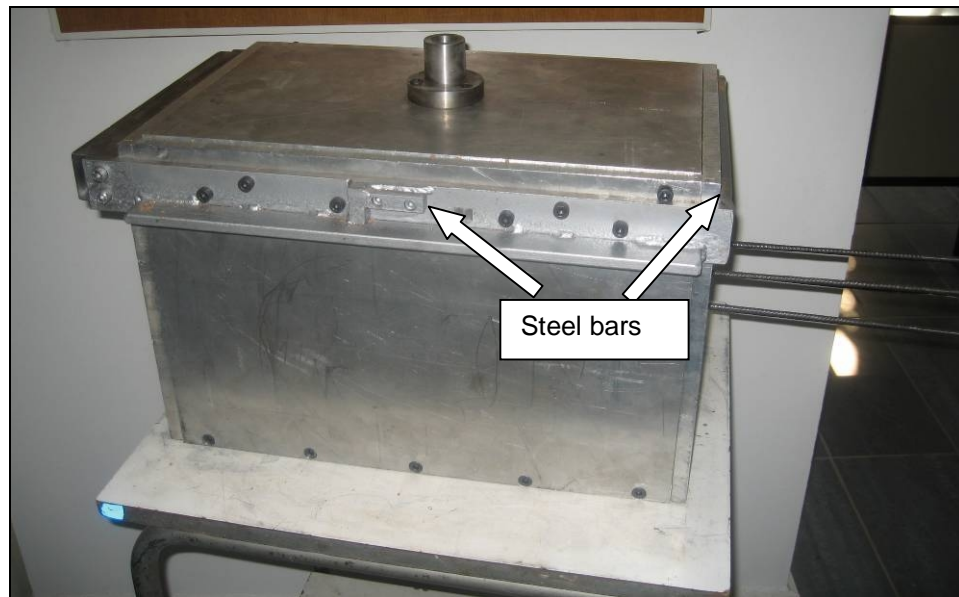


Figure 3.5 A view of model box with dimensions of 300 mm width, 300 mm height, 500 mm length

3.2.2 PULL-OUT DEVICE

The loading unit of a GeoNor tri-axial testing machine is used as the pull-out device (Figure 3.1). The capacity of the loading unit is 100 kN and it permits the pull-out tests to be conducted in a displacement-rate-controlled manner. This type of test allows one to obtain the load-displacement characteristics of nails for the peak and post-peak states of shearing (Junaideen et al., 2004).

The determination of the displacement-rate of the pull-out test is another important issue. A loading rate between 0.000081 and 8.1 mm/min could be

achieved using this testing machine. A comparison of the displacement speed used in different studies on Table 3.1 suggests a rate between 0,1-1,3 mm/min in pull-out tests. Besides, the displacement-rates employed during the direct shear test and the tri-axial tests on soil sample are also considered for the determination of an appropriate displacement-rate for the pull-out tests. The strength tests on soil samples were performed according to TS1900-2, which specifies displacement-rates of 0,6mm/min and 0,8 mm/min for the direct shear tests and tri-axial tests, respectively. Therefore, a displacement rate of 0,6 mm/min is employed for the pull-out tests.

Table 3.1 The displacement-rates and the box dimensions in various pull-out tests

Study	Year	Author	Dimensions of the box	Displacement Speed (mm/min)
Pull-out resistance of single and double nails in a model sand box	2003	Hong et al.	600(l)x800(w)x400(h)	0,1
Comparison of interface shear strength of soil nails measured by both direct shear box tests and pull-out tests	2005	Chu et al.	710(l)x570(w)x610(h)	0,5
Laboratory study of soil-nail interaction in loose, completely decomposed granite	2004	Junaideen et al.	2000(l)x1600(w)x1400(h)	1,3
Soil nail pullout interaction in loose fill materials	2006	Pradhan et al.	2000(l)x1600(w)x1400(h)	1,0

3.2.3 APPLICATION OF OVERBURDEN PRESSURE

As mentioned previously, the loading unit of the GeoNor tri-axial test machine is used as the pull-out device. The piston of the test device operates vertically and due to this reason the pull-out tests are performed in this direction. As a result, the overburden pressure on the test box is applied laterally during the tests. The horizontal pressure is applied by a specially designed frame in which short steel bars are welded on the box to support the steel arm that holds the piston connecting to the movable aluminum plate. The piston is connected to a hydraulic jack that can supply 100 kPa pressure that corresponds to an approximately 5-6 m of overburden height. The details of this set-up are given in Figure 3.6.

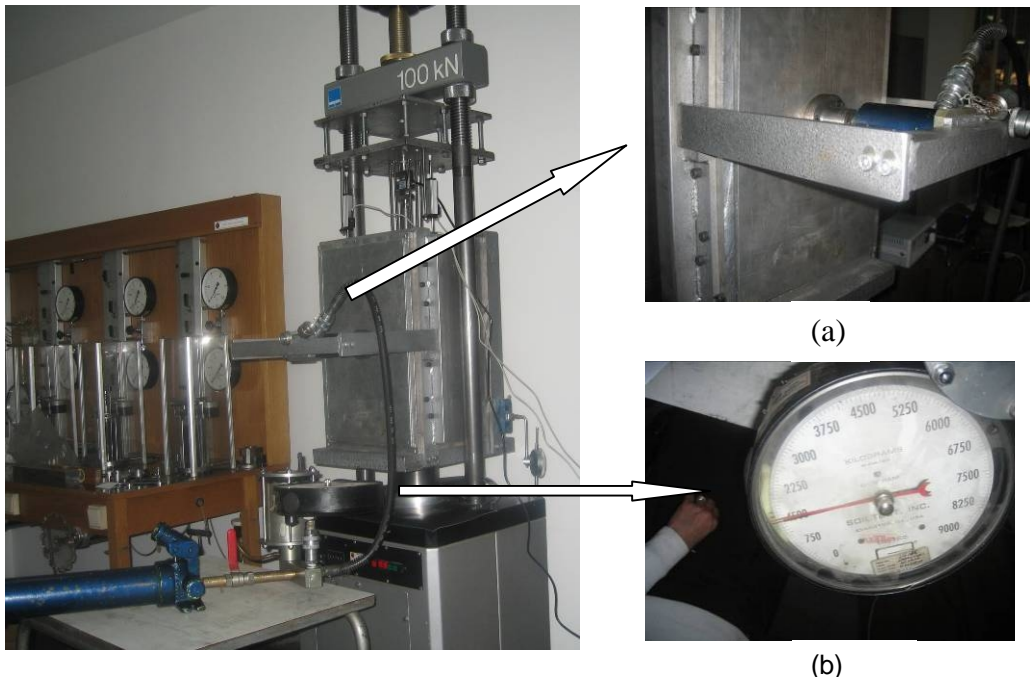


Figure 3.6 The details of the overburden pressure applicator (a) specially designed frame in which short steel bars are welded on the box, (b) a hydraulic jack

3.2.4 MEASURING EQUIPMENT

During the test, by the help of the pull-out device the nail(s) is pulled along its longitudinal direction. A 500 kgf load-cell is installed between the central nail and the pulling device to measure the pull-out force. The class of the load cell is 0.5 according to EN ISO 7500-1. The displacement of the nail during the test is measured by means of two linear variable differential transformers, LVDT's, having a maximum capacity of 50 mm. The measurement uncertainties of two LVDT's are ± 3.2 and $\pm 9.1 \mu\text{m}$, respectively. By using TDG data logger and CoDA Locomotive Software, the test data is recorded by the computer at every 500 ms. The measuring equipments are shown in Figure 3.7. During the tests, the pull-out load versus displacement plots are monitored on the computer.

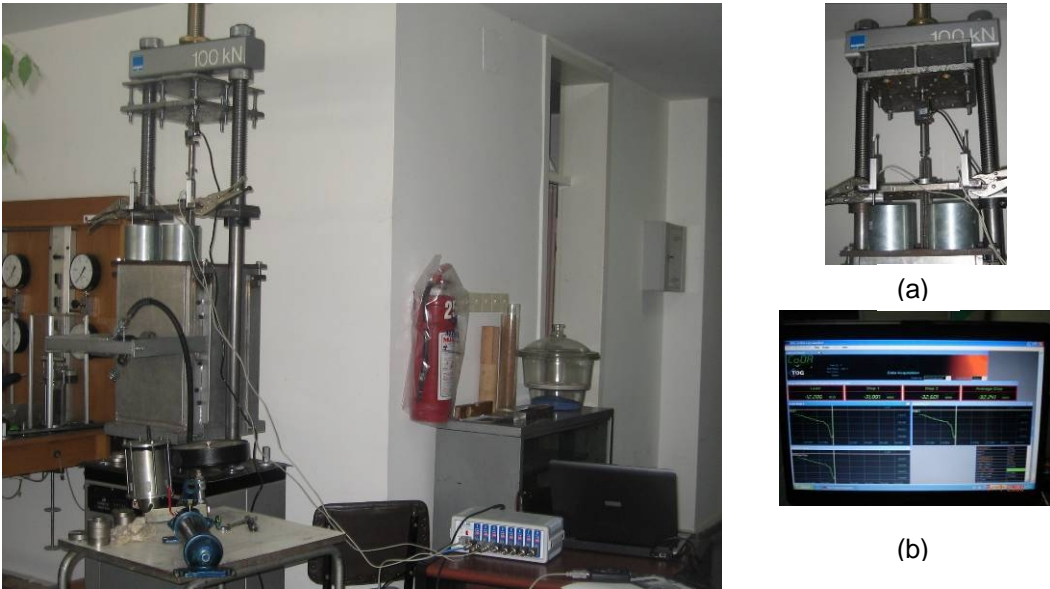


Figure 3.7 Measurement and monitoring devices used in the experiments
(a) LVDT's and load-cell, (b) Monitor of the computer during recording data

3.3 SOIL SAMPLE PREPARATION

In the first phase of the preparation work, the soil sample is sieved from Number 4 (4.75 mm) sieve. Then, the sample is spread out, mixed, and finally placed into plastic bags with an amount of approximately 30 kg.

Five days before the pull-out tests, the samples are taken out from plastic bags for determination of the water content. After obtaining the actual water content of the sample, amount of additional water necessary to obtain the optimum water content is calculated. The additional water is mixed with soil in large trays as shown in Figure 3.8. Since the sample is clay, the absorption of the water by clay is provided by mixing and molding for approximately an hour. The details of this procedure are shown in Figure 3.9.



Figure 3.8 Addition of water to the sample in order to obtain the optimum water content



Figure 3.9 Mixing and molding of the sample

One day after mixing with water, the water content of the sample is measured again in order to determine whether the optimum water content is achieved or not. Then, the soil sample is placed into the model box by using the method described in Section 3.5. During the compaction, special care is given to the sample in order to avoid loss of water.

3.4 SOIL NAILS

The nails used in the experiments are 6 mm diameter ribbed steel bars. As stated previously, the aspect ratio of the nails is determined as 60. Therefore, 360 mm long soil nails are placed into the model box during the placement of the clay into the box. Experiments are performed for both single and group nails that are placed in a scattered pattern as in field applications. An application of soil nails on a road cut is give in Figure 3.10, and in Figure 3.11, the details of pull-out tests for single and group soil nails are shown.

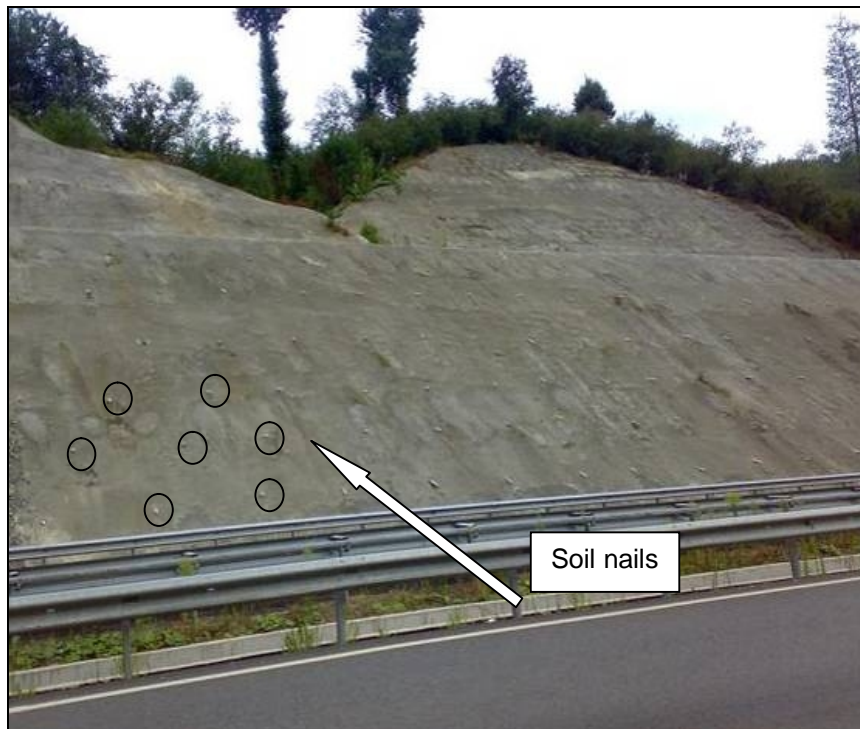


Figure 3.10 An application of soil nails on a road cut



Figure 3.11 Pull-out test details of single nail and group nails

3.5 PLACEMENT OF THE SOIL SAMPLE

The static pressure method is used to compact the clay in the model box. The soil layers to be compacted are placed parallel to the longitudinal direction of nail lengths and the compaction of each layer is performed by using a 100 ton capacity testing machine and a specially designed frame that provides a uniform load distribution on each layer. This special designed frame is composed of two steel plates that are connected to each other with four steel bars. These plates are connected to the testing machine with a thick steel pipe. The dimensions of the plates are chosen such that it can fit into the model box. The details of the compaction process are shown in Figure 3.12. Two sequences of layer thicknesses, shown in Figure 3.13, are used for two different nail configurations.

The amount of material for each compaction layer was calculated, and the soil to be compacted is placed as layers in the box. The details of the soil placement is shown in Figure 3.14. On top of each layer, the compacted material is trimmed and a new layer of soil is spread. Next, the soil is leveled and a plastic cover is placed to avoid sticking of soil to the frame during compaction. The measured amount of material is then placed inside the mold and the compaction is performed for other layers. Finally, the degree of compaction is checked by measuring two different oppositely placed tape measures as shown in Figure 3.15.



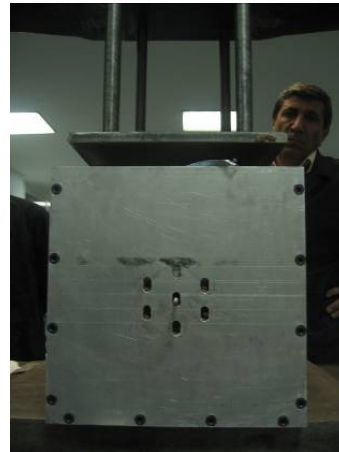
(a)



(b)

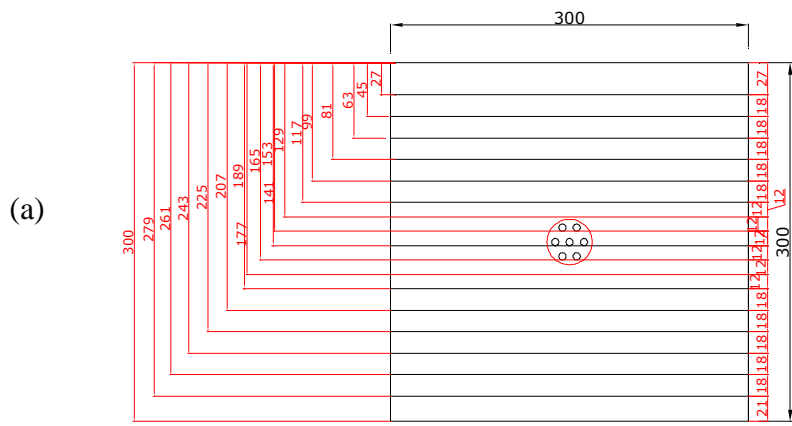


(c)

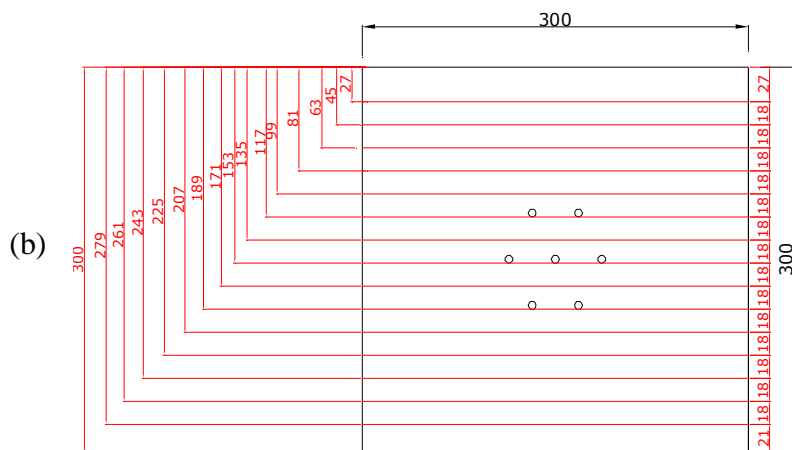


(d)

Figure 3.12 Details of the compaction process of the soil sample: (a) Thick steel pipe to provide connection between frame and press machine, (b) two steel plates that are connected to each other with four steel, (c),(d) view of special designed frame composed of two steel plates that are connected to each other with four steel bars during compaction



Spacing 2xD (12 mm)



Spacing 6xD (36mm)

Figure 3.13 The sequences of thicknesses of soil layers placed in model box for (a) 12 mm and (b) 36 mm nail spacing tests

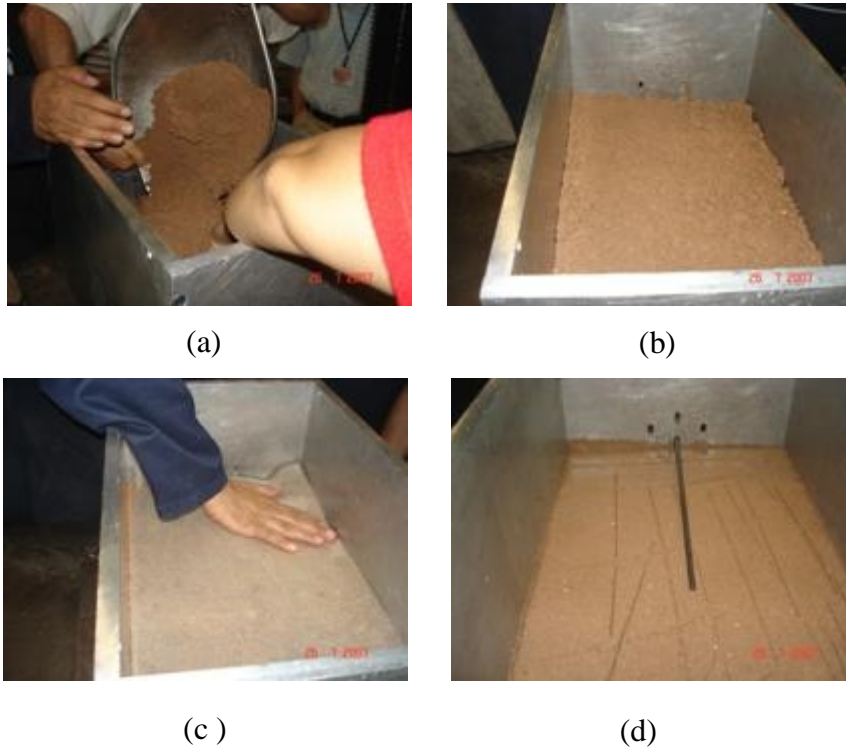


Figure 3.14 Compaction of clay: (a) Placing of the measured amount of material inside the mold, (b) leveling of the material, (c) placing of plastic cover and (d) trimming and placing of soil nail

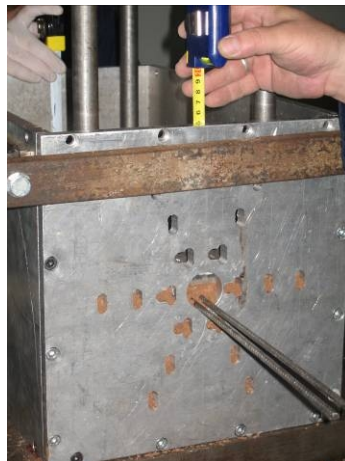


Figure 3.15 Measurement of compaction

3.6 PULL-OUT TEST PROCEDURE

The model box filled with the compacted soil is placed into the pull-out device. As shown in Figure 3.16, the box is fixed to the plate located on the piston. The placement of the box is provided by the steel bars and bolts. During the pull-out tests, the loading unit pulls the box downwards with a constant displacement-rate such that the frame on which the nails are mounted is stationary.

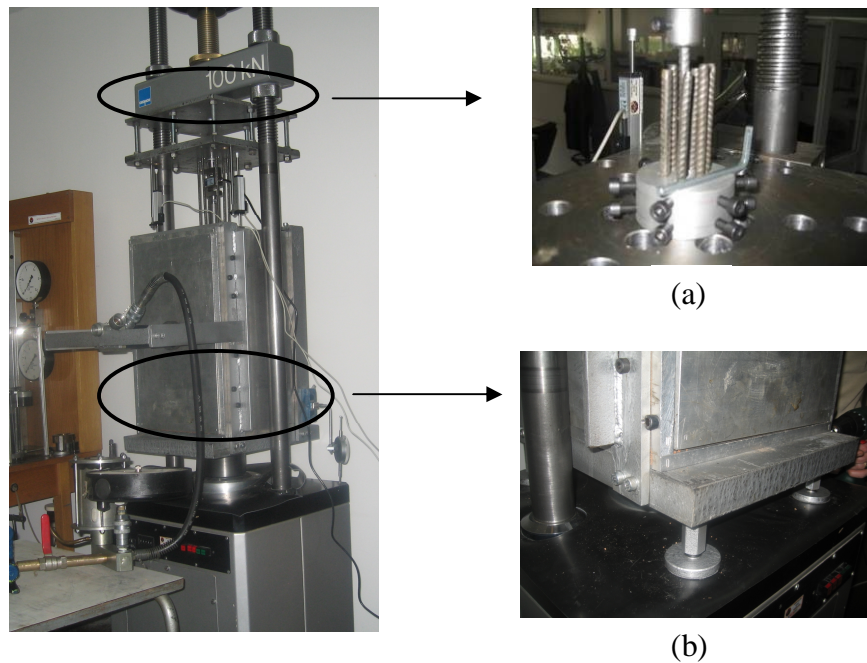


Figure 3.16 The placement of the model box: (a) Fixed part of the nails, (b) fixing the box to the piston

After putting the model box into the pull-out frame, the overburden pressure (100 kPa) is applied in the horizontal direction. As seen in Figure 3.17, the pressure is applied uniformly to the vertical surface of the model box by a frame containing a piston that is connected to the hydraulic pump.

The soil nails are mounted on the upper part of the frame by the help of plates. Mounting of the single and group nails with 2Ø and 6Ø spacing patterns are rather different: The single nail or the central nail of nail groups is connected to the load-cell, and then the load-cell is connected to the fixed plate located above the box (Figure 3.18). In tests with nail groups, 2Ø spaced soil nails are fixed to the lower plate with the help of a special apparatus shown in Figure 3.19, whereas 6Ø spaced soil nails are fixed to the lower plate with special bolts shown in Figure 3.20.



Figure 3.17 Application of the overburden pressure

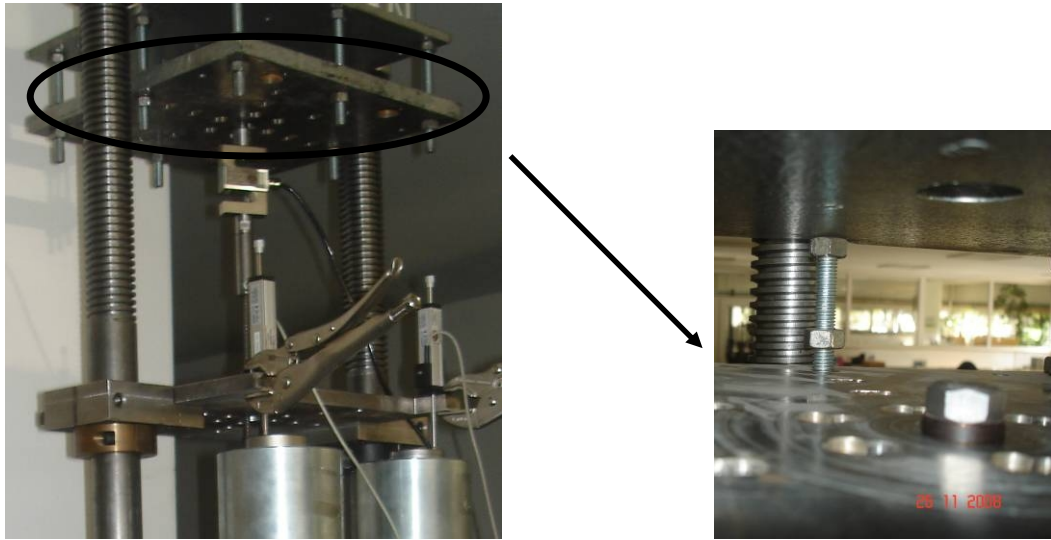


Figure 3.18 Connection details of the load-cell, single nail and the plate

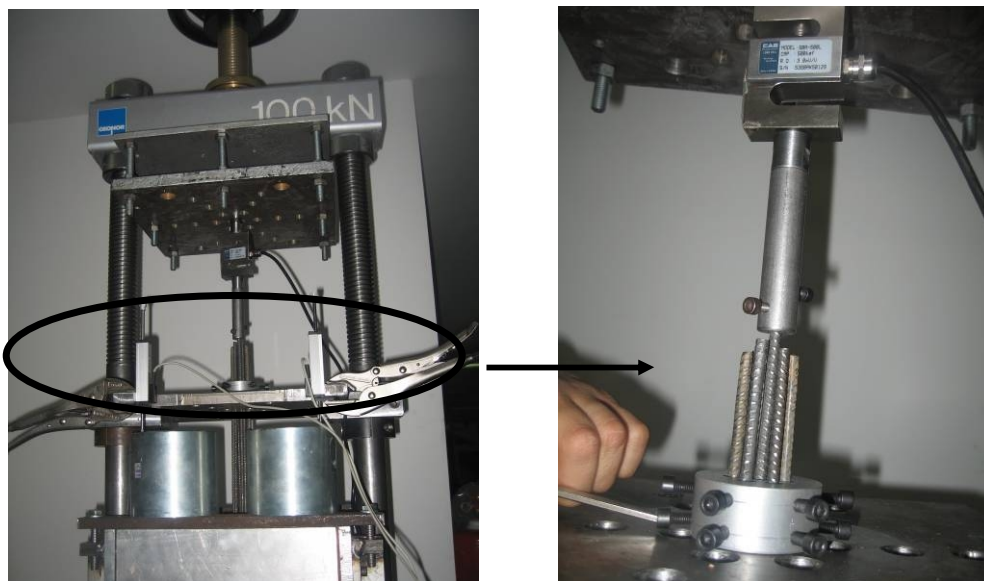


Figure 3.19 Connection details of 2Ø spaced soil nails



Figure 3.20 Connection details of 6Ø spaced soil nails

As stated before, two linear variable displacement transformers (LVDT's) and a load-cell are used to measure the displacement and the pull-out load during the tests. Placement of the measuring devices is shown in Figure 3.21. The LVDT's are located at the opposite corners of the upper surface of the model box and the load-cell is placed on the central nail for measuring the pull-out load during the tests.

When the testing machine is started, the load piston begins to displace the model box downwards with a constant rate of 0.6 mm/min. Since the nails are mounted at the fixed frame during the tests, they remain stationary, but they are pulled-out of soil during the test (Figure 3.22).

During each pull-out test, the data gathered by the measuring devices is transferred to the computer by a data logger. The data is recorded with a sampling rate of 500 ms and the variation of displacement with exerted load on nail is plotted. In addition, the ultimate pull-out load is determined at the end of each test.

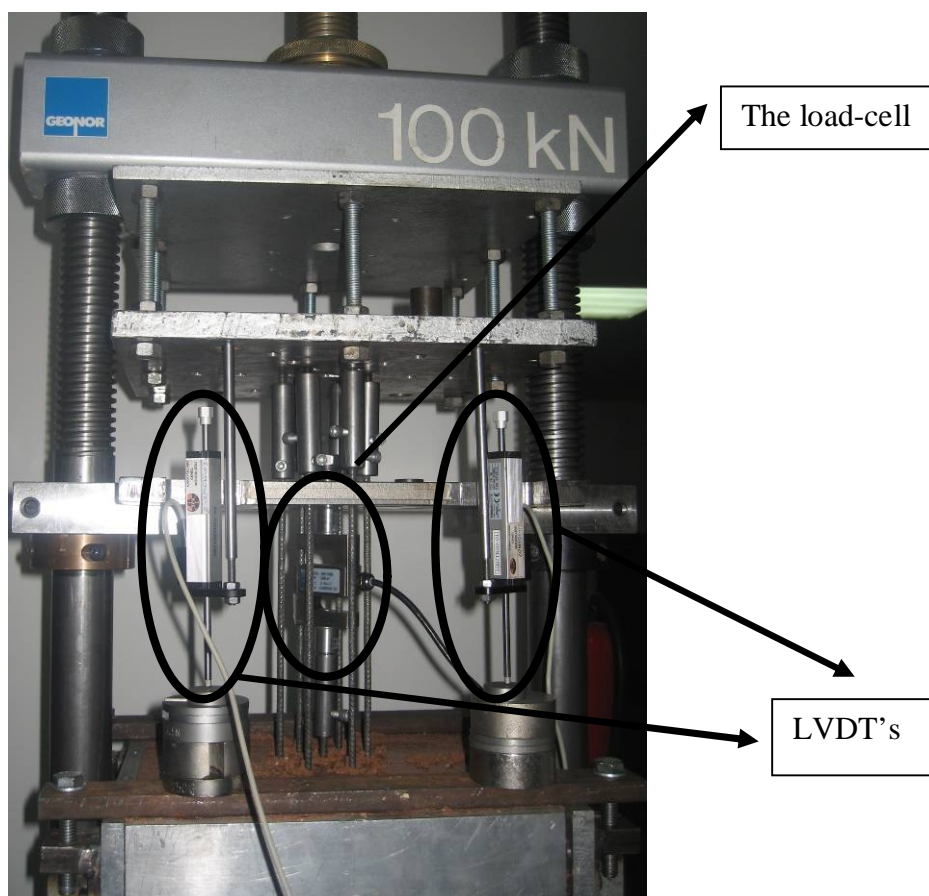


Figure 3.21 Measuring devices: LVDT's and the load-cell

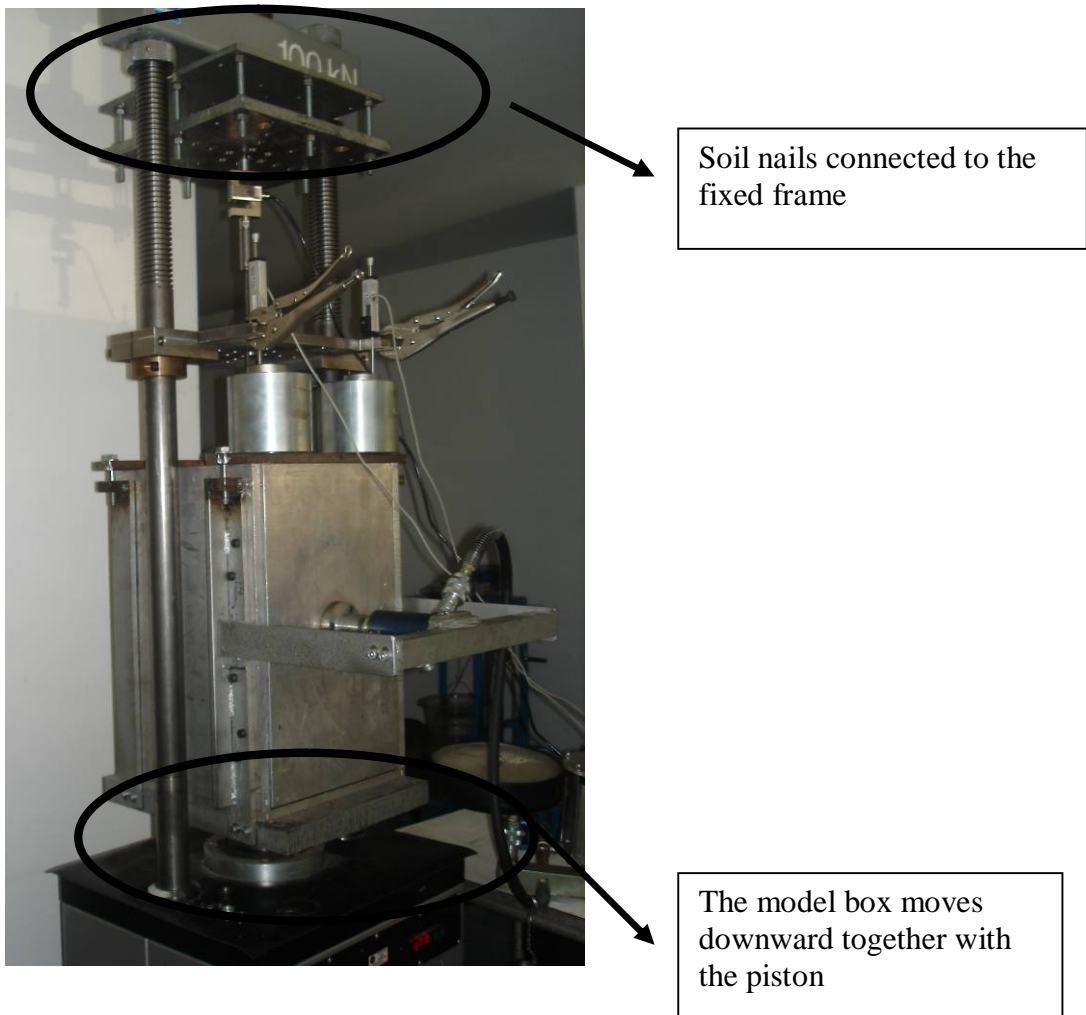


Figure 3.22 Details of the pull-out test

CHAPTER 4

RESULTS OF THE PULL-OUT TESTS

4.1 NAIL SPACING AND NAIL LAYOUT

Nail spacing and nail layout are the two important aspects in the design of soil nail walls. Nicholson (1986) stated that the nail spacing varying between 6 and 10 times the nail diameter is common in the United States, whereas a nail spacing as wide as 15 times the nail diameter is commonly used in Europe (Hong et al., 2003). On the other hand, Phear et al. (2005) recommended that, the nail spacing should not exceed one nail per 2-4 m² as the nailed ground may no longer behave as a coherent reinforced block. Hong Kong Special Administrative Region published a technical note about the design of steel nails for soil cuts (GEO, 2005). In this guidance note, it is mentioned that too wide nail spacing is not effective in preventing the local instability between the soil nail heads, and the nails too close to each other may not be cost-effective and may intersect during drilling. In addition, it is stated that the rows of the soil nails should be staggered to improve the stability of slope face through the enhanced development of soil arching and the usage of staggered horizontal nail rows are recommended.

In the first set of the tests, the pull-out capacity of a single nail is determined, and in the view of the results of the study performed by Nicholson (1986), the effect of group behavior on the pull-out capacity of the central nail is

investigated next. At the beginning of the tests with group nails, the group effect of 6Ø, 8Ø, 10Ø, and 12Ø spacing was considered. However, when the results were compared with the single nail tests, the tests performed for 6Ø nail-spacing showed no group effect on the pull-out capacity of a nail. Therefore, the spacings greater than 6Ø (8Ø, 10Ø and 12Ø) were not tested. In order to observe the group effect on soil-nails, practically for research purposes, a spacing of 2Ø is chosen, although at site no spacing less than 6Ø can be used. In 2Ø spacing nail pattern, the nails are located 12 mm (center to center) apart from each other. This configuration is preferred due to the difficulties involved in the application of laboratory tests with the spacing below 2Ø.

4.2 PULL-OUT TESTS

First two trials for the pull-out tests are performed in the Structural Mechanics Laboratory of Middle East Technical University with a local set-up. However, due to the problems pertaining to the collection of data, these test results could not be used. As mentioned previously, the test set-up is re-established in the Laboratory of the Technical Research Department of General Directorate of Highways. Ten tests are performed but the results of eight tests (three single nail, two 2Ø and three 6Ø spacing) are evaluated due to some technical problems encountered during two tests. For each test, approximately 82 kg of Ankara Clay with uniform properties is placed in the model box. In order to examine the soil properties and shear strength parameters in each test, the clay samples are retrieved from the model box to perform tri-axial tests (UU) after each pull-out test. The strength parameters obtained for each test are given in Table 4.1. The details of the work done for the determination of these parameters for each test are given in Appendix B. It is observed that the soil properties in all tests are quite

uniform. The strength parameters of the samples from the tests T6, T8 T9 and the samples from the tests T4, T5, T10 and T12 are particularly similar, considering the variability inherent in the sampling procedure and the moisture content of soil.

Table 4.1 Strength parameters of the soil samples used in pull-out tests

NAME	STATUS	STRENGTH PARAMETERS	
		c (kPa)	ϕ ($^{\circ}$)
T3	SINGLE	74	19
T6	SINGLE	117	11
T12	SINGLE	108	16
T9	2 \emptyset	121	11
T10	2 \emptyset	107	8
T4	6 \emptyset	101	18
T5	6 \emptyset	107	13
T8	6 \emptyset	121	17

In Table 4.2 the maximum measured pull-out loads obtained during the tests are given for different nailing patterns. For group nails, the maximum pull-out load is measured for the central nail. The group effect on the pull-out

capacity of a (central) nail with 2Ø nail-spacing is significant when compared to that for 6Ø nail-spacing.

Table 4.2 Maximum measured pull-out loads during the tests

TEST NAME	STATUS	MAX. MEASURED PULL-OUT LOAD DURING TESTS (kN)
T3	SINGLE	0.772
T6	SINGLE	0.737
T12	SINGLE	0.798
T9	2Ø	0.690
T10	2Ø	0.664
T4	6Ø	0.789
T5	6Ø	0.781
T8	6Ø	0.735

In Table 4.3, the maximum pull-out loads and the corresponding shear strength parameters obtained by tri-axial compression tests are tabulated. As seen in this table, the shear strength parameters differ insignificantly from each other except the test T3. The result of the measured pull-out capacity of a single-nail in test T3 is very close to the capacities measured in other single-nail tests (T6 and T12), although the shear strength parameters of sample gathered from test T3 is significantly different from those of other tests. This can be possibly be attributed to the local differences in the characteristics and/or moisture content of the clay as well as the sampling and variations involved in sampling and testing processes.

In addition, the pull-out responses (i.e., displacement versus pull-out load) of single nails and central nails of the groups recorded during the tests are given in Figures 4.1 to 4.8. In Figures 4.9 to 4.11 the pull-out responses of nails during the tests for single nails, for the central nail of the groups with $2\emptyset$ spacing, and for the central nail of the groups with $6\emptyset$ spacing are compared, respectively. Finally, in Figure 4.12 pull-out responses obtained in all tests are plotted together for the purpose of comparison.

Table 4.3 Measured pull-out loads and the corresponding strength parameters measured for each test.

NAME	STATUS	MEASURED PULL-OUT LOAD (kN)	STRENGTH PARAMETERS	
			c (kPa)	ϕ ($^{\circ}$)
T3	SINGLE	0.772	74	19
T6	SINGLE	0.737	117	11
T8	6 \emptyset	0.735	121	17
T9	2 \emptyset	0.690	121	11
T12	SINGLE	0.798	108	16
T4	6 \emptyset	0.789	101	18
T5	6 \emptyset	0.781	107	13
T10	2 \emptyset	0.664	107	8

Test 3 (Single Nail)

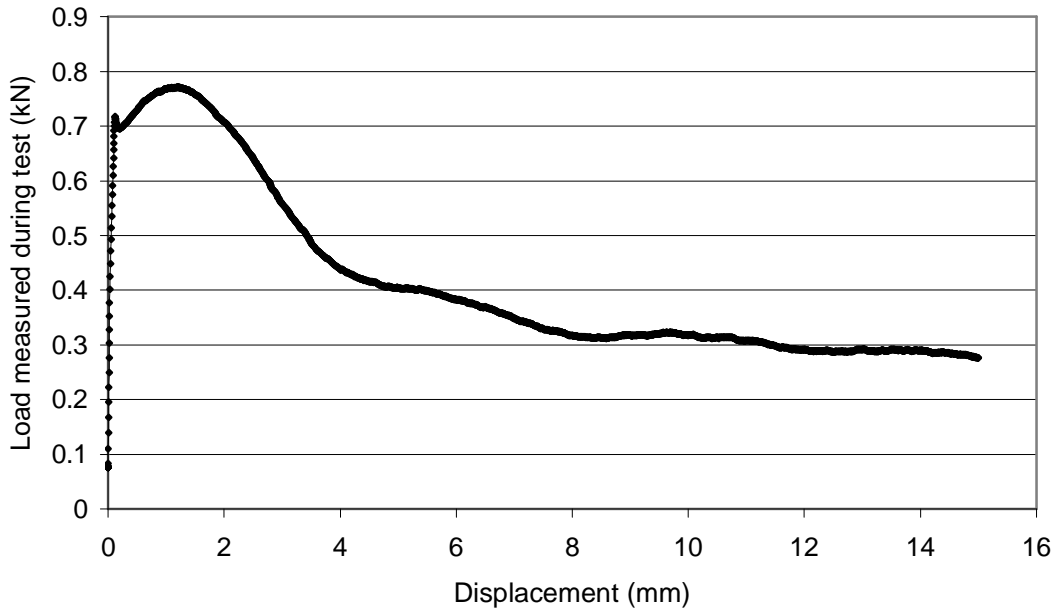


Figure 4.1 Pull-out response of the single nail in test T3.

Test 6 (Single Nail)

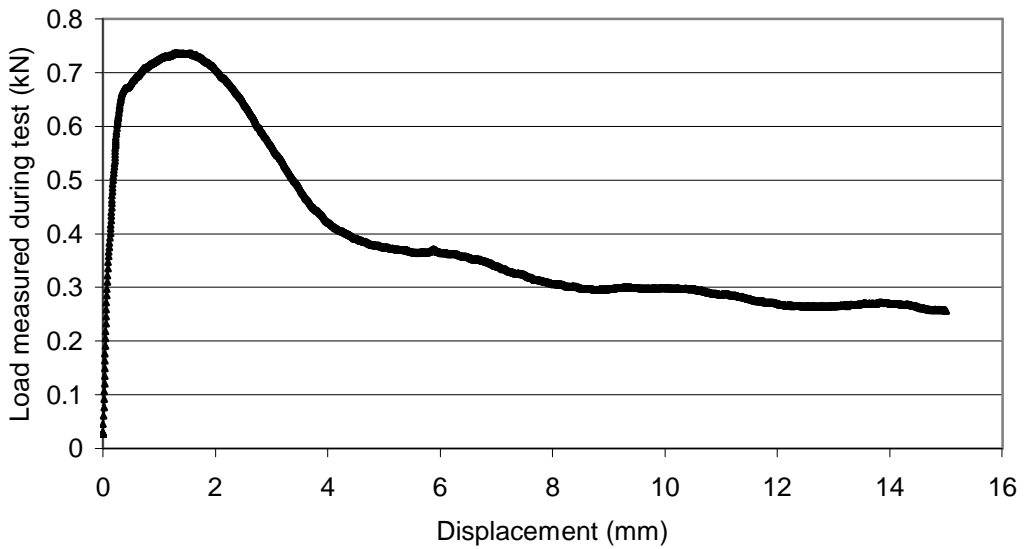


Figure 4.2 Pull-out response of the single nail in test T6

Test 12 (Single Nail)

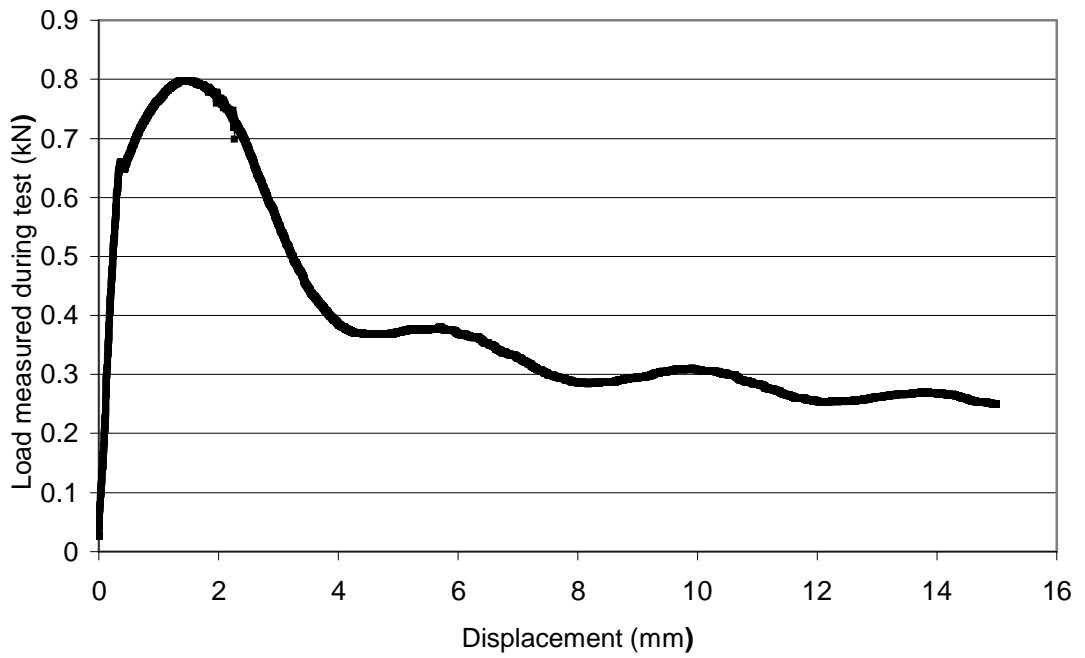


Figure 4.3 Pull-out response of the single nail in test T12

Test 9 (Group 2Ø)

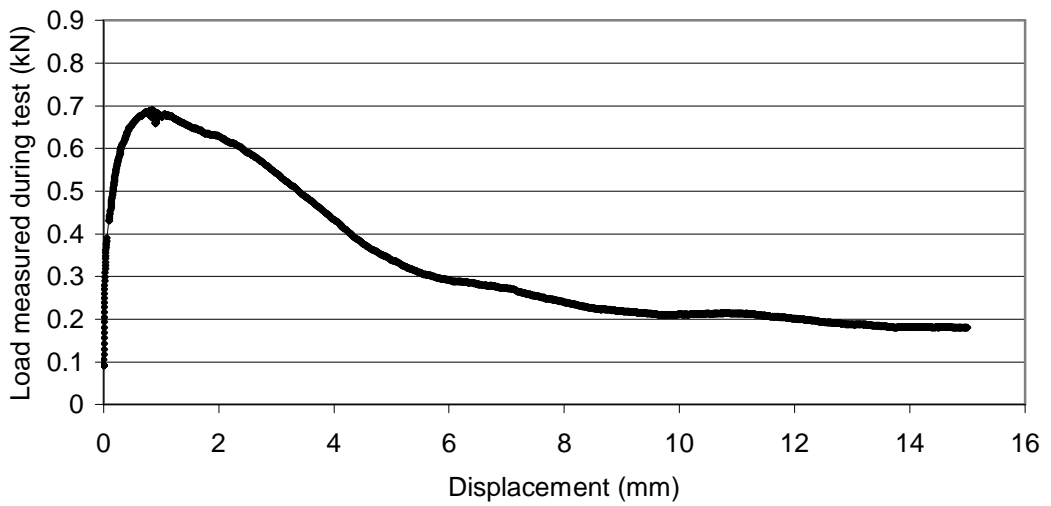


Figure 4.4 Pull-out response of the central nail in test T9

Test 10 (Group 2Ø)

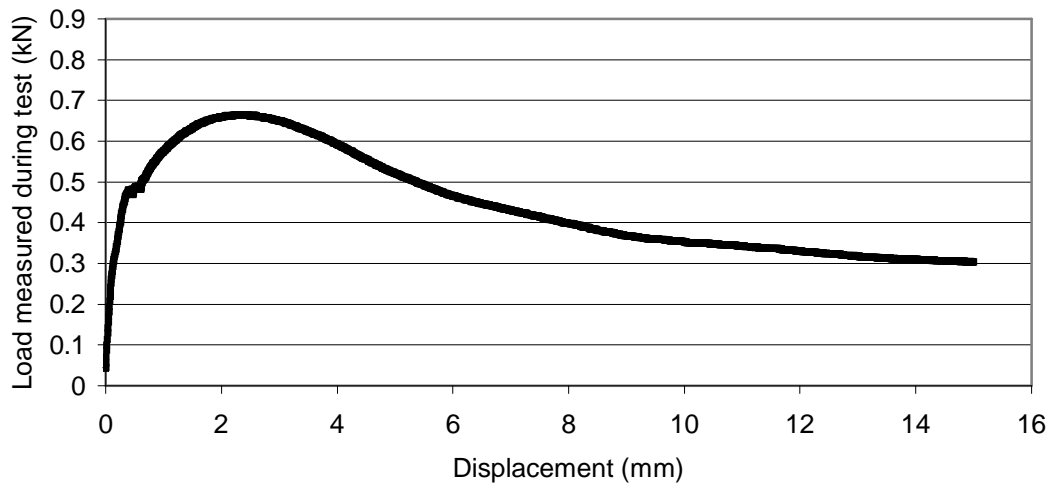


Figure 4.5 Pull-out response of the central nail in test T10

Test 4 (Group 6Ø)

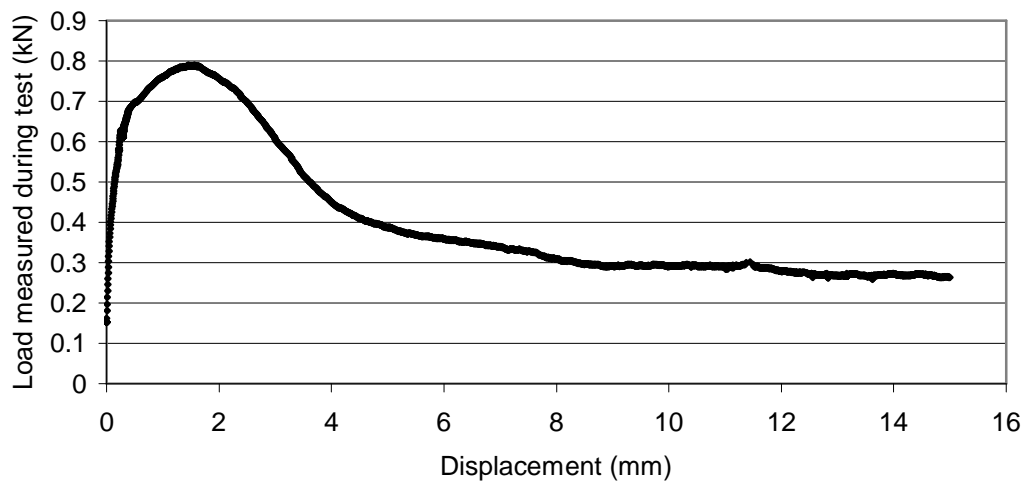


Figure 4.6 Pull-out response of the central nail in test T4

Test 5 (Group 6Ø)

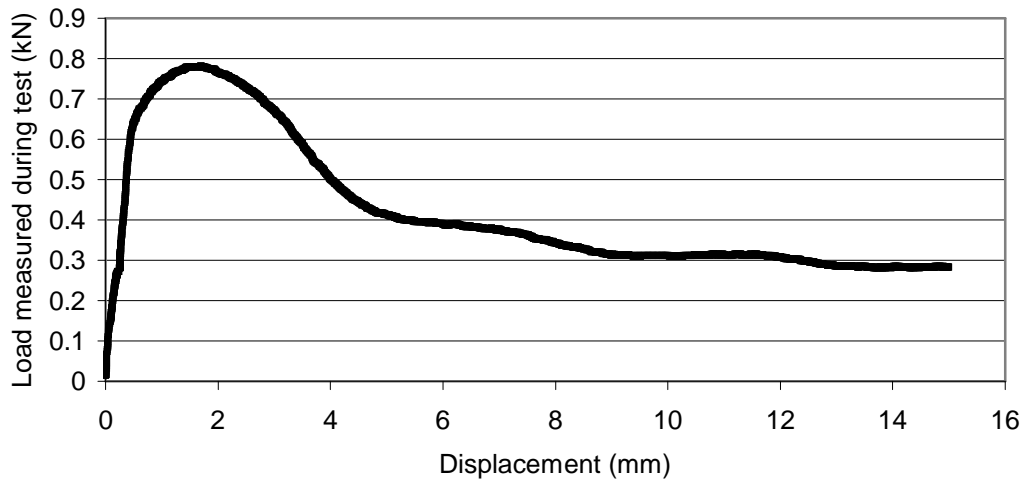


Figure 4.7 Pull-out response of the central nail in test T5

Test 8 (Group 6Ø)

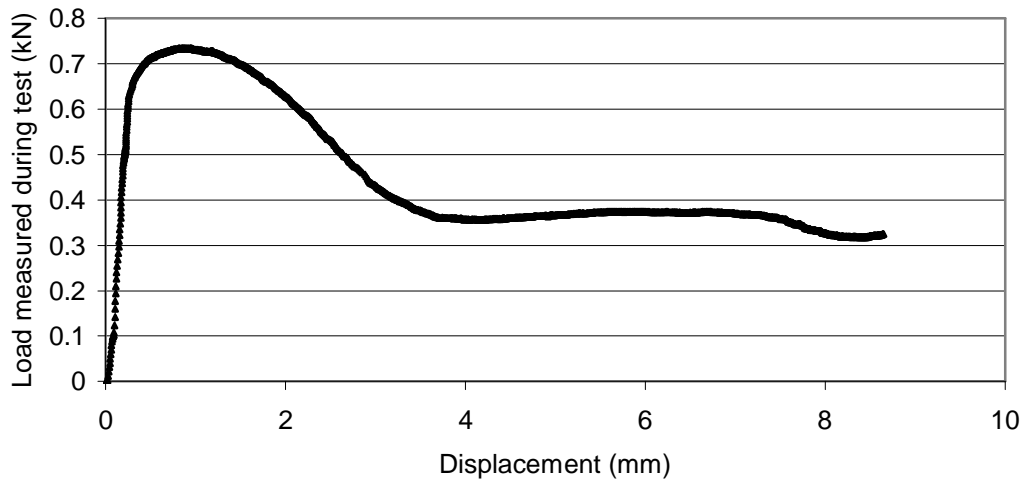


Figure 4.8 Pull-out response of the central nail in test T8.

Single Pull-Out Tests

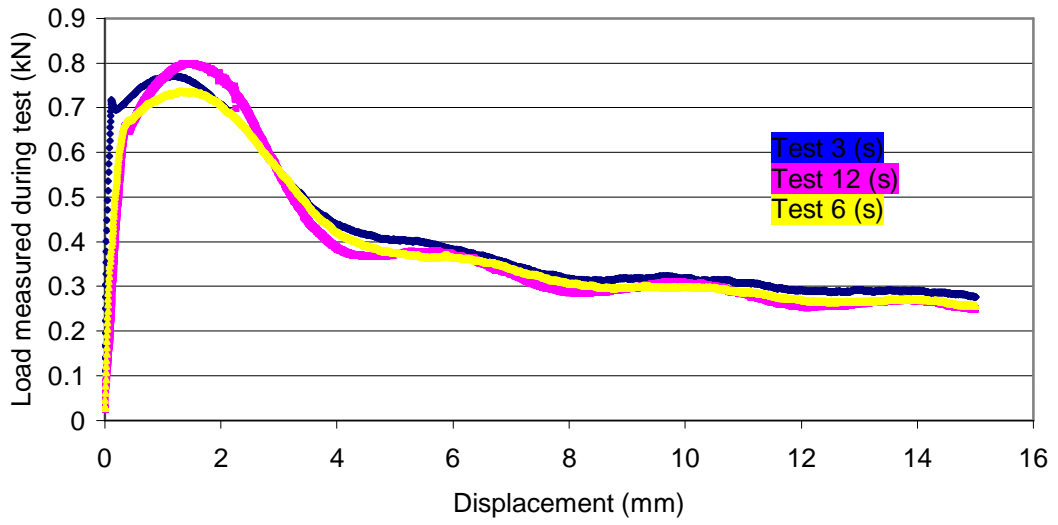


Figure 4.9 Pull-out responses of single nails.

Group 2Ø Pull-out Tests

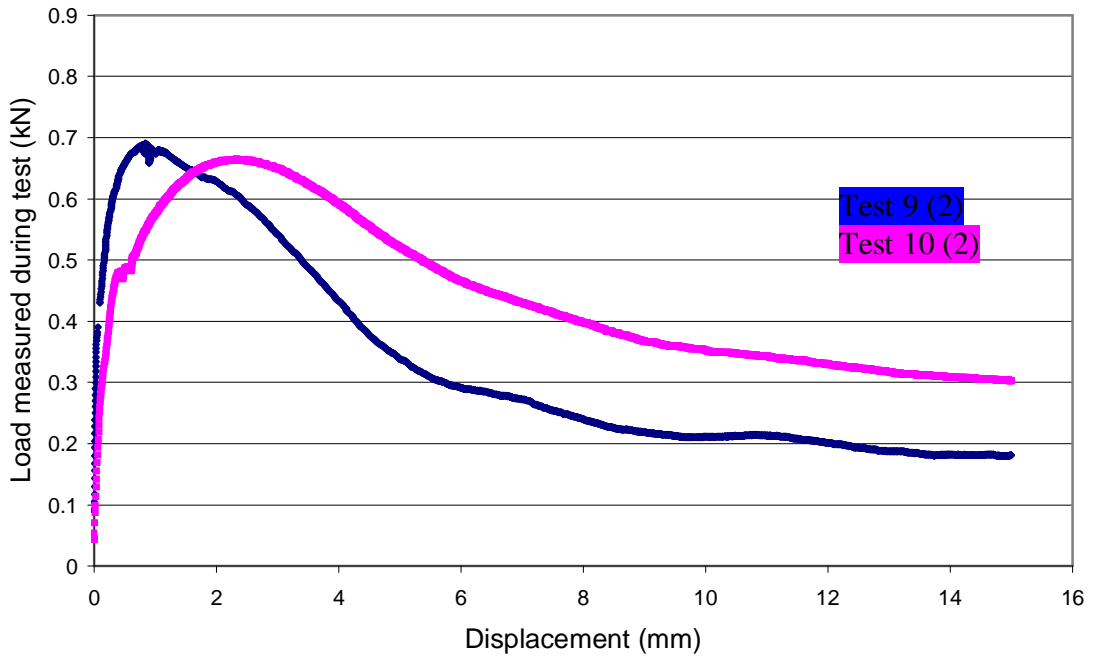


Figure 4.10 Pull-out responses of nails in groups with 2Ø spacing.

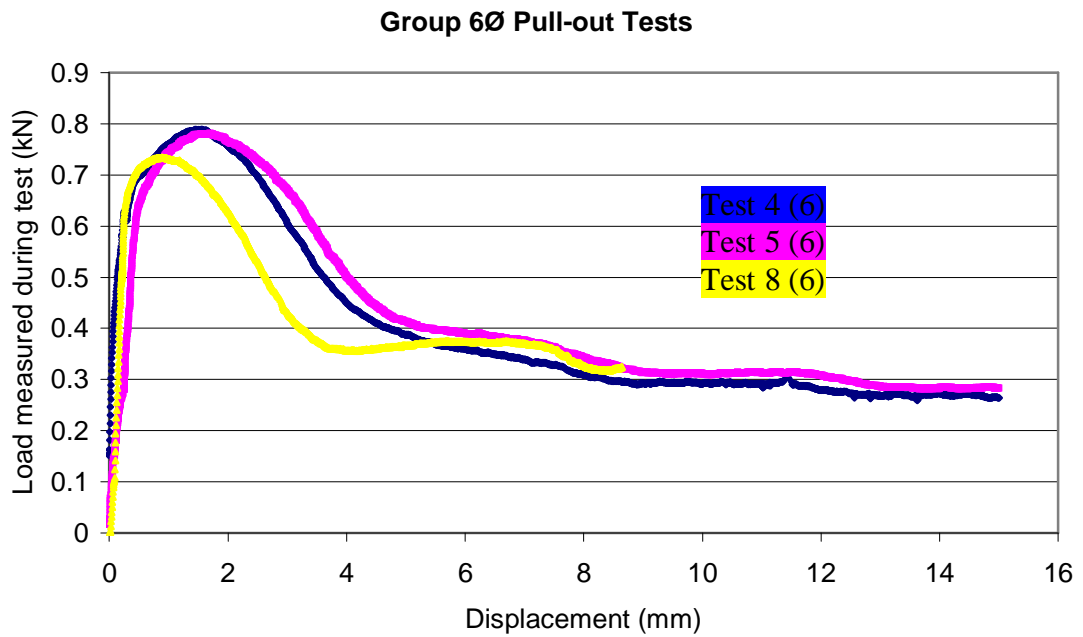


Figure 4.11 Pull-out responses of nails in groups with 6Ø spacing

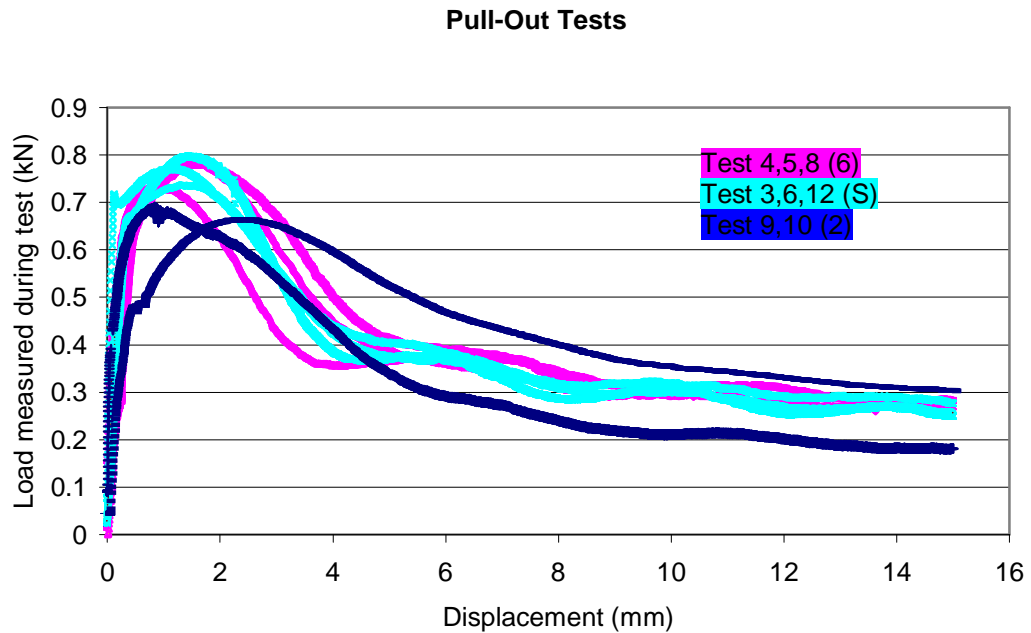


Figure 4.12 Comparison of the results of the pull-out tests with single nails, 2Ø and 6Ø nail spacing.

Finally, in Figure 4.13, the pull-out capacities of the single nails and the central nails of the groups with different nail spacings are compared. It is observed that the nail groups with $2\varnothing$ spacing show reductions in pull-out capacity due to the group effect, whereas tests with $6\varnothing$ spacing do not reflect any significant group effect.

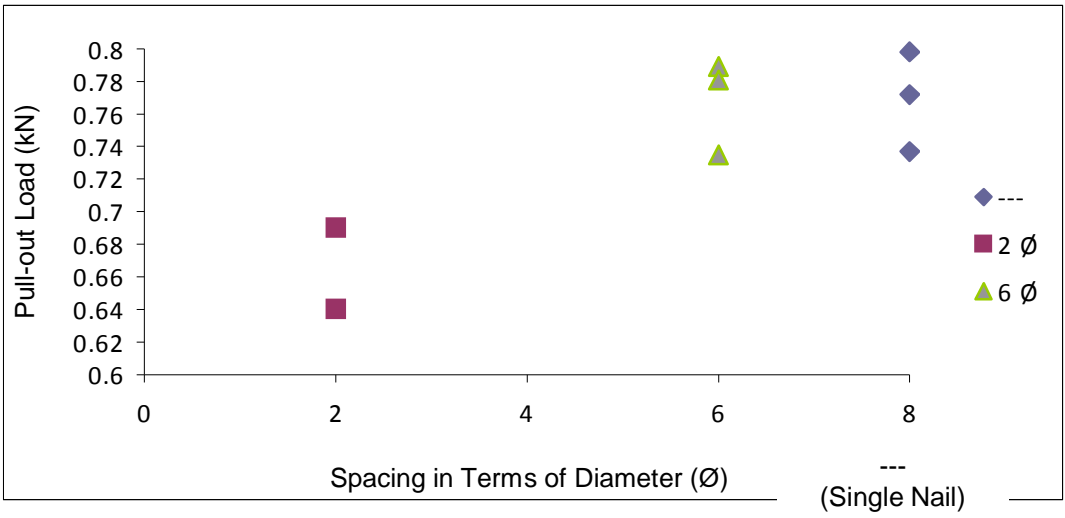


Figure 4.13 Maximum pull-out capacity of the nails tested

CHAPTER 5

NUMERICAL ANALYSES

5.1 INTRODUCTION

A three dimensional finite element based program, PLAXIS 3D FOUNDATION - Version 2 (Brinkgreve et al., 2007) that is developed by Delft University of Technology, is used to simulate the pull-out tests. This software is especially developed for the analysis of deep and shallow foundations using finite element method.

A pile embedded in soil can be modeled using PLAXIS 3D FOUNDATION by employing several slender beam elements coupled with 3D solid (continuum) elements. Skin and foot interfaces of the pile are defined in order to provide a realistic interaction between the pile and the soil elements. The embedded pile is able to cross through the bulk soil elements at any position which provides ease in the modeling of pile groups. In this study, this technique is used in modeling single and group nails. In the following parts, the details of the numerical models used for the analyses and the results obtained are presented.

5.2 MODELLING THE PULL-OUT TEST

In order to model the pull-out tests, the material boundaries and the boundary conditions are defined first. Next, prior to generating the finite element mesh, the soil and material properties and the pull-out load are specified. Finally, the numerical analyses are performed and the pull-out capacity of the single nails and the central nails of the models are computed. These phases are explained in the following.

5.2.1 DIMENSIONS OF THE MODEL

The dimensions of the numerical model are chosen as 30 cm x 30 cm x 50 cm, which is the same as the dimensions of the model box. The diameters of the soil nails are taken as 6 mm and the length of them are taken as 360 mm. In the analyses, the central nail is located at the midpoint of the box surface. The other nails are located in a scatter design, as it is applied in situ. In addition, the nail spacing is varied between 2 to 8 times the diameters of the soil nail in order to investigate the effect of group behavior on the pull-out capacity of the nails. These details are implemented in the numerical models.

5.2.2 BOUNDARY CONDITIONS

Actual dimensions of the test model are used in the numerical model. The vertical boundaries of the model (30 x 50 cm in dimensions), excluding one face on which the overburden pressure is applied by a hydraulic pump, are fixed in normal direction and set free in two orthogonal directions. The top plate (30 x 30 cm) is set free as it is in the pull-out test set-up. Finally, the

bottom boundary of the model is fixed in all directions. Boundary conditions of the model is given in Figure 5.1. The load corresponding to the overburden pressure is applied on one of the vertical boundaries (30 x 50 cm).

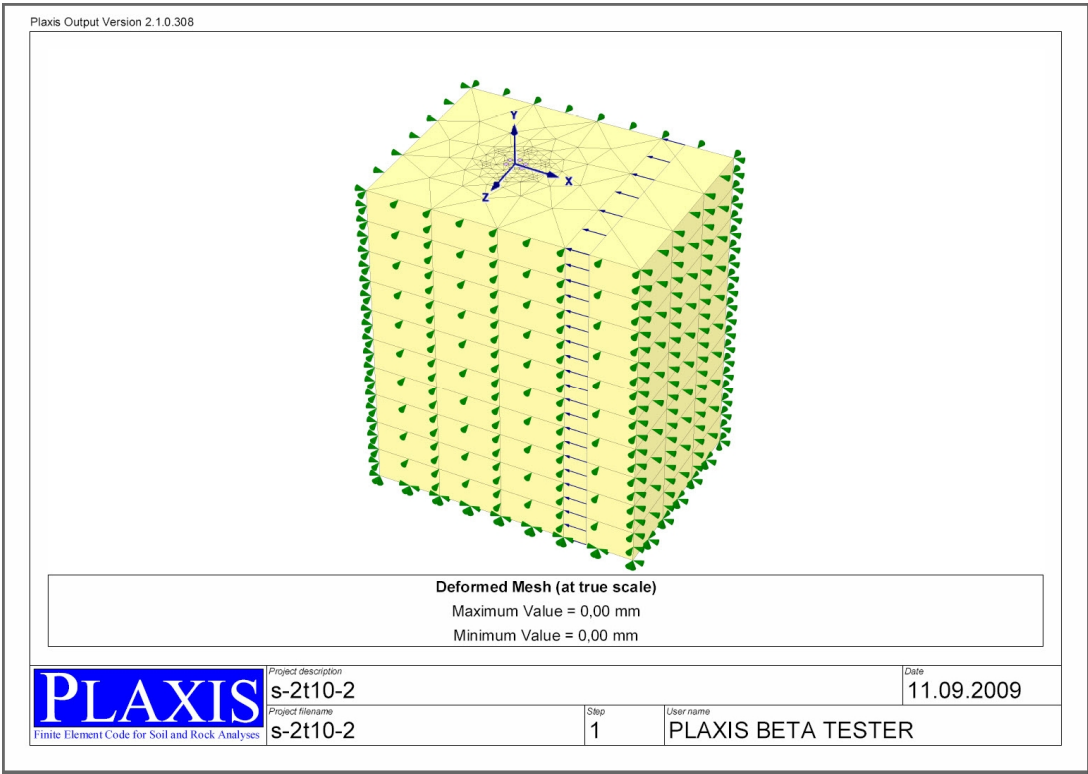


Figure 5.1 Boundary conditions of the model

5.2.3 SOIL PARAMETERS

In order to model the soil behavior, Mohr Coulomb model is used in the analyses. The parameters of the model, such as Young’s Modulus (E),

Poissons ratio (μ), cohesion (c), friction angle (ϕ), and dilatancy (ψ) used in the model can be determined from suitable laboratory tests.

Hence, Young's Modulus (E), cohesion (c), and friction angle (ϕ) are estimated from the results of the tri-axial compression (UU) tests. The p-q diagrams obtained from the test results are plotted and given in Appendix B. The intercept (a) and inclination angle (α) are determined employing the p-q diagrams (Figure 5.2).

The corresponding parameters of Mohr-Coulomb failure criterion are calculated by the following equations:

$$\phi = \sin^{-1} (\tan \alpha) \tag{5.1}$$

$$c = a / \cos (\phi) \tag{5.2}$$

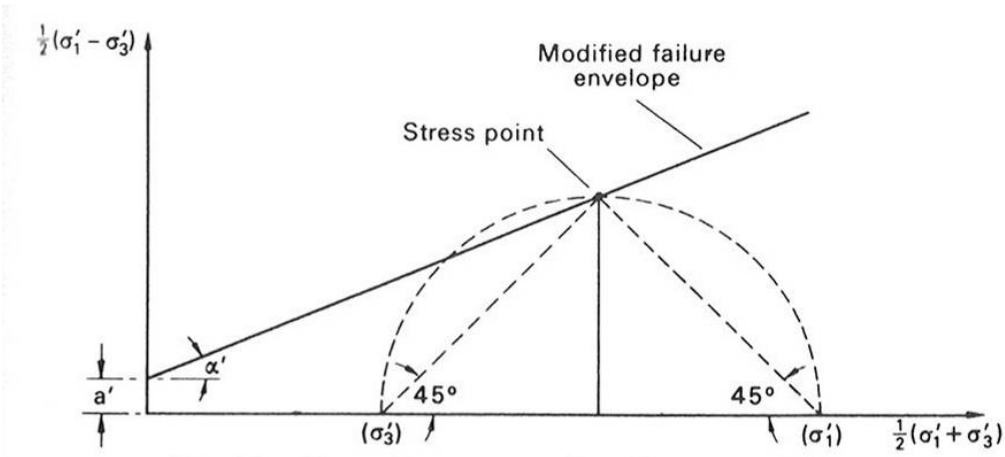


Figure 5.2 The general presentation of the p-q diagrams (Craig, 1986)

The secant moduli corresponding to the half of the peak deviator stress in are calculated using stress strain curves obtained in tri-axial tests (Lambe et al., 1979), and Poissons ratio (μ) is calculated from the following relation (Brinkgreve et al., 2007):

$$K_o = \mu / (1 - \mu) \quad (5.3)$$

Whereas, the coefficient of the earth pressure (K_o) is determined from the following expression (Jaky, 1944)

$$K_o = 1 - \sin \phi \quad (5.4)$$

The soil parameters employed in the numerical analyses are given in Table 5.1. The dilatancy (ψ) of the soil is taken as zero.

Table 5.1 The soil parameters employed in numerical analyses

NAME	γ (kN/m ³)	E (kPa)	μ	STRENGTH PARAMETERS	
				c (kPa)	ϕ (^o)
T3	18.14	25000	0.403	74	19
T6	18,14	25000	0.447	117	11
T8	18.42	35000	0.414	121	17
T9	18.46	30000	0.432	121	11
T12	18.40	45000	0.420	108	16
T4	18.30	32500	0.409	101	18
T5	18.52	21000	0.437	107	13
T10	18.27	30000	0.463	107	8

The soil parameters are entered in the program via “General” tab of the material data set window. Since the soil samples used in the experiments are prepared at their optimum water content with maximum dry density, the model soil is presumed to be unsaturated. Therefore, the drained option on Material Type menu is used. The soil parameters such as Young’s Modulus (E), Poissons ratio (μ), cohesion (c), friction angle (ϕ), and dilatancy (ψ) are

entered to the program in “Parameters” tab of material data set window. The input and output data of the numerical analyses are presented in Appendix C.

5.2.4 MODELLING OF SOIL NAILS

In the study by Engin et al. (2007), the pile compression and tension tests performed in Frankfurt and Kuwait were used to validate the accuracy of a single pile model, which was built by the embedded pile option of PLAXIS 3D FOUNDATION. The results showed that the numerical results and site tests are in reasonable agreement for both test types. Hence, the embedded pile option of the software is used to model the soil nails. In the embedded pile option, the soil-pile interaction is modeled by means of special interface elements.

When the embedded pile option of the program is used, the installation effects on the piles are not taken into consideration. Due to this reason, the piles that cause limited disturbance to the surrounding soil could be modeled. In the pull-out tests, the soil nails are located inside the model box during the compaction of the soil, so that the soil in the vicinity of nails is presumably undisturbed during the installation of nails.

In the program, a data set for modeling a pile is composed of material properties of surrounding soil and pile, geometric properties, and the soil-pile interaction. In the analyses, an elastic – plastic model is used to describe the behavior of the interface elements which is determined by considering equivalent local skin resistance. The skin resistance is defined as the force in kN per unit pile length. In the analyses, the layer dependent skin resistance with an overall maximum value is used for modeling the pull-out

tests. The skin resistance value is calculated from the correlation suggested by Cartier et al. (1983) and the obtained value is given as a cut-off value. The equivalent local skin resistance, T_{max} , used in the analyses is given in Table 5.2.

Table 5.2 Skin resistance data used in the analyses

NAME OF THE TEST	STATUS	T_{max} (kN/m) $T = Pc' + 2D\sigma_v' \tan \phi'$
T3	SINGLE	1.807
T6	SINGLE	2.438
T8	6Ø	2.647
T9	2Ø	2.513
T12	SINGLE	2.379
T4	6Ø	2.293
T5	6Ø	2.293
T10	2Ø	2.185

The axial load is applied at the nail head to simulate the pull-out response of the soil nails. In addition, a distributed stress of 100 kPa is given horizontally

on one side of the rectangular prism in order to simulate the overburden pressure on the physical model.

5.2.5 FINITE ELEMENT MESH

The finite element mesh generation is quite important in finite element analyses in the sense that both precision and economy requirements should be reasonably satisfied. On the other hand, the element type and the number of elements used in the analyses directly effect the calculation time. In the 3-D finite element mesh, the soil elements used in the models are 15-node wedge elements shown in Figure 5.3 (Brinkgreve et al., 2007).

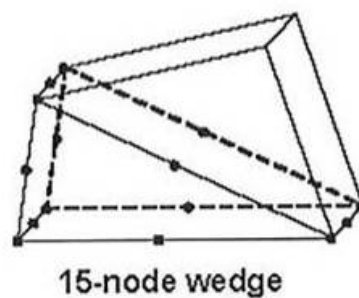


Figure 5.3 Finite element used for soil modelling.

A series of analyses are performed in order to determine the mesh size. Coarse, medium and fine mesh generation options of the program are used with 15-noded wedge elements in order to obtain three different meshes for analyses. The views and the detailed information about each option are given in Figures 5.4 to 5.6. The number of elements and nodes for each mesh is stated in Table 5.3.

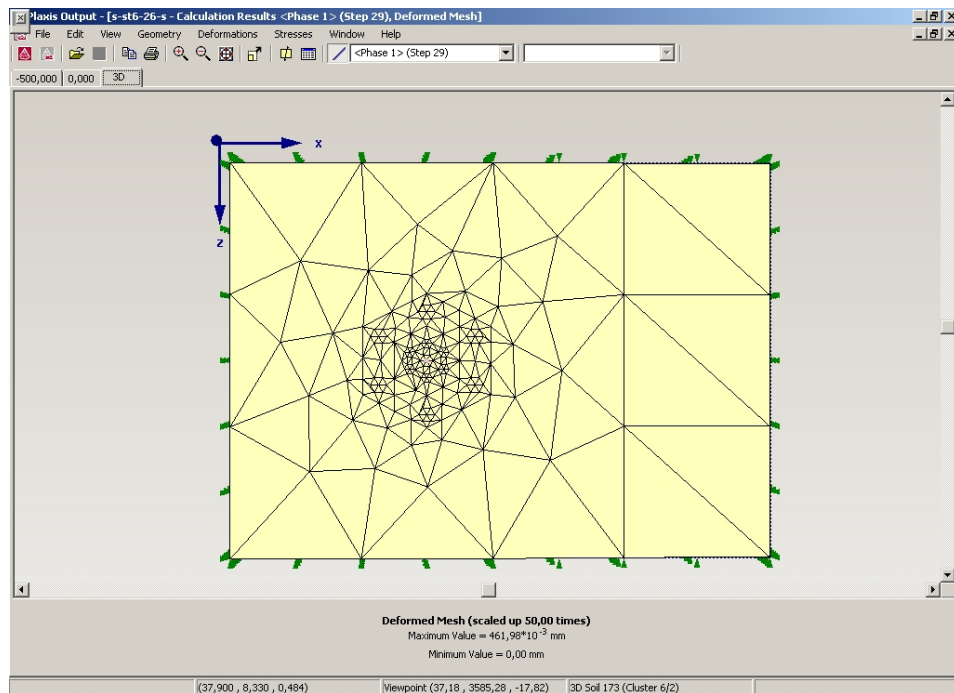


Figure 5.4 Top view of the coarse mesh

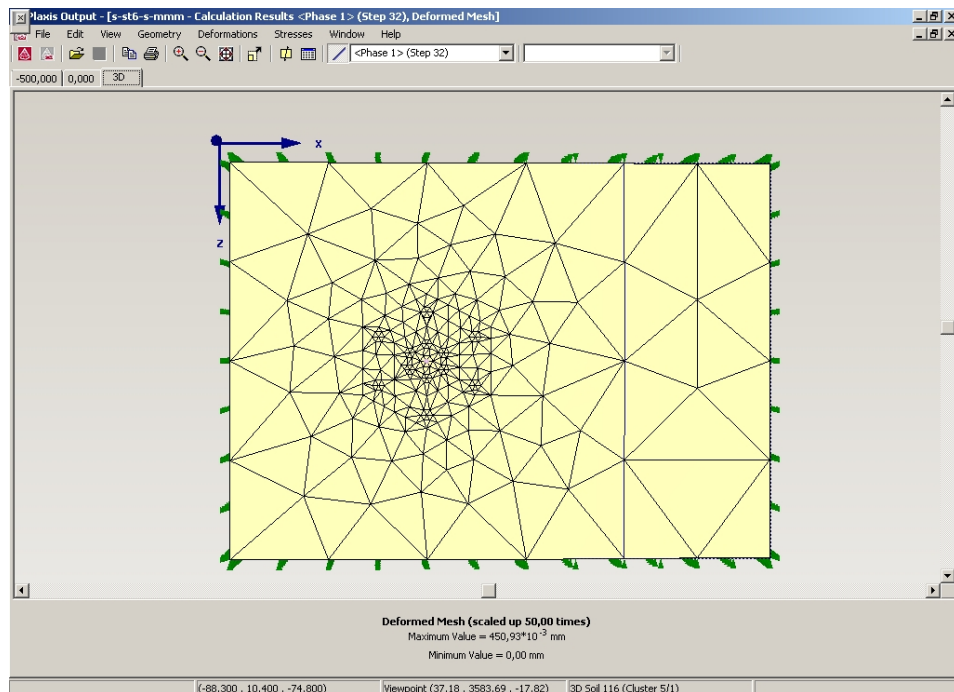


Figure 5.5 Top view of the medium mesh

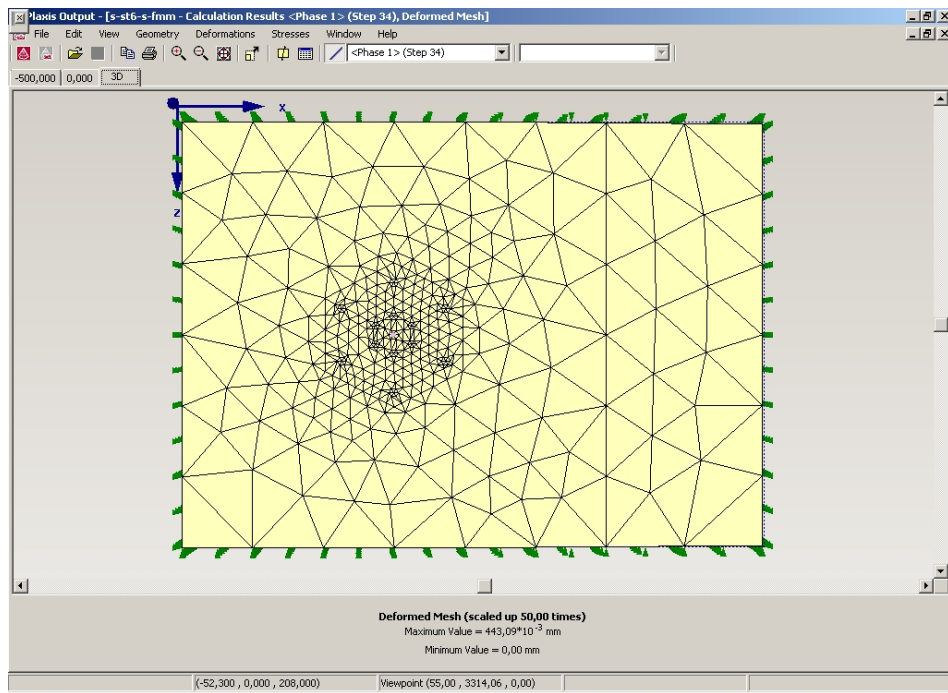


Figure 5.6 Top view of the fine mesh

After generating the three meshes with different sizes, a single soil nail pull-out test is simulated with each mesh. The results of these analyses, given in Table 5.3, show that there is no significant difference in the pull-out capacities computed with different mesh-sizes. Therefore, the coarse mesh is employed in the rest of the numerical analyses.

Table 5.3 Pull-out loads calculated by PLAXIS 3D FOUNDATION with different mesh densities

Mesh Type	Pull-out Capacity (kN)	Number of Elements	Number of Nodes
Coarse	0.811	3340	9484
Medium	0.814	6912	19002
Fine	0.809	11712	31802

5.2.6 CALCULATION STAGES

Several sequential calculation phases that correspond to a construction or loading stage can be described in the program. Since the program allows staged analyses of the models, two stages to simulate the pull-out tests are considered. In the first stage, the 3-D box is modeled only with an embedded pile in the soil together with the overburden pressure. In this phase, K_0 procedure that considers only the soil weight is selected. As a result of this procedure, the initial stresses are set up in such a way that the vertical stresses are generated in equilibrium with the self weight of the soil, however horizontal stresses are calculated from the specified value of K_0 . In the second stage, in addition to the first stage, a 1 kN pull-out force is applied to the embedded pile. At this phase, plastic calculation is defined since an elastic-plastic deformation analysis is performed. The same procedure for defining the calculation stages is used for group piles.

5.3 RESULTS OF THE NUMERICAL ANALYSES

Using the parameters given in Tables 5.1 and 5.2, the numerical analyses are performed. The computed deformed shapes of the mesh and pull-out loads on nails are given in Figures 5.7 through 5.16. In the figures for the deformed shapes, the area of influence of the nail can be easily observed. In the 2Ø spaced nails the influence area surrounding the nails intersects each other. On the other hand, the influence area of 6Ø spaced nails does not intersect each other and seems like of a single nail. These deformed shapes are in good agreement with the performed tests since both of them confirm that group effect is significant only for 2Ø spacing nails. Finally, the comparison of the pull-out capacities obtained by the numerical analyses with the test results is given in Table 5.4.

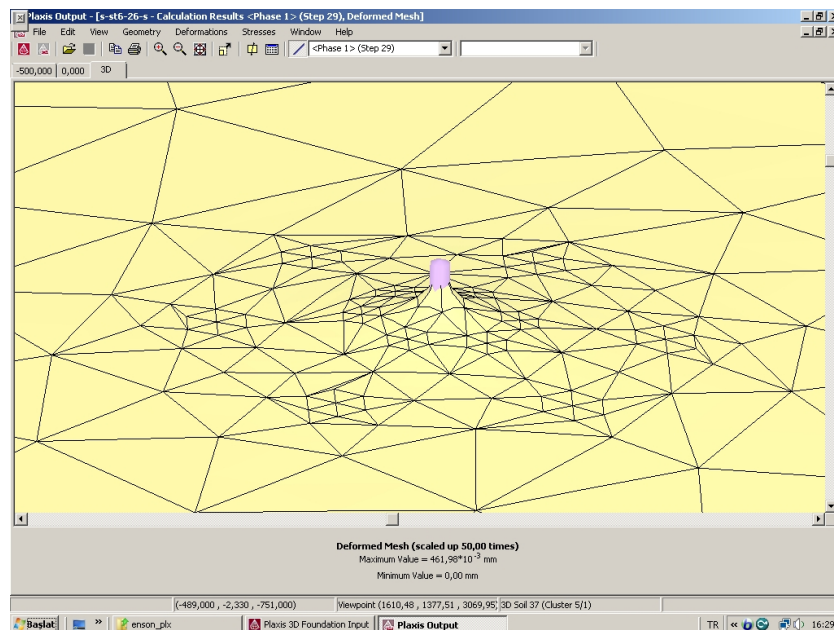


Figure 5.7 Deformed mesh of Test 6 (Single Nail)

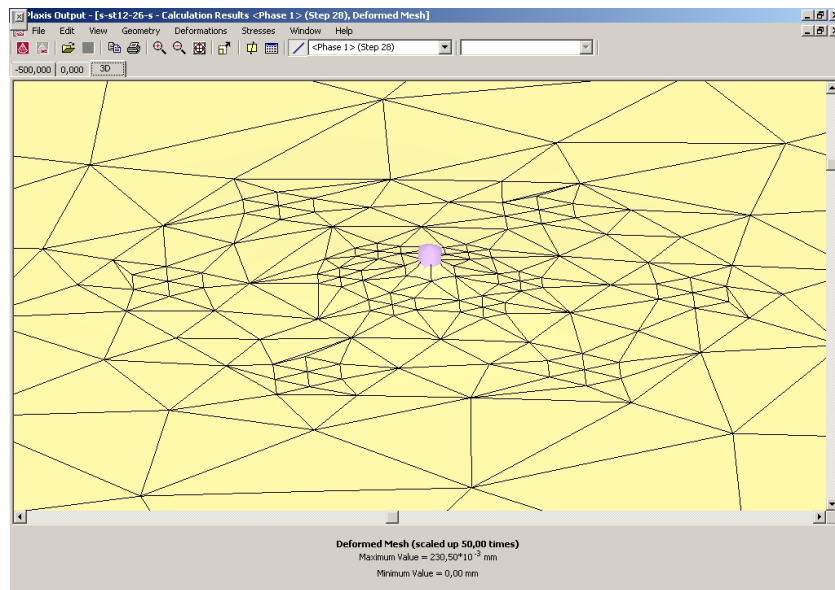


Figure 5.8 Deformed mesh of Test 12 (Single Nail)

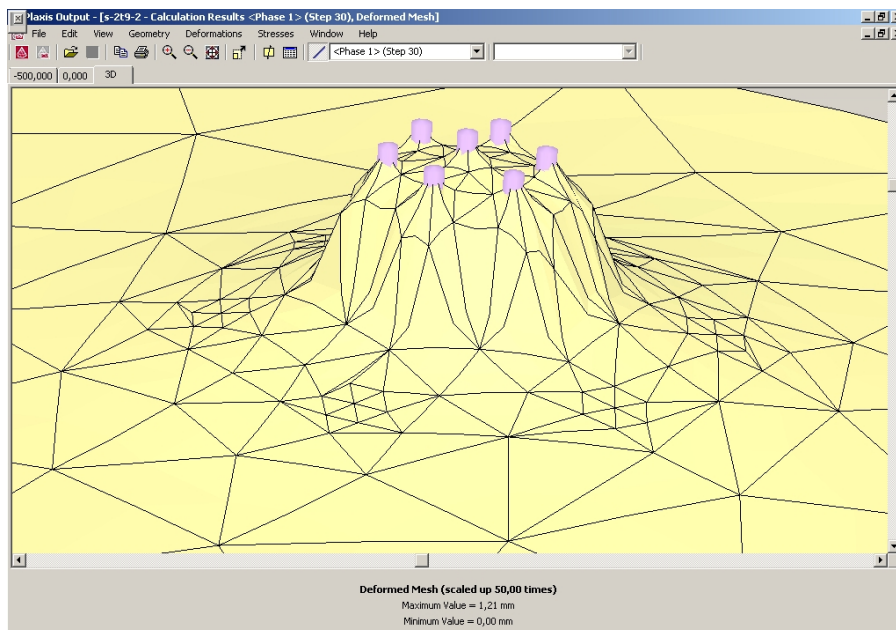


Figure 5.9 Deformed mesh of Test 9 (2Ø spaced group)

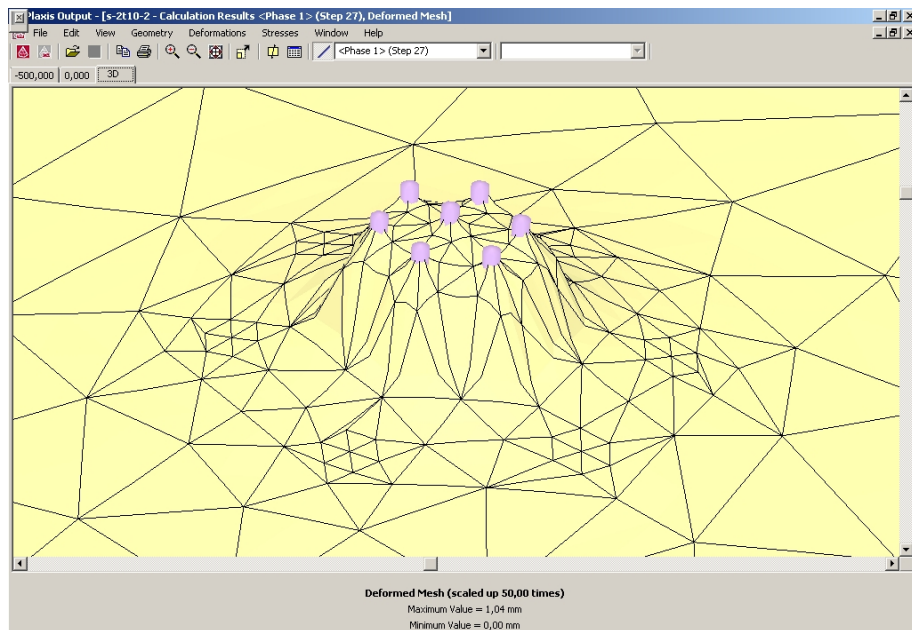


Figure 5.10 Deformed mesh of Test 10 (2Ø spaced group)

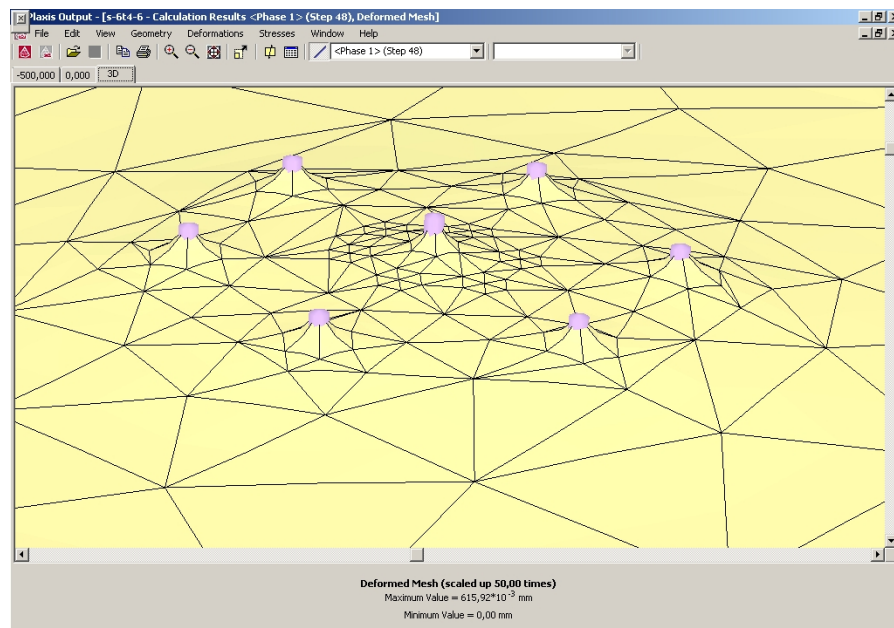


Figure 5.11 Deformed mesh of Test 4 (6Ø spaced group)

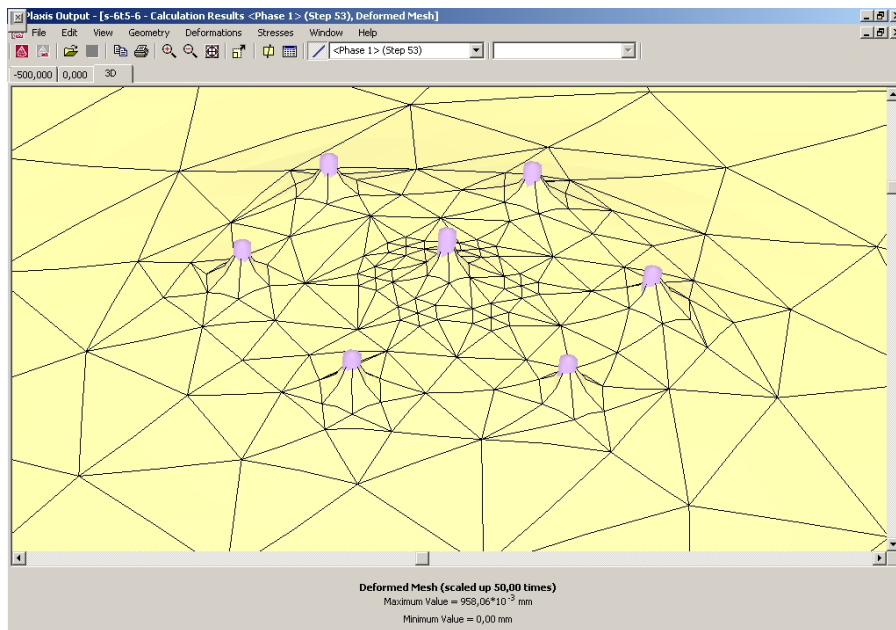


Figure 5.12 Deformed mesh of Test 5 (6Ø spaced group)

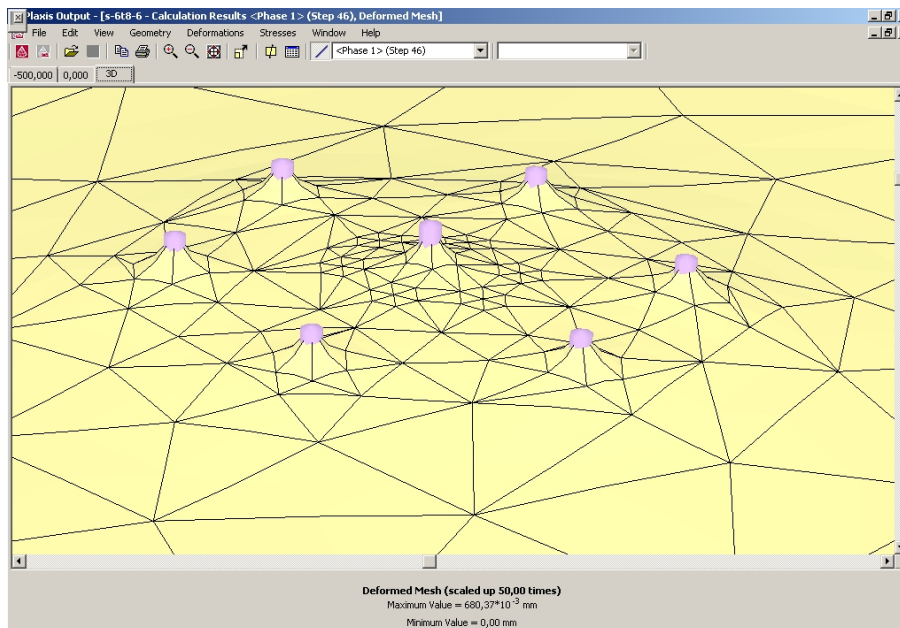


Figure 5.13 Deformed mesh of Test 8 (6Ø spaced group)

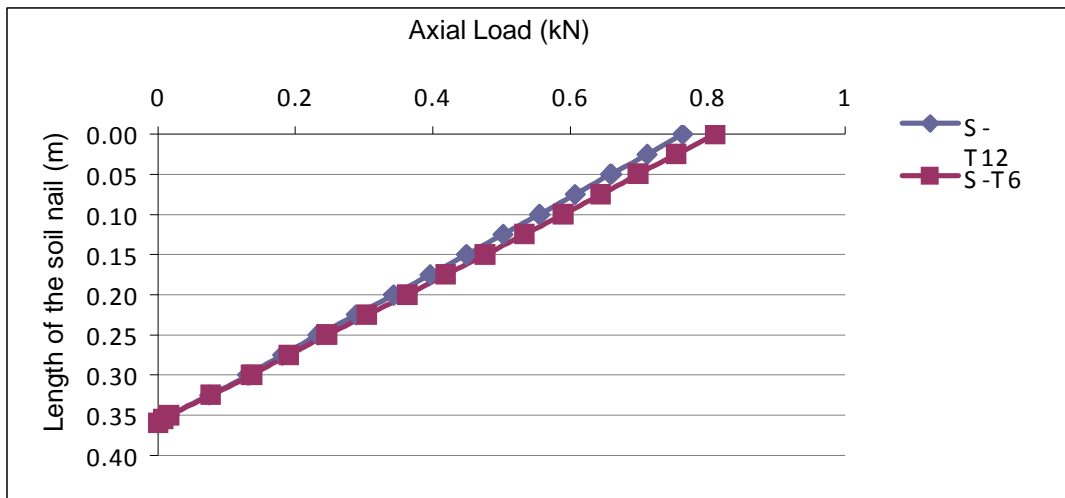


Figure 5.14 Axial force on the single nail tests (T12 and T6)

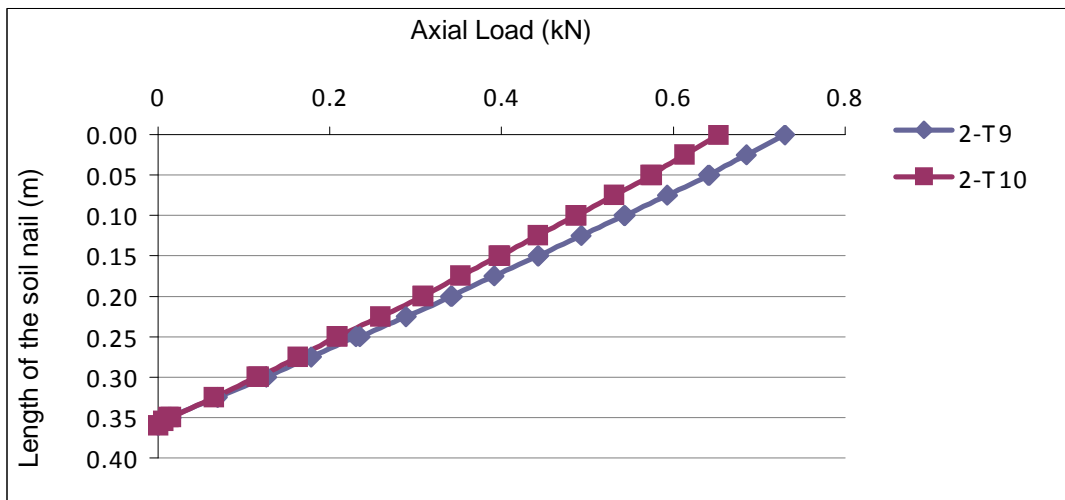


Figure 5.15 Axial force on the central nail in 2 Ø spaced nail groups (T9 and T10)

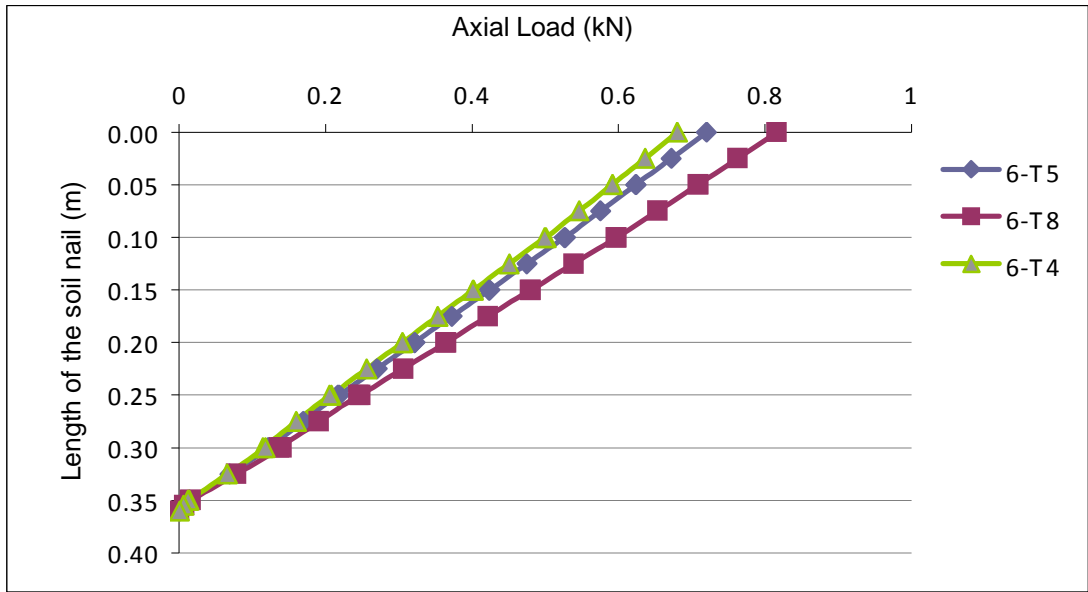


Figure 5.16 Axial force on the central nail in 6Ø spaced nail groups (T4, T5 and T8)

As seen in Table 5.4, there is a variation of 1% to 13% between the measured and calculated values of pull-out loads, except for test T3. It is concluded that, the results of numerical simulation are in good agreement with those of the pull-out tests. If the comparison of variation between the measured and calculated values is made, in literature, 9% to 13% difference between the measured and calculated pull-out loads was reported by Su (2006) in a study on the compacted completely decomposed granite fill. The difference of 31.5% in test 3 can be attributed to the possible errors involved in the measurement of strength parameters.

Table 5.4 Comparison of the maximum pull-out loads measured during tests and calculated from numerical analyses

NAME	STATUS	c (kPa)	\emptyset ($^{\circ}$)	MAX. MEASURED PULL-OUT LOAD DURING TEST (kN)	CALCULATED MAX. AXIAL FORCE FROM PLAXIS 3D (kN)	DIFFERENCE (%)
T3	SINGLE	74	19	0.772	0.528	31,6%
T6	SINGLE	117	11	0.737	0.811	-10.0%
T12	SINGLE	108	16	0.798	0.764	4,3%
T9	2 Φ	121	11	0.690	0.730	-5,5%
T10	2 Φ	107	8	0.664	0.653	1,7%
T4	6 Φ	101	18	0.789	0.680	13,8%
T5	6 Φ	107	13	0.781	0.720	7,8%
T8	6 Φ	121	17	0.735	0.816	-11,0%

5.4 COMPARISON OF DEFORMED MESH AND THE EXPERIMENTS

The pull-out behavior of the soil nails followed during the experiments are in good agreement with the deformed shapes obtained from the numerical analyses. Comparison of the deformed meshes obtained by the numerical analyses and the photographs taken during the experiments are given in Figures 5.17 and 5.18. The behavior of the group nails with $2\emptyset$ or $6\emptyset$ spacing in numerical model is similar to that observed during the model tests.

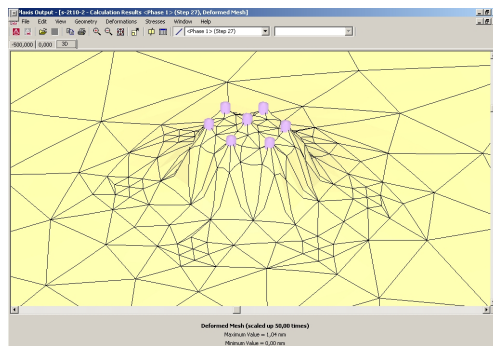


Figure 5.17 Comparison of the deformed mesh of the numerical analyses and the photograph taken during the experiment T10

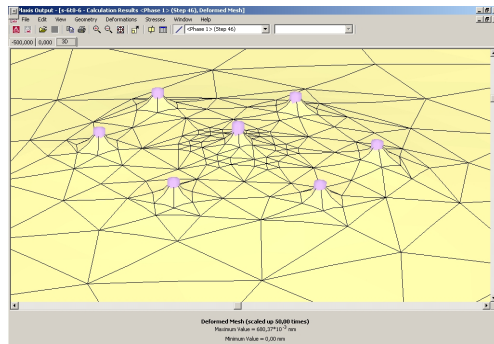


Figure 5.18 The comparison of the deformed mesh of the numerical analyses and photograph taken during the experiment T8

5.5 A PARAMETRIC STUDY

In order to investigate the effect of group behavior on the central nail, several numerical analyses are performed for different spacing. The material properties and the configurations of the experiments are used in the analyses. The results of these parametric analyses are presented in Tables 5.5 and Figure 5.19. It is concluded that the reduction in pull-out load for 4Ø, 6Ø and 8Ø spaced group nails vary between 1,5% to 5,7% of the pull-out load. Based on these results it can be stated that the group effect is negligible for 4Ø, 6Ø and 8Ø spaced group nails. On the other hand, for 2Ø spaced group nails, the reduction of the pull-out load varies between 11,4% and 19,1% of the pull-out load, which shows the reducing effect of group behavior on the pull-out capacity of the nails.

Table 5.5 Summary of the results of the parametric study (Calculated maximum axial force and the reduction of the pull-out loads for different spaced nail groups in terms of pull-out load percentage)

NAME	SINGLE	2Ø		4Ø		6Ø		8Ø	
	CALC. MAX. AXIAL FORCE (kN)	CALC. MAX. AXIAL FORCE (kN)	DIFF. WRT. SINGE NAIL (%)	CALC. MAX. AXIAL FORCE (kg)	DIFF. WRT. SINGE NAIL (%)	CALC. MAX. AXIAL FORCE (kg)	DIFF. WRT. SINGE NAIL (%)	CALC. MAX. AXIAL FORCE (kg)	DIFF. WRT. SINGE NAIL (%)
T3	0.528	0.427	19.1	0.499	5.5	0.498	5.7	0.503	4.7
T4	0.715	0.585	18.2	0.677	5.3	0.680	4.9	0.686	4.1
T5	0.747	0.638	14.6	0.720	3.6	0.720	3.6	0.725	3.0
T6	0.811	0.704	13.2	0.784	3.3	0.792	2.3	0.792	2.3
T8	0.853	0.705	17.4	0.809	5.2	0.816	4.3	0.820	3.9
T9	0.842	0.730	13.3	0.817	3.0	0.820	2.6	0.821	2.5
T10	0.737	0.653	11.4	0.723	1.9	0.726	1.5	0.726	1.5
T12	0.764	0.633	17.2	0.722	5.5	0.727	4.8	0.732	4.2

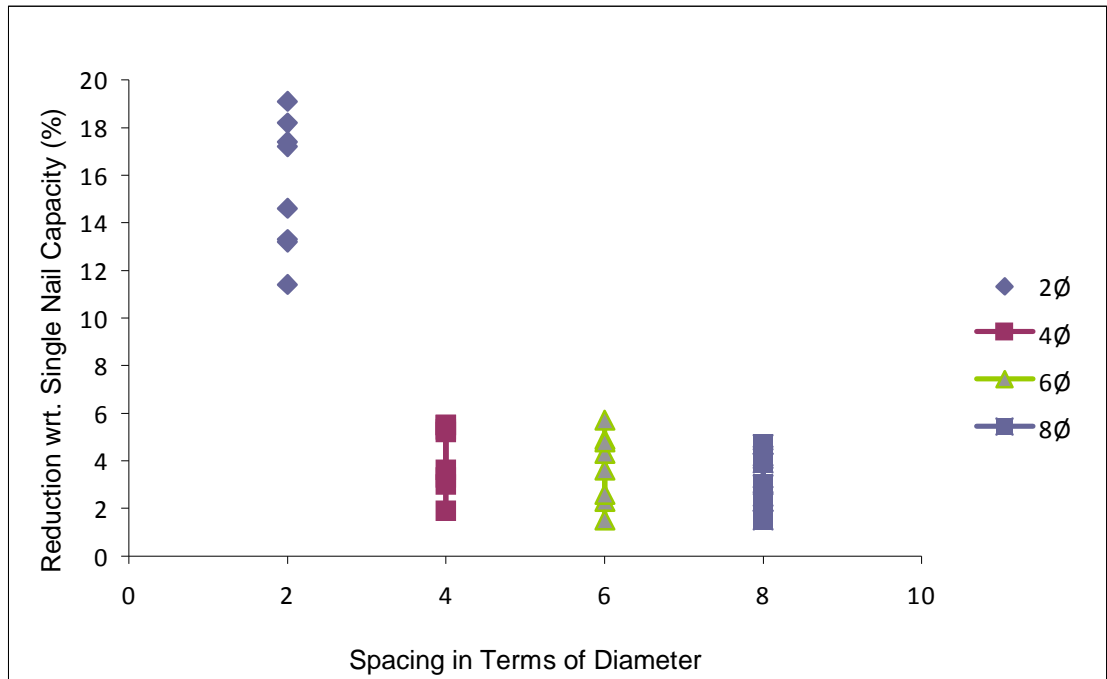


Figure 5.19 Reduction in the pull-out capacity of group nails with respect to single nail capacity

CHAPTER 6

SUMMARY, DISCUSSION AND CONCLUSION

6.1 SUMMARY

In this study, a literature review on the soil nailing is presented first. The history of the soil nailing, failure modes of the soil nailed structures and the fundamentals of soil nail behavior including the development of loads in soil nails and the role of other components of the system are summarized. Emphasis is given on the importance and difficulty on the prediction of soil nail interface. Then, the techniques used to estimate the pull-out resistance by several researchers are presented. Among these, the pull-out tests are focused, and the factors affecting the pull-out resistance are presented briefly.

A pull-out set up is developed in this study for testing the behavior of soil nails in high plastic clay. Before performing the pull-out tests, the characteristics of the soil sample are determined by laboratory methods. In addition, the most appropriate sample preparation technique is decided by comparing several methods. The internal dimensions of the aluminum model box are 300 mm, 300 mm and 500 mm. In all tests 360 mm long, 6 mm diameter ribbed reinforcing bars are used and an overburden pressure of 100 kPa is applied to the sample. The pull-out displacement speed used in

the tests is 0.6 mm/min. The pull-out load and the displacement behavior is recorded by using a load cell at the nail head and two LVDT's measuring the relative movement of the detruide nails and the box. The tests are performed for single nails and for the group nails that are placed in a scattered pattern as in field applications. After each pull-out test, samples are taken from the model box to determine the soil characteristics.

In the second part of the study, numerical modeling is carried out via finite element method and using PLAXIS 3D FOUNDATION (Brinkgreve et al., 2007), a three dimensional software. The measured and simulated pull-out forces are compared with each other. By and large, the agreement between the tests and the numerical analyses is observed to be satisfactory. In addition to these comparison studies, a parametric study is performed with varying spacing to investigate the reduction of the pullout resistance of the central nail regarding the nail spacing.

6.2 DISCUSSION

In view of the previous studies presented in Chapter 1, one can conclude that the shear strength parameters of the soil sample are the most important parameters that effect pull-out capacity of soil nails. In this study, in order to compare the results of different pull-out tests, soil samples of similar properties are prepared for each individual test. As mentioned in the previous sections, approximately 82 kg of high plastic clay is compacted into the model box for each test and great care is given during the soil sample preparation (the details of sample preparation are given in Chapter 3 briefly).

After each experiment, the shear strength parameters of the soil sample are obtained by tri-axial compression tests and the results are given in Table 4.1.

The results of shear strength tests showed that the soil used in the models has quite uniform strength properties. Regarding the shear strength parameters, the test results can be evaluated in two groups. The first group consists of the tests T6, T8, T9 while the second group consists of T4, T5, T10 and T12 tests (Table 4.3). When the results of the first group tests are compared, it is observed that the pull-out capacities of nails measured in the tests with a single nail and in the tests with a group of nails with 6 \emptyset spacing are very close to each other: The result of single nail test (T6) and 6 \emptyset spacing group test (T8) are 0.737 and 0.735 kN respectively. On the other hand 0.690 kN is measured for 2 \emptyset spaced group nails (T9). If the results of the second group is evaluated, similar behavior can be observed: 0.798 kN for single nail (T12), and 0.789 – 0.781 kg for group nails with 6 \emptyset spacing in tests T4 and T5. For 2 \emptyset spaced groups, a 0.664 kg pull-out load is measured for nails (T10), similar to the reduction observed in the first group of tests. Hence, 2 \emptyset spaced group nails cause 6.4% and 16.8% reduction in pull-out capacity, and 6 \emptyset spaced nails cause reductions between 0.3% and 2.1%, when the results for two test groups are combined.

The numerical models of the pull-out tests are developed in order to analyze each test by using a 3D finite element program. The details of the program and the input data are presented in Chapter 5. The variation between the measured and the calculated pull-out forces varied between 9-13% in a previous study by Su (2006). In this study, if the result of test T3 is excluded, there is 2% to 14% variation between the computed and measured pull-out capacities. The measured and the computed pull-out capacities are in good agreement for both single and group nails. Additionally, the group behavior of the nails with 2 \emptyset or 6 \emptyset spacing in numerical model is similar to that observed during the model tests as presented in section 5.4.

A parametric study is performed in order to compare the pull-out capacity for the nail patterns having spacings from $2\emptyset$ to $6\emptyset$ with same strength parameters. There is a 11%-19% reduction in the pull-out capacity of the soil nails in groups with $2\emptyset$ spacing. On the other hand, relatively very low reduction in the pull-out capacity is computed for the nail groups with $4\emptyset$, $6\emptyset$, and $8\emptyset$ spacing. The computed reductions are consistent with the test results.

Details of the study on the correlations of shear strength parameters with the pull-out capacity of the soil nails are presented in Chapter 1. As an alternative to the pull-out tests, the pull-out capacity of the driven nails can be calculated from the empirical relation suggested by Cartier et al. (1983). The pull-out capacities of the soil nails in the tests are compared with those according to Cartier et al. in Table 6.1. The relative difference of measured and calculated pull-out forces vary between 5%-31% for single and group nails.

Another way to estimate the pull-out resistance of the soil nails is to use the bond strength values suggested in the previous studies. As stated earlier, a databank consisting of the ultimate pull-out stress is previously formed by Elias and Juran (1991) and the estimated bond strength of the soil nails in soil and rock is presented in Table 1.1. In this table, the ultimate pull-out resistance of the soil nail for stiff clay is given as 40-60 kN/m^2 and 40-100 kN/m^2 for stiff clayey silt. The ultimate pull-out force which is calculated from the measured data, varies between 97-117 kN/m^2 which is close to the upper bound of the limits suggested for the stiff clayey silt. The pull-out capacity of the soil nails in the design are usually estimated either by employing previous experience in comparable conditions,

or by employing empirical relationships between geotechnical parameters and the nail capacity. As seen from the empirical relations, the pull-out capacity of a nail is most sensitive to the shear strength parameters of soil. Hence, the pull-out capacity should be carefully estimated when using the information given by previous studies.

Table 6.1 Comparison of the pull-out capacity measured and calculated according to Cartier et al. (1983).

Status	Test	Measured Pullout Force (kN)	Measured Pullout Force (kN/m)	Calculated Pull-out Force(kN/m) $T=Pc' + 2D\sigma_v' \tan\phi'$	Difference (%)
SINGLE	T6	0.737	2.047	2.438	-19.1
SINGLE	T3	0.772	2.144	1.807	15.7
SINGLE	T12	0.798	2.217	2.379	-7.3
2Ø	T9	0.690	1.917	2.513	-31.1
2Ø	T10	0.664	1.844	2.185	-18.4
6Ø	T4	0.789	2.192	2.293	-4.6
6Ø	T5	0.781	2.169	2.293	-5.7
6Ø	T8	0.735	2.042	2.647	-29.6

6.3 CONCLUSIONS

The pull-out resistance of group nails is investigated in clay type soil in order to determine the influence of nail spacing in group applications. During the tests, the pull-out capacity of soil-nail is measured for single and group nails with different spacing. It is observed in model tests with high plastic clay that, there is a reduction in the pull-out capacity of a nail in $2\emptyset$ spaced group within the limitations of this study. For a nail group with $6\emptyset$ spacing, the pull-out capacity is not affected from the neighboring nails. In all tests, the plots of the pull-out load on nail versus nail displacement show that, the peak value of load is followed by a sharp reduction. The peak pull-out load is mobilized within the first few millimeters of the nail displacements.

The results of the tests are compared with those of the numerical (finite-element) analyses. It is seen that, the results are in good agreement. In addition, a parametric study is carried on the pull-out capacity of the soil nails in groups with different spacing. It is observed that the reduction of pull-out capacity for $2\emptyset$ spacing varies between 11% and 19%. On the other hand, the reductions in the pull-out capacity of two groups of tests are 6.4% and 16.8%, respectively. Hence, the results of numerical analyses are in good agreement with those of the model tests.

6.4 RECOMMENDATIONS FOR THE FUTURE STUDIES

In this research, a set-up for pull-out tests is designed and an experimental study is carried out on the pull-out capacity of the soil nails in high plastic clay for single and group nail applications. For modeling group nails a scattered design, a hexagonal pattern used in situ, is applied. In view of the findings, the following issues may be considered for future studies:

- The effect of the overburden pressure on the pull-out capacity of the nails in clay can be investigated.
- The pull-out capacity of the nails for different L/D (nail length to nail diameter) ratios can be investigated.

REFERENCES

Aminfar, M.H., 1998. *Centrifuge modeling soil nailed slopes*. PhD Thesis, University of Wales, Cardiff., UK.

Bolton, M.D., Stewart, D.I., 1990. *The response of nailed walls to the elimination of suction in clay*. Proceedings of the International Reinforced Soil Conference, Glasgow, UK.

Brinkgreve, R.B.J., Swolfs, W.M., Beuth, L., Broere, W., Bonnier, P.G., Hartman, E., El-Mossallamy, Y., Slot, M., Waterman, D., Wolfersdorff, P.A., Haag D., 2007. *Plaxis 3D FOUNDATION Version 2 Manuals*.

Cartier, G., Gigan, J.P., 1983. *Experiments and observations on soil nailing structures*. In *Improvement of Ground: Proceedings of the 8th European Conference on Soil Mechanics and Foundation Engineering*, Helsinki, Finland, pp. 473-476.

Chu, L.M., Yin, J.H., 2005. *Comparison of interface shear strength of soil nails measured by both direct shear box tests and pull-out tests*. *Journal of Geotechnical and Geoenvironmental Engineering*, Vol.131, pp. 1097-1107.

Chu, L.M., Yin, J.H., 2005. *A Laboratory device to test the pull-out behavior of soil nails*. Geotechnical Testing Journal, 28, pp. 499-513.

Craig R.F., 1986. *Soil Mechanics*, 4th edition, English Language Book Society.

Demirel, Z., Kadiođlu, M., Aray, S., ;Orhan, F., Alp, A., 2003. *Toprak ve stabilizasyon laboratuvarı el kitabı*. Karayolları Genel Müdürlüğü, Teknik Araştırma Dairesi Başkanlığı, Üstyapı Şubesi Müdürlüğü.

Elias,V. Juran, I., 1991. *Soil nailing for stabilization of highway slopes and excavations*. Federal Highway Administration Report Ref FHWA-RD-89-198, Washington DC, USA.

Engin, H.K., Septanika, E.G., Brinkgreve, R.B.J., 2007. *Load-settlement behavior of large diameter bored piles in over-consolidated clay*. Proceedings of the 7th International Symposium on Geotechnical Engineering, Rhodes, Greece.

Engin, H.K., Septanika, E.G., Brinkgreve, R.B.J., 2008. *Estimation of pile group behavior using embedded piles*. The 12th International Association for Computer and Advances in Geomechanics, India, pp. 3231-3238.

Franzen, G., 1998. *A laboratory and field study of pullout capacity*. PhD Thesis, Chalmers Univ. of Technology, Göteborg, Sweden.

FHWA-SA-96-072, 1993a. *FHWA International Scanning Tour for Geotechnology, September-October 1992-Soil Nailing Summary Report*. US. Department of Transportation Federal Highway Administration, Washington, D.C.

FHWA-SA-93-026, 1993b. *French National Research Project Clouterre, 1991-Recommendations Clouterre 1991*. US. Department of Transportation Federal Highway Administration, Washington, D.C.

FHWA-SA-93-068, 1994. *Soil nailing field inspector's manual*. US. Department of Transportation Federal Highway Administration, Washington, D.C.

FHWA, 1994. *FHWA Ground Nailing Demonstration Project Guideline, Manual and Workshop* US. Department of Transportation Federal Highway Administration, Washington, D.C.

FHWA-SA-96-069R, 1998. *Manual for Design and Construction Monitoring of Soil Nail Walls*. U.S. Department of Transportation Federal Highway Administration.

FHWA-0-IF-03-017, 2003. *Geotechnical Engineering Circular No.7, Soil Nail Walls*. U.S. Department of Transportation Federal Highway Administration.

Frydman, S. Baker, R., Levy, A., 1994. *Modeling of the soil nailing excavation process*. Centrifuge 94, Singapore, pp. 669-674.

Gammage, P.J. (1997). *Centrifuge modelling of soil nailed walls*. PhD Thesis, University of Wales, Cardiff, UK.

Gassler, G. & Gudehus, G., 1981. *Soil nailing - some aspects of a new technique*. Proceedings of the 10th International Conference on Soil Mechanics and Foundation Engineering, Stockholm, Sweden, Vol. 3, pp. 665-670.

Gassler, G., 1983. *Discussion on ground movement analysis of earth support system*. Journal of the Geotechnical Engineering Division, ASCE, 109.

Gassler, G. 1992. *Discussion leader's report: slopes and excavations*. In Earth Reinforcement Practice: Proceedings of the International Symposium on Earth Reinforcement Practice, Fukuoka, Kyushu, Japan, pp. 955-960.

Geotechnical Engineering Office (GEO), 2005. *Good practice in design of steel soil nails for soil cut slopes*. GEO Technical Guidance Note No:23, Civil Engineering Department, The Government of the Hong Kong Special Administrative Region, Hong Kong.

Guilloux, A., Schlosser, F., 1982 . *Soil nailing: practical applications in recent development in ground improvement techniques*. Proceedings of the International Symp., Asian Institute of Technology, Bangkok, Thailand, pp. 389-397

Hong, Y.S., Chen, R.H., 2000. *Nonlinear analysis of model nail pullout behavior*. Proceedings of the Conference on Computer Applications in Civil and Hydraulic Engineering, Taichung, Taiwan, Republic of China, pp. 629-637

Hong Y.S., Wu C.S., Yang S.H., 2003. *Pullout resistance of single and double nails in a model sandbox*. Canadian Geotechnique . J. 40, pp. 1039-1047

Ingold, T.S., 1982. *Reinforced earth*. Thomas Telford Ltd. London.

Jaky, Y., 1944. *The coefficient of earth pressure at rest*. J. Soc. Hung. Eng. Arch, pp. 355-358

Jewell, R.A., 1990. *Review of theoretical models for soil nailing*. In performance of Reinforced Soil Structures Proceedings of the International Reinforced Soil Conference, Glasgow, UK, pp.265-275.

Jewell, R.A., Pedley, M.J. 1992. *Analysis for soil reinforcement with bending stiffness*. ASCE Journal of Geotechnical Engineering, Vol 118, pp. 1505-1528.

Junaideen, L.G., Tham L.G., Law, K.T., Lee, C.F., Yue, Z.Q. 2004. *Laboratory study of soil-nail interaction in loose, completely decomposed granite*. Canadian Geotechnique. J. 41, pp. 274-286.

Karayolu Teknik Şartnamesi, 2006. Karayolları Genel Müdürlüğü, pp. 66.

Lambe, T.W., Withman, R.V., 1979. *Series in soil engineering*, John Wiley and Sons, New York.

Mitchell J.K., Villet C.B., 1987. *Reinforcement of earth slopes and embankments*. National Cooperative Highway Research Program Report 290, Transportation Research Board, Washington D.C

Morgan, N., 2002. *The influence of variation in effective stress on the serviceability of soil nailed slopes*. PhD Thesis. University of Dundee, UK.

Morris, J.D., 1999. *Physical and numerical modeling of grouted nails in clay*. PhD Thesis, University of Oxford, UK.

Ng, C.W.W., Laak, P.V., Tang, W.H., Li, X.S., Shen, C.K. *The Hong Kong Geotechnical Centrifuge and Its Unique Capabilities*. <http://www.earthquakecountry.info/roots/objects/12478.pdf>, 19.09.2009.

Nicholson, P.J., 1986. *Soil nailing a wall*. Civil Engineering, ASCE, 56(12), pp. 37-39.

O'Rourke, T.D., Druschel, S.J., Netravali, A.N., 1990. *Shear strength characteristics of sand-polymer Interfaces*. Journal of Geotechnical Engineering, 116(3), pp. 451-469.

Pedley, M.J., Jewell, R.A., Milligan, G.W.E., 1990. *A large scale experimental study of soil reinforcement interaction*. Ground Engineering. Part 1, pp. 44-48, Part 2, pp. 45-49.

Phear, A., Dew, C., Ozsoy, B., Wharmby N.J., Judge, J., Barley A.D., 2005. *Soil Nailing –Best Practice*, CIRIA.

Powell, G.E., and Watkins, A.T. 1990. *Improvement of marginally stable existing slopes by soil nailing in Hong Kong*. Proceedings of the International Reinforced Soil Conference, Glasgow, U.K., pp. 241-247.

Pradhan, B., Tham, L.G., Yue Z.Q., Junaideen S.M., Lee, C.F., 2006. *Soil-nail pullout interaction in loose fill materials*. International Journal of Geomechanics, pp. 238-247.

Rabcewicz L., 1964. *The New Austrian Tunnelling Method*. Part 1, Water Power, pp. 453-457, Part 2, Water Power, pp. 511-515

Shen, C.K., Bang, S., and Herrman, L.R., 1981. *Ground movement analysis of earth support system*. Journal of the Geotechnical Engineering Division, ASCE, 107(GT12), pp. 1609-1624.

Shen, C.K., Bang, S., Kim, Y.S., Mitchell, J.F., 1982. *Centrifuge modelling of lateral earth support*. ASCE Journal of Geotechnical Engineering Division, Vol. 108, No GT09, pp. 1150-1164.

Su, L.J., 2006. *Laboratory pull-out testing study on soil nails in compacted completely decomposed granite fill*. PhD Thesis, Hong Kong Polytechnic University.

Su, L.J., Chan, T.C.F., Yin, J.H., Shiu, Y.K., Chiu, S.L., 2008. *Influence of overburden pressure on soil nail pullout resistance in a compacted fill*. Journal of Geotechnical and Geoenvironmental Engineering, pp. 1339-1347.

Tei, K., 1993. *A study of soil nailing in sand*. PhD Thesis. University of Oxford, UK.

TS 1900-2, 2006. *İnşaat mühendisliğinde zemin laboratuvar deneyleri-Bölüm 2: Mekanik özelliklerin tayini*. Türk Standartları Enstitüsü.

Wagner, A.A., 1957. *The use of unified soil classification system by the Bureau of Reclamation*. Proceedings of the 4th International Conference on Soil Mechanics and Foundation, London.

Wang, Z., Richwien, W., 2002. *A study of soil-reinforcement interface friction*. Journal of Geotechnical Geoenvironmental Engineering. pp. 92-94.

APPENDIX A

HYDROMETER TEST RESULTS

GENERAL DIRECTORATE OF HIGHWAYS
TECHNICAL RESEARCH DEPARTMENT
SUPERSTRUCTURE DIV

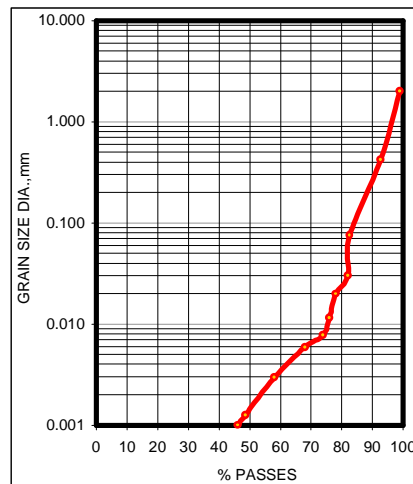
HYDROMETER TEST FORM

Project : Soil Mech. Div. Date : 05.12.2007
Site No : Ebru Akis's Research Study Starting Time (T) : 09:31
Lab. No : 14/49

SIEVES		RETAINED	Σ RETAINED	Σ RETAINED	Σ PASSING	Σ SAMPLE
No.	mm	g	g	%	%	% PASSING
No.10	2.00	0.00	0.00	0.00	100.0	99.0
No.40	0.42	3.20	3.20	6.40	93.6	92.7
No.200	0.075	5.12	8.32	16.64	83.4	82.5

Specific Weight (γ) = 2.697 Dr Sample Weight. (W) = 50 Spec.W. Fact (a) = 1.01

DATA READING INTERVAL, min	DATA READING TIME	HYDROMETER READING, g/ml	TEMPERATURE, °C	CORRECTION FACTOR FOR TEMP.	CORRECTED DATA READING	SUSPENSION %	Σ SAMPLE SUSP. %	MAXIMUM GRAIN SIZE DIA., mm	CORRECTION FACTORS				CORRECTED GRAIN SIZE
									k _n	k _i	k _g	d = d ₁ × k _n × k _i × k _g	
f	T=t+f	r	S	±M	R=±M	P	P1	d ₁	k _n	k _i	k _g	d = d ₁ × k _n × k _i × k _g	
2	09:26	43	23	-2.1	40.9	82.8	82.0	0.0400	0.96	0.77	1.02	0.0302	
5	09:29	41	23	-2.1	38.9	78.8	78.0	0.0260	0.96	0.78	1.02	0.0199	
15	09:39	40	23	-2.1	37.9	76.8	76.0	0.0150	0.96	0.78	1.02	0.0116	
30	09:54	39	23	-2.1	36.9	74.7	74.0	0.0100	0.96	0.79	1.02	0.0078	
60	10:24	36	23	-2.1	33.9	68.7	68.0	0.0074	0.96	0.81	1.02	0.0059	
250	13:34	31	23	-2.1	28.9	58.5	57.9	0.0036	0.96	0.83	1.02	0.0030	
1440	09:24	26	24	-1.8	24.2	49.1	48.6	0.0015	0.95	0.86	1.02	0.0013	



% GRAVEL (>2 mm)	1.0
% COARSE SAND (2-0.42 mm)	6.3
% FINE SAND (0.42-0.075 mm)	10.1
% SILT (0.075-0.002 mm)	28.9
% CLAY (0.002-0.001 mm)	7.6
% COLLOIDAL CLAY (< 0.001 mm)	46.1

APPENDIX B

DETERMINATION OF SOIL PARAMETERS

STRESS-STRAIN DIAGRAMS

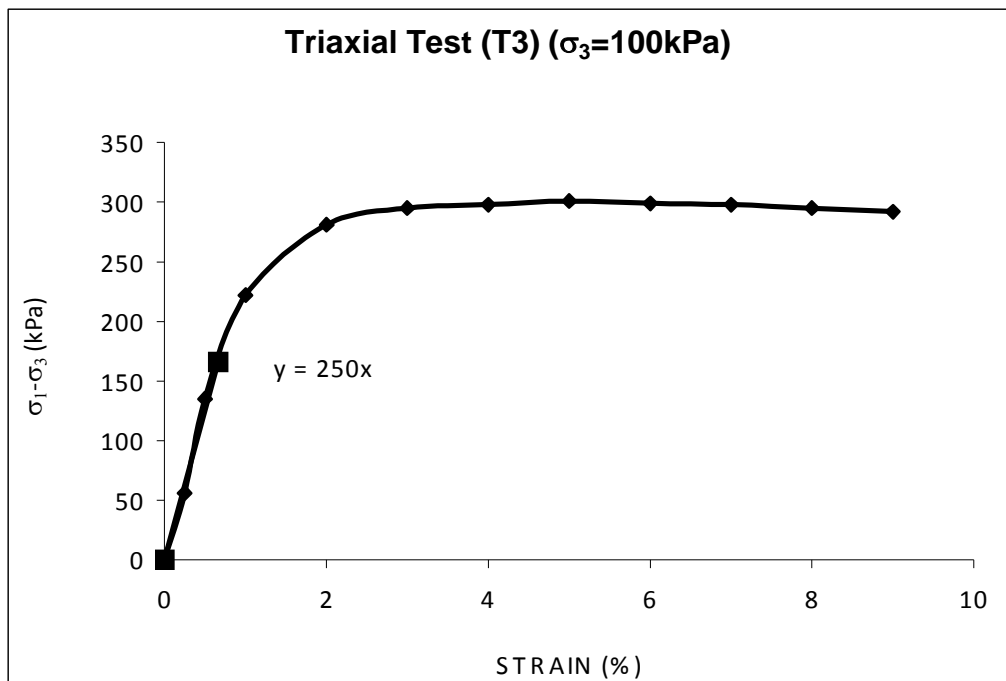


Figure B.1 Stress-strain diagram of tri-axial test T3

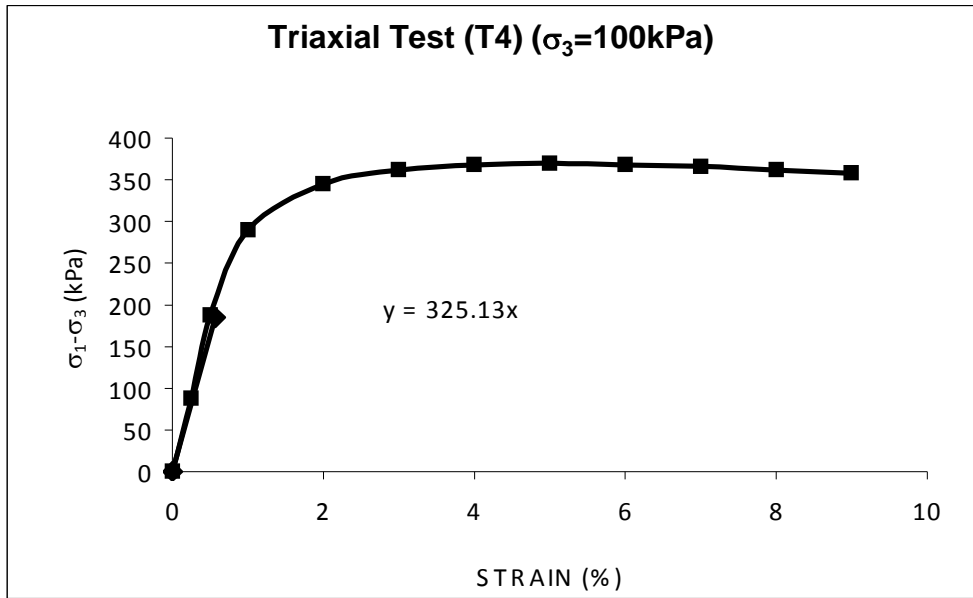


Figure B.2 Stress-strain diagram of tri-axial test T4

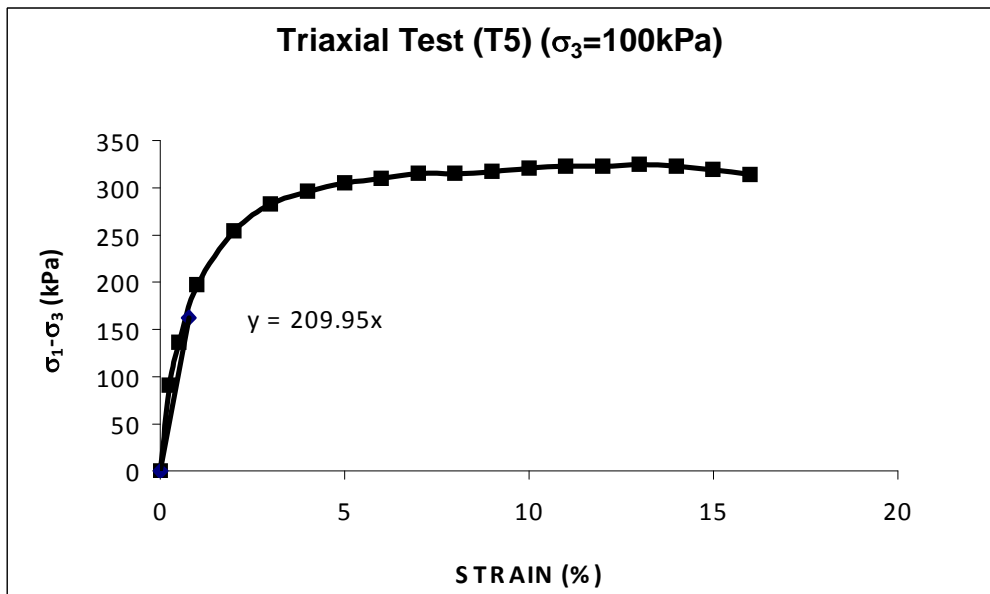


Figure B.3 Stress-strain diagram of tri-axial test T5

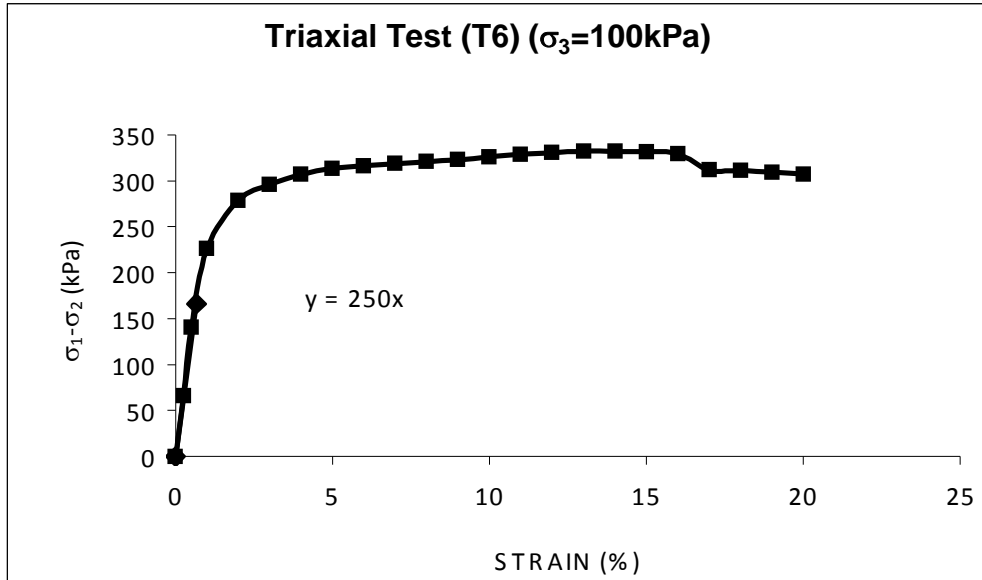


Figure B.4 Stress-strain diagram of tri-axial test T6

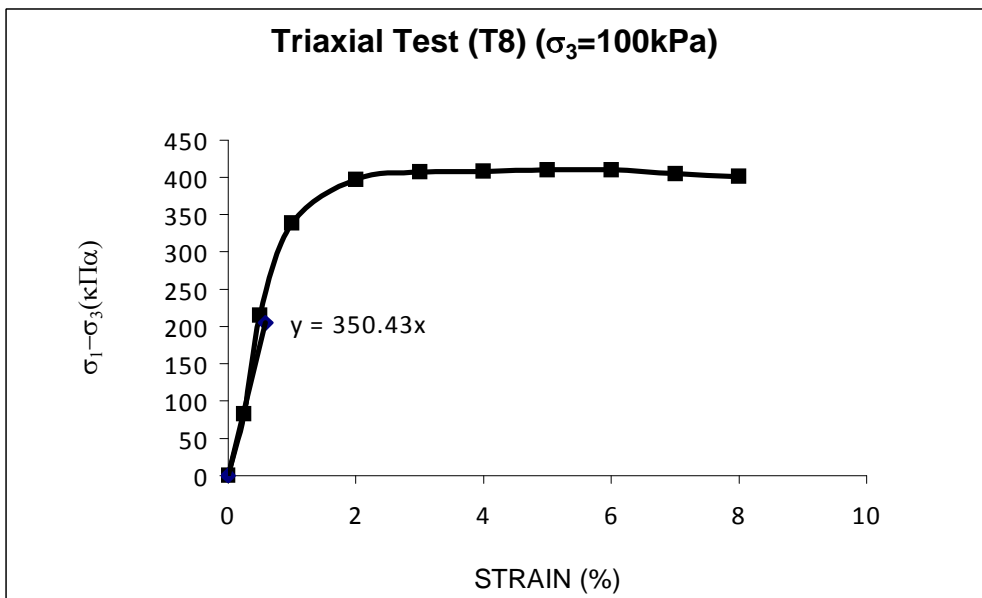


Figure B.5 Stress-strain diagram of tri-axial test T8

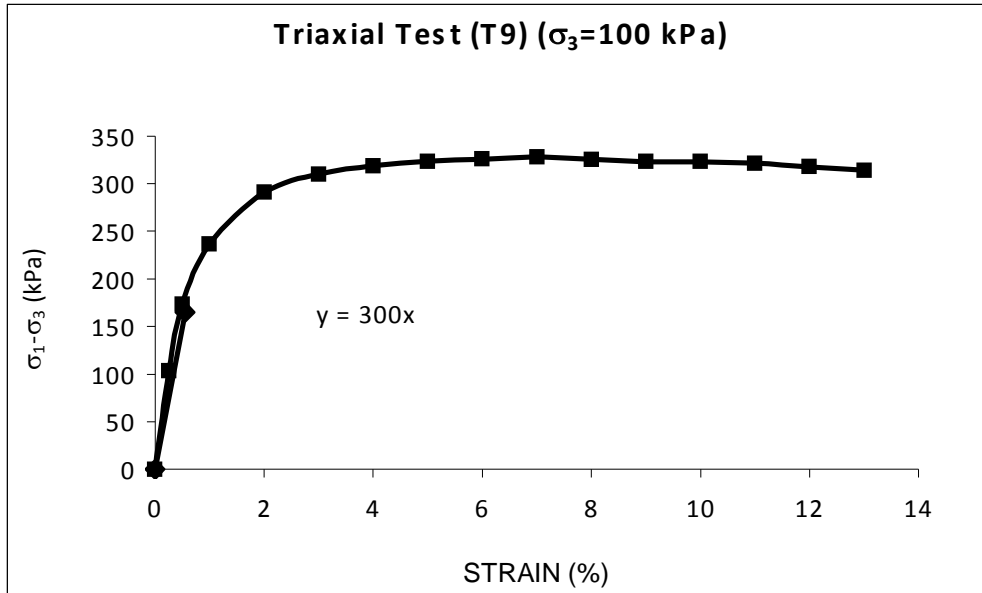


Figure B.6 Stress-strain diagram of tri-axial test T9

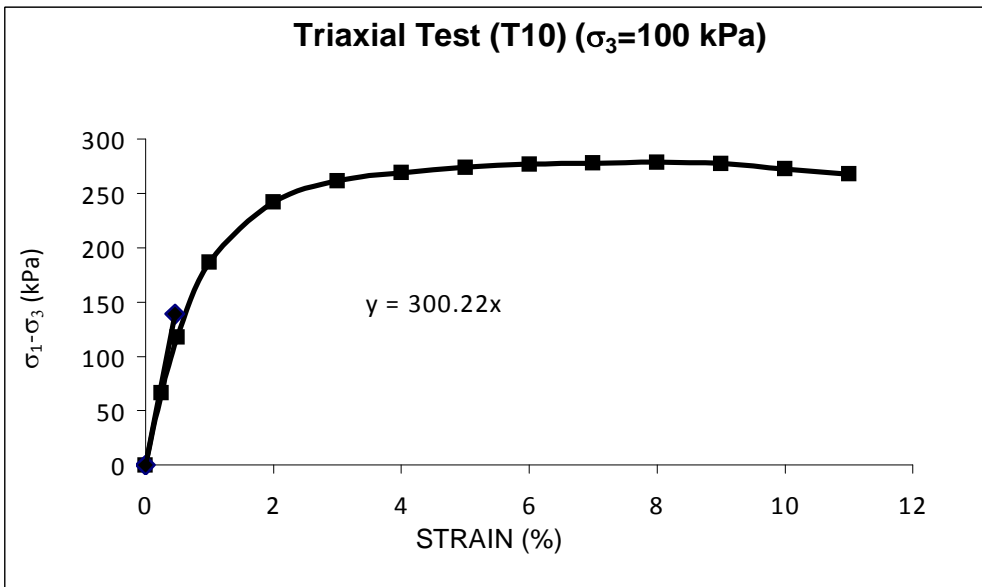


Figure B.7 Stress-strain diagram of tri-axial test T10

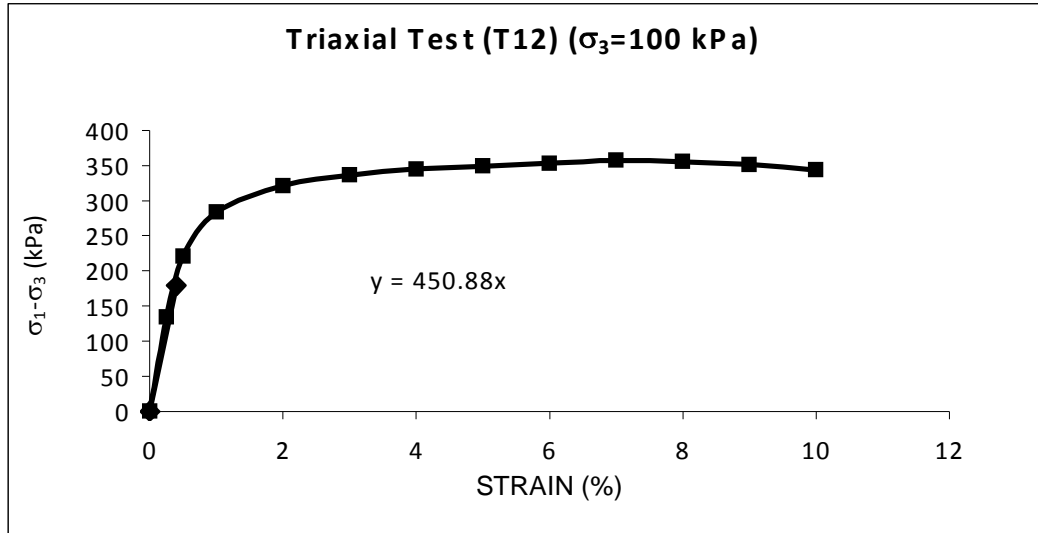


Figure B.8 Stress-strain diagram of tri-axial test T12

DETERMINATION OF SHEAR STRENGTH PARAMETERS

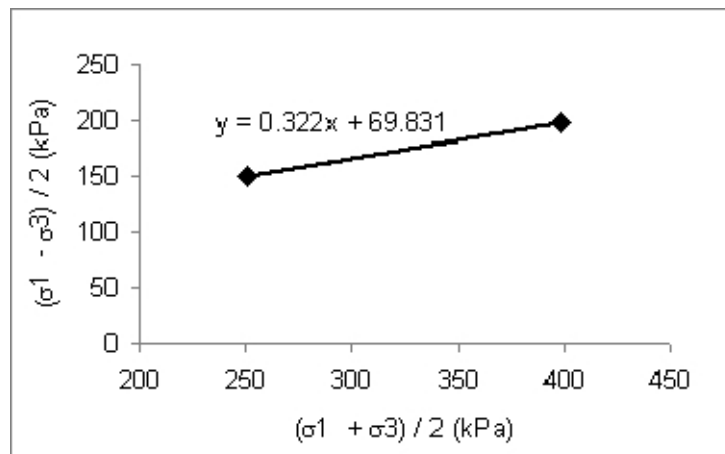


Figure B.9 The results of tri-axial test T3

Table B.1 Shear strength parameters of test T3

$\tan\alpha$	a	c (kPa) $c=a/\cos\phi$	ϕ ($^{\circ}$) $\phi=\sin^{-1}(\tan\alpha)$
0.322	69.831	74	19

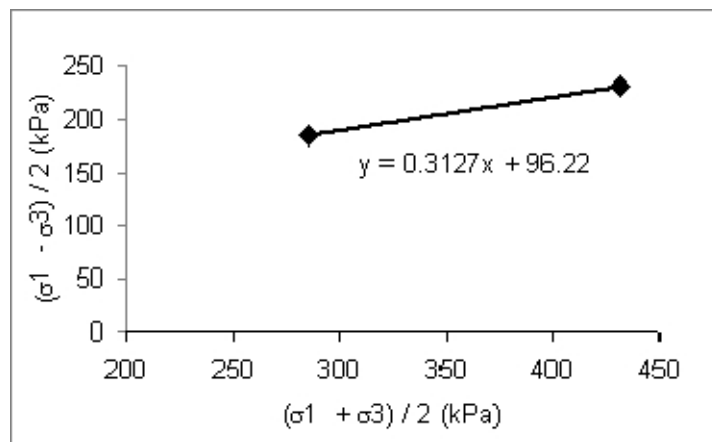


Figure B.10 The results of tri-axial test T4

Table B.2 Shear strength parameters of test T4

$\tan\alpha$	a	c (kPa) $c=a/\cos\phi$	ϕ ($^{\circ}$) $\phi=\sin^{-1}(\tan\alpha)$
0.313	96.22	101	18

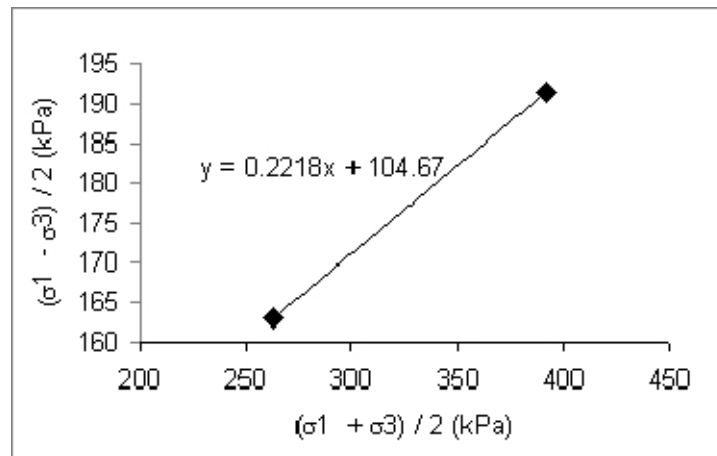


Figure B.11 The results of tri-axial test T5

Table B.3 Shear strength parameters of test T5

$\tan\alpha$	a	c (kPa) $c=a/\cos\phi$	ϕ ($^\circ$) $\phi=\sin^{-1}(\tan\alpha)$
0.222	104.67	107	13

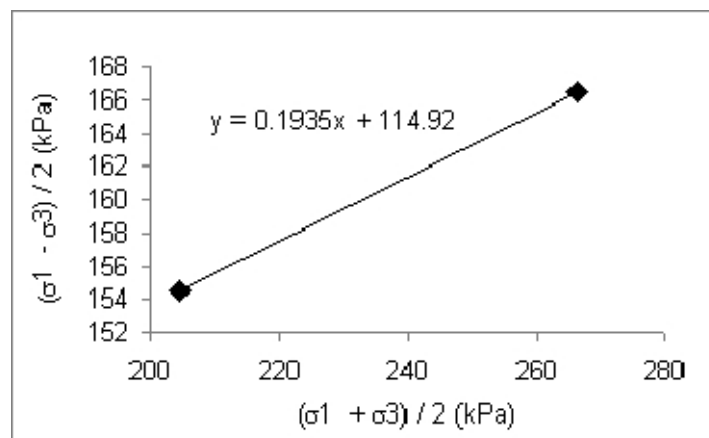


Figure B.12 The results of tri-axial test T6

Table B.4 Shear strength parameters of test T6

$\tan\alpha$	a	c (kPa) $c=a/\cos\phi$	ϕ ($^{\circ}$) $\phi=\sin^{-1}(\tan\alpha)$
0.194	114.92	117	11

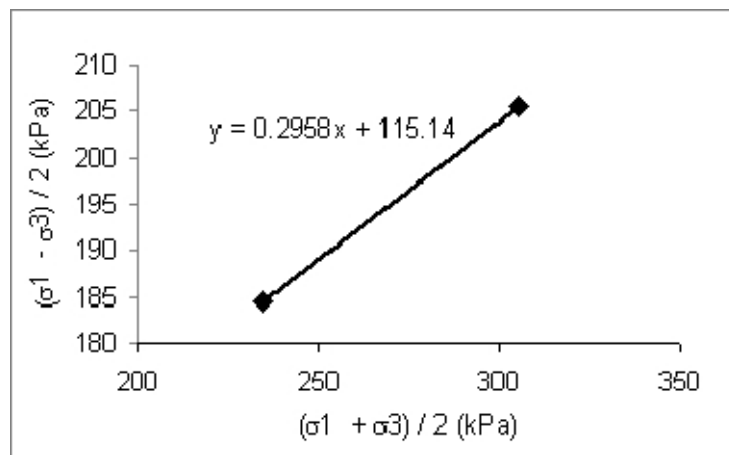


Figure B.13 The results of tri-axial test T8

Table B.5 Shear strength parameters of test T8

$\tan\alpha$	a	c (kPa) $c=a/\cos\phi$	ϕ ($^{\circ}$) $\phi=\sin^{-1}(\tan\alpha)$
0.296	115.14	121	17

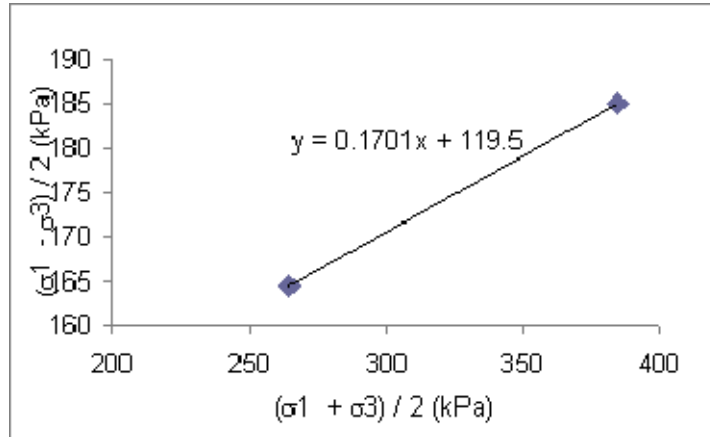


Figure B.14 The results of tri-axial test T9

Table B.6 Shear strength parameters of test T9

$\tan\alpha$	a	c (kPa) $c=a/\cos\phi$	ϕ ($^\circ$) $\phi=\sin^{-1}(\tan\alpha)$
0.170	119.5	121	11

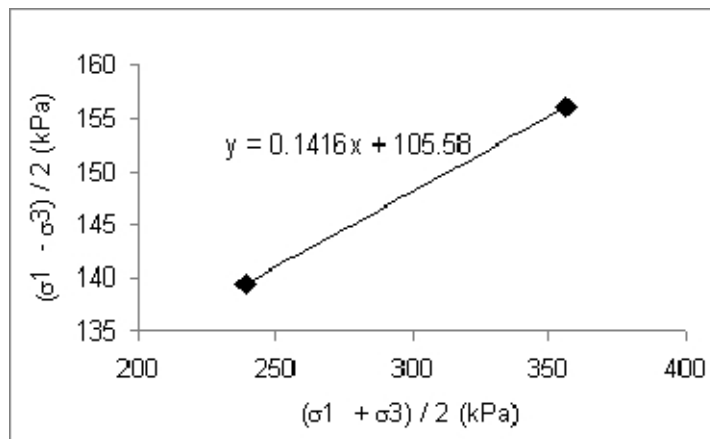


Figure B.15 The results of tri-axial test T10

Table B.7 Shear strength parameters of test T10

$\tan\alpha$	a	c (kPa) $c=a/\cos\phi$	$\phi (^{\circ})$ $\phi=\sin^{-1}(\tan\alpha)$
0.142	105.58	107	8

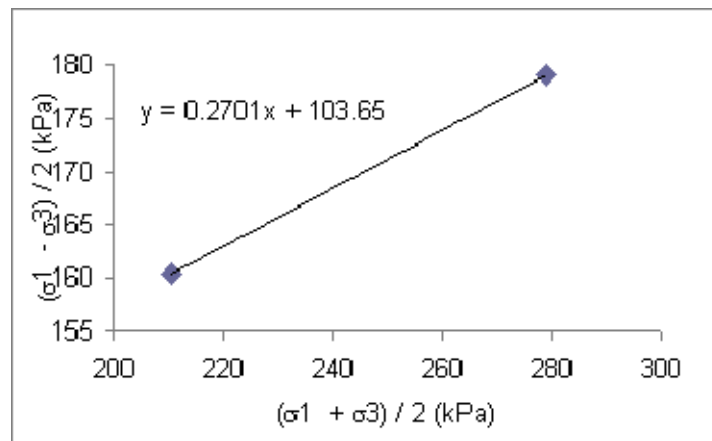


Figure B.16 The results of tri-axial test T12

Table B.8 Shear strength parameters of test T12

$\tan\alpha$	a	c (kPa) $c=a/\cos\phi$	$\phi (^{\circ})$ $\phi=\sin^{-1}(\tan\alpha)$
0.27	103.65	108	16

APPENDIX C

INPUT AND OUTPUT DATA OF PLAXIS 3D FOUNDATION SOFTWARE

The image shows a software dialog box titled "Mohr-Coulomb - Ankara Clay-t3". It has three tabs: "General", "Parameters", and "Interfaces", with "General" selected. The dialog is divided into several sections:

- Material Set:** Identification: Ankara Clay-t3; Material model: Mohr-Coulomb; Material type: Drained.
- General properties:** γ_{unsat} : 1,814E-08 kN/mm³; γ_{sat} : 1,814E-08 kN/mm³.
- Permeability:** k_x : 1,000 m/day; k_y : 1,000 m/day; k_z : 1,000 m/day.
- Comments:** A large empty text area.
- Buttons:** "Advanced...", "Next", "OK", and "Cancel".

Figure C.1.a Input data of single nail (T3)

Mohr-Coulomb - Ankara Clay-t3

General Parameters Interfaces

Stiffness

E_{ref} : 0,025 kN/mm²

ν (nu) : 0,403

Strength

c_{ref} : 7,400E-05 kN/mm²

ϕ (phi) : 19,000 °

ψ (psi) : 0,000 °

Alternatives

G_{ref} : 8,909E-03 kN/mm²

E_{oed} : 0,055 kN/mm²

Advanced...

Next OK Cancel

Figure C.1.b Input data of single nail (T3)

Pile Properties

Material set

Nail-t3

Comments

Properties

E : 200,000 kN/mm²

γ : 7,810E-09 kN/mm³

Predefined Type

Massive Circular Pile

Diameter : 6,000 mm

User-defined Type

A : 28,274 mm²

I_3 : 63,617 mm⁴

I_2 : 63,617 mm⁴

I_{23} : 0,000 mm⁴

Skin Resistance

Linear

$T_{top, max}$: 1,690 kN/mm

$T_{bot, max}$: 1,690 kN/mm

Multi-linear

Define...

Layer dependent

T_{max} : 1,807E-03 kN/mm

Base Resistance

F_{max} : 0,000 kN

OK Cancel

Figure C.1.c Input data of single nail (T3)

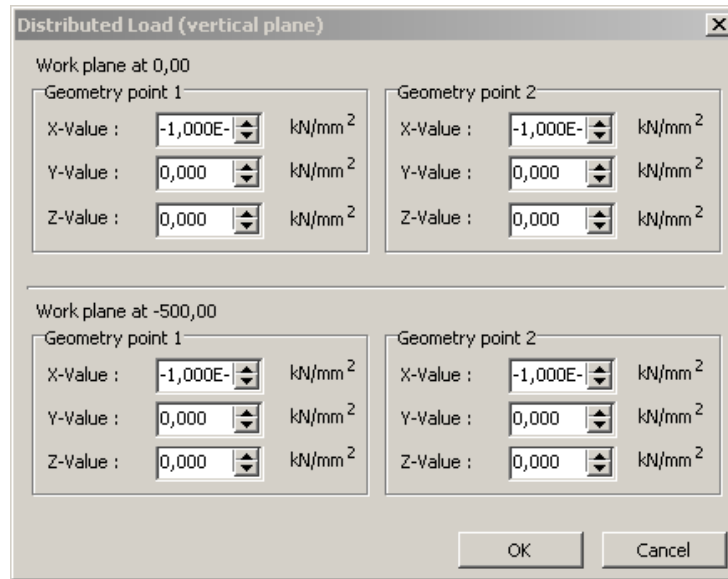


Figure C.1.d Input data of single nail (T3)

Plaxis - Finite Element Code for Soil and Rock Analyses

Project description	: s-st3-26-s	Output Version 2.1.0.308
User name	: PLAXIS BETA TESTER	Step : 26
Project filename	: s-st3-26-s	Date : 11.09.2009
Output	: Load Information - Point Load	Page : 1

ID	Node	Workplane	X [mm]	Y [mm]	Z [mm]	F _x [kN]	F _y [kN]	F _z [kN]
1	9264	0,000	0,000	0,000	0,000	0,000	1,000	0,000

Figure C.1.e Input data of single nail (T3)

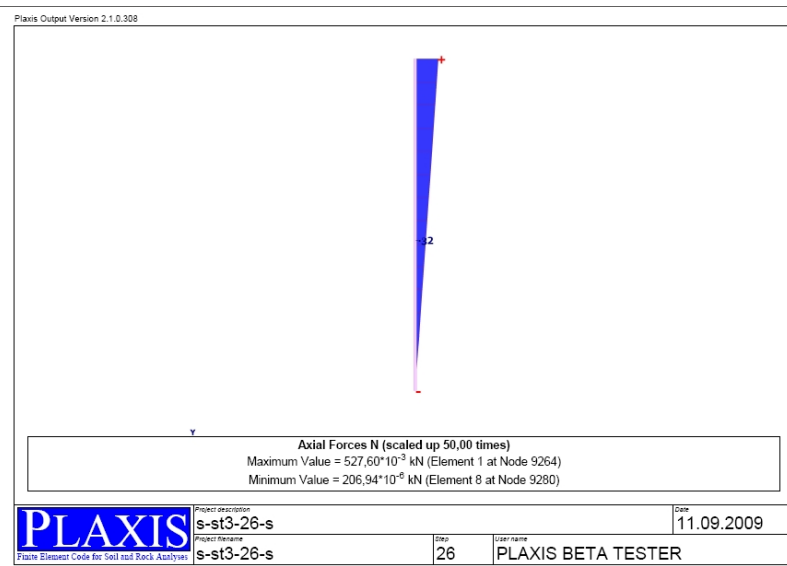


Figure C.1.f Output data of single nail (T3)

Mohr-Coulomb - Ankara Clay-t6

General Parameters Interfaces

Material Set

Identification:

Material model:

Material type:

General properties

γ_{unsat} : kN/mm³

γ_{sat} : kN/mm³

Comments

Permeability

k_x : m/day

k_y : m/day

k_z : m/day

Figure C.2.a Input data of single nail (T6)

Mohr-Coulomb - Ankara Clay-t6

General Parameters Interfaces

Stiffness

E_{ref} : 0,025 kN/mm²

ν (nu) : 0,447

Strength

c_{ref} : 1,170E-04 kN/mm²

ϕ (phi) : 11,000 °

ψ (psi) : 0,000 °

Alternatives

G_{ref} : 8,639E-03 kN/mm²

E_{oed} : 0,090 kN/mm²

Advanced...

Next OK Cancel

Figure C.2.b Input data of single nail (T6)

Pile Properties

Material set: Nail-t6

Comments:

Properties

E : 200,000 kN/mm²

γ : 7,810E-09 kN/mm³

Predefined Type

Massive Circular Pile

Diameter : 6,000 mm

User-defined Type

A : 28,274 mm²

I_3 : 63,617 mm⁴

I_2 : 63,617 mm⁴

I_{23} : 0,000 mm⁴

Skin Resistance

Linear

$T_{top, max}$: 1,690 kN/mm

$T_{bot, max}$: 1,690 kN/mm

Multi-linear

Define...

Layer dependent

T_{max} : 2,438E-03 kN/mm

Base Resistance

F_{max} : 0,000 kN

OK Cancel

Figure C.2.c Input data of single nail (T6)

Distributed Load (vertical plane)

Work plane at 0,00

Geometry point 1		Geometry point 2	
X-Value :	-1,000E- kN/mm ²	X-Value :	-1,000E- kN/mm ²
Y-Value :	0,000 kN/mm ²	Y-Value :	0,000 kN/mm ²
Z-Value :	0,000 kN/mm ²	Z-Value :	0,000 kN/mm ²

Work plane at -500,00

Geometry point 1		Geometry point 2	
X-Value :	-1,000E- kN/mm ²	X-Value :	-1,000E- kN/mm ²
Y-Value :	0,000 kN/mm ²	Y-Value :	0,000 kN/mm ²
Z-Value :	0,000 kN/mm ²	Z-Value :	0,000 kN/mm ²

OK Cancel

Figure C.2.d Input data of single nail (T6)

Plaxis - Finite Element Code for Soil and Rock Analyses

Project description	: s-st6-26-s	Output Version 2.1.0.308
User name	: PLAXIS BETA TESTER	Step : 29
Project filename	: s-st6-26-s	Date : 11.09.2009
Output	: Load Information - Point Load	Page : 1

ID	Node	Workplane	X [mm]	Y [mm]	Z [mm]	F _x [kN]	F _y [kN]	F _z [kN]
1	9264	0,000	0,000	0,000	0,000	0,000	1,000	0,000

Figure C.2.e Input data of single nail (T6)

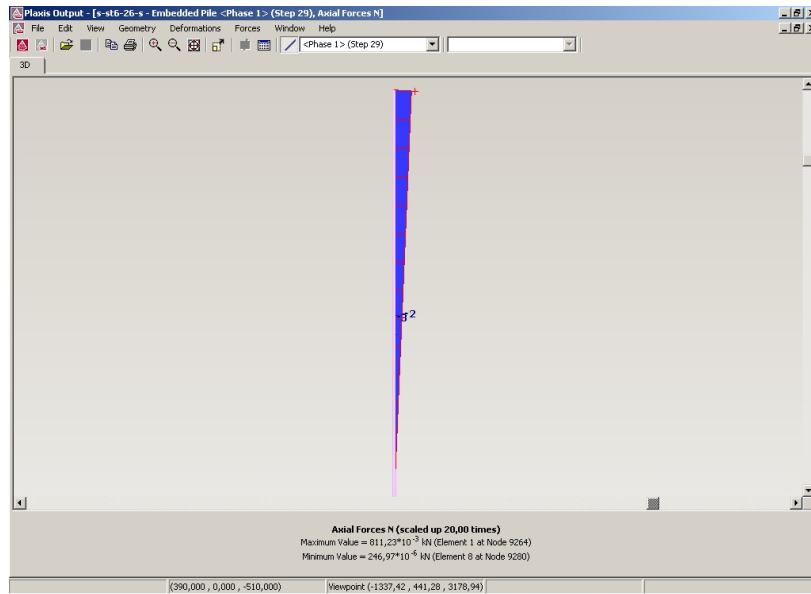


Figure C.2.f Output data of single nail (T6)

Figure C.3.a Input data of single nail (T12)

Mohr-Coulomb - Ankara Clay-t12

General Parameters Interfaces

Stiffness

E_{ref} : 0,045 kN/mm²

ν (nu) : 0,420

Strength

c_{ref} : 1,080E-04 kN/mm²

ϕ (phi) : 16,000 °

ψ (psi) : 0,000 °

Alternatives

G_{ref} : 0,016 kN/mm²

E_{oed} : 0,115 kN/mm²

Advanced...

Next OK Cancel

Figure C.3.b Input data of single nail (T12)

Pile Properties

Material set

Nail-t12

Comments

Properties

E : 200,000 kN/mm²

γ : 7,810E-09 kN/mm³

Predefined Type

Massive Circular Pile

Diameter : 6,000 mm

User-defined Type

A : 28,274 mm²

I_3 : 63,617 mm⁴

I_2 : 63,617 mm⁴

I_{23} : 0,000 mm⁴

Skin Resistance

Linear

$T_{top, max}$: 1,690 kN/mm

$T_{bot, max}$: 1,690 kN/mm

Multi-linear

Define...

Layer dependent

T_{max} : 2,379E-03 kN/mm

Base Resistance

F_{max} : 0,000 kN

OK Cancel

Figure C.3.c Input data of single nail (T12)

Distributed Load (vertical plane)

Work plane at 0,00

Geometry point 1	X-Value : -1,000E- kN/mm ²	Geometry point 2	X-Value : -1,000E- kN/mm ²
Y-Value : 0,000 kN/mm ²		Y-Value : 0,000 kN/mm ²	
Z-Value : 0,000 kN/mm ²		Z-Value : 0,000 kN/mm ²	

Work plane at -500,00

Geometry point 1	X-Value : -1,000E- kN/mm ²	Geometry point 2	X-Value : -1,000E- kN/mm ²
Y-Value : 0,000 kN/mm ²		Y-Value : 0,000 kN/mm ²	
Z-Value : 0,000 kN/mm ²		Z-Value : 0,000 kN/mm ²	

OK Cancel

Figure C.3.d Input data of single nail (T12)

Plaxis - Finite Element Code for Soil and Rock Analyses

Project description	: s-st12-26-s	Output Version 2.1.0.308
User name	: PLAXIS BETA TESTER	Step : 28
Project filename	: s-st12-26-s	Date : 11.09.2009
Output	: Load Information - Point Load	Page : 1

ID	Node	Workplane	X [mm]	Y [mm]	Z [mm]	F _x [kN]	F _y [kN]	F _z [kN]
1	9264	0,000	0,000	0,000	0,000	0,000	1,000	0,000

Figure C.3.e Input data of single nail (T12)

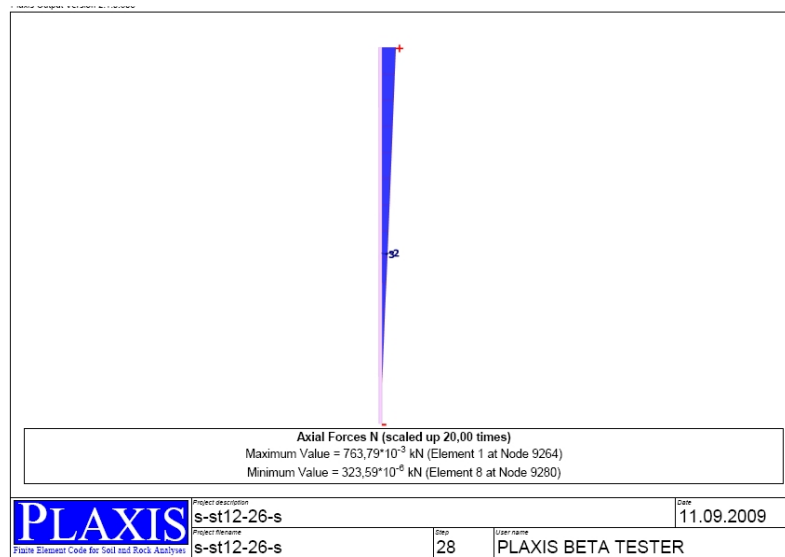


Figure C.3.f Output data of single nail (T12)

Mohr-Coulomb - Ankara Clay-t9

General Parameters Interfaces

Material Set

Identification: Ankara Clay-t9

Material model: Mohr-Coulomb

Material type: Drained

General properties

γ_{unsat} : 1,846E-08 kN/mm³

γ_{sat} : 1,846E-08 kN/mm³

Comments

Permeability

k_x : 1,000 m/day

k_y : 1,000 m/day

k_z : 1,000 m/day

Advanced...

Next OK Cancel

Figure C.4.a Input data of 2 \emptyset spaced nail group (T9)

Mohr-Coulomb - Ankara Clay-t9

General Parameters Interfaces

Stiffness

E_{ref} : 0,030 kN/mm²

ν (nu) : 0,432

Strength

c_{ref} : 1,210E-04 kN/mm²

ϕ (phi) : 11,000 °

ψ (psi) : 0,000 °

Alternatives

G_{ref} : 0,010 kN/mm²

E_{oed} : 0,087 kN/mm²

Advanced...

Next OK Cancel

Figure C.4.b Input data of 2Ø spaced nail group (T9)

Pile Properties

Material set: Nail-t9

Comments:

Properties

E : 200,000 kN/mm²

γ : 7,810E-09 kN/mm³

Predefined Type

Massive Circular Pile

Diameter : 6,000 mm

User-defined Type

A : 28,274 mm²

I_3 : 63,617 mm⁴

I_2 : 63,617 mm⁴

I_{23} : 0,000 mm⁴

Skin Resistance

Linear

$T_{top, max}$: 1,690 kN/mm

$T_{bot, max}$: 1,690 kN/mm

Multi-linear

Define...

Layer dependent

T_{max} : 2,513E-03 kN/mm

Base Resistance

F_{max} : 0,000 kN

OK Cancel

Figure C.4.c Input data of 2Ø spaced nail group (T9)

Figure C.4.d Input data of 2Ø spaced nail group (T9)

Plaxis - Finite Element Code for Soil and Rock Analyses

Project description	: s-2t9-2	Output Version 2.1.0.308
User name	: PLAXIS BETA TESTER	Step : 30
Project filename	: s-2t9-2	Date : 11.09.2009
Output	: Load Information - Point Load	Page : 1

ID	Node	Workplane	X [mm]	Y [mm]	Z [mm]	F _x [kN]	F _y [kN]	F _z [kN]
1	9264	0,000	0,000	0,000	0,000	0,000	1,000	0,000
2	9281	0,000	12,000	0,000	-6,000	0,000	1,000	0,000
3	9298	0,000	12,000	0,000	6,000	0,000	1,000	0,000
4	9315	0,000	0,000	0,000	-12,000	0,000	1,000	0,000
5	9349	0,000	-12,000	0,000	-6,000	0,000	1,000	0,000
6	9366	0,000	-12,000	0,000	6,000	0,000	1,000	0,000
7	9332	0,000	0,000	0,000	12,000	0,000	1,000	0,000

Figure C.4.e Input data of 2Ø spaced nail group (T9)

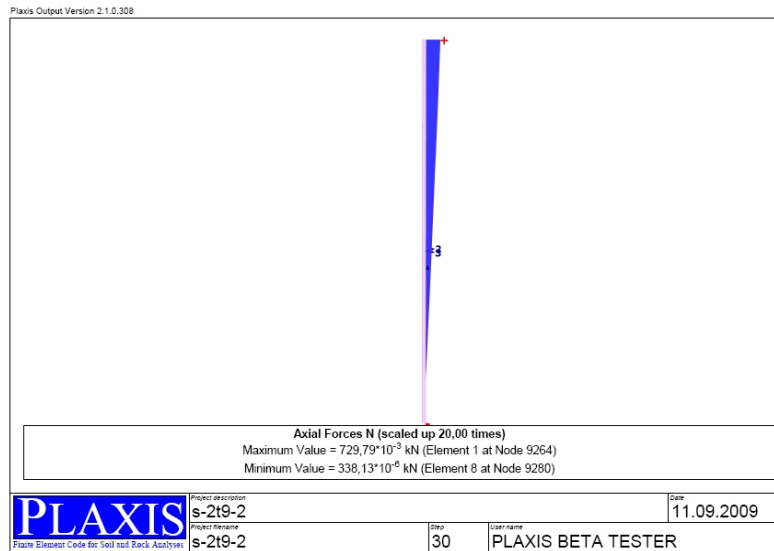


Figure C.4.f Input data of 2Ø spaced nail group (T9)

Mohr-Coulomb - Ankara Clay-t10

General | Parameters | Interfaces

Material Set

Identification:

Material model:

Material type:

General properties

γ_{unsat} : kN/mm³

γ_{sat} : kN/mm³

Comments

Permeability

k_x : m/day

k_y : m/day

k_z : m/day

Advanced...

Next OK Cancel

Figure C.5.a Input data of 2Ø spaced nail group (T10)

Mohr-Coulomb - Ankara Clay-t10

General Parameters Interfaces

Stiffness

E_{ref} : 0,030 kN/mm²

ν (nu) : 0,463

Strength

c_{ref} : 1,070E-04 kN/mm²

ϕ (phi) : 8,000 °

ψ (psi) : 0,000 °

Alternatives

G_{ref} : 0,010 kN/mm²

E_{oed} : 0,149 kN/mm²

Advanced...

Next OK Cancel

Figure C.5.b Input data of 2Ø spaced nail group (T10)

Pile Properties

Material set

Nail-t10

Comments

Properties

E : 200,000 kN/mm²

γ : 7,810E-09 kN/mm³

Predefined Type

Massive Circular Pile

Diameter : 6,000 mm

User-defined Type

A : 28,274 mm²

I_3 : 63,617 mm⁴

I_2 : 63,617 mm⁴

I_{23} : 0,000 mm⁴

Skin Resistance

Linear

$T_{top, max}$: 1,690 kN/mm

$T_{bot, max}$: 1,690 kN/mm

Multi-linear

Define...

Layer dependent

T_{max} : 2,185E-03 kN/mm

Base Resistance

F_{max} : 0,000 kN

OK Cancel

Figure C.5.c Input data of 2Ø spaced nail group (T10)

Distributed Load (vertical plane)

Work plane at 0,00

Geometry point 1	Geometry point 2
X-Value : -1,000E- kN/mm ²	X-Value : -1,000E- kN/mm ²
Y-Value : 0,000 kN/mm ²	Y-Value : 0,000 kN/mm ²
Z-Value : 0,000 kN/mm ²	Z-Value : 0,000 kN/mm ²

Work plane at -500,00

Geometry point 1	Geometry point 2
X-Value : -1,000E- kN/mm ²	X-Value : -1,000E- kN/mm ²
Y-Value : 0,000 kN/mm ²	Y-Value : 0,000 kN/mm ²
Z-Value : 0,000 kN/mm ²	Z-Value : 0,000 kN/mm ²

OK Cancel

Figure C.5.d Input data of 2Ø spaced nail group (T10)

Plaxis - Finite Element Code for Soil and Rock Analyses

Project description : s-2t10-2	Output Version 2.1.0.308
User name : PLAXIS BETA TESTER	Step : 27
Project filename : s-2t10-2	Date : 11.09.2009
Output : Load Information - Point Load	Page : 1

ID	Node	Workplane	X [mm]	Y [mm]	Z [mm]	F _x [kN]	F _y [kN]	F _z [kN]
1	9264	0,000	0,000	0,000	0,000	0,000	1,000	0,000
2	9281	0,000	12,000	0,000	-6,000	0,000	1,000	0,000
3	9298	0,000	12,000	0,000	6,000	0,000	1,000	0,000
4	9315	0,000	0,000	0,000	-12,000	0,000	1,000	0,000
5	9349	0,000	-12,000	0,000	-6,000	0,000	1,000	0,000
6	9366	0,000	-12,000	0,000	6,000	0,000	1,000	0,000
7	9332	0,000	0,000	0,000	12,000	0,000	1,000	0,000

Figure C.5.e Input data of 2Ø spaced nail group (T10)

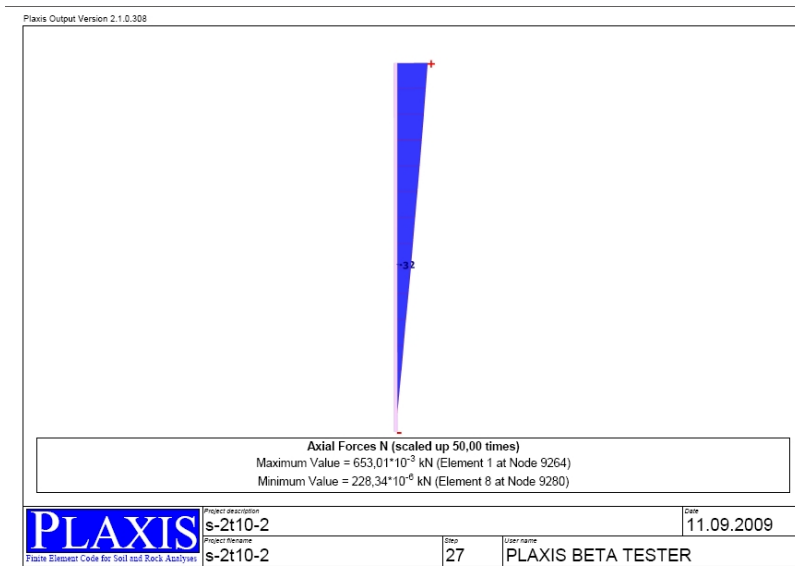


Figure C.5.f Input data of 2Ø spaced nail group (T10)

Mohr-Coulomb - Ankara Clay-t4

General Parameters Interfaces

Material Set

Identification:

Material model:

Material type:

General properties

γ_{unsat} : kN/mm³

γ_{sat} : kN/mm³

Comments

Permeability

k_x : m/day

k_y : m/day

k_z : m/day

Figure C.6.a Input data of 6Ø spaced nail group (T4)

Mohr-Coulomb - Ankara Clay-t4

General Parameters Interfaces

Stiffness

E_{ref} : 0,033 kN/mm²

ν (nu) : 0,409

Strength

c_{ref} : 1,010E-04 kN/mm²

ϕ (phi) : 18,000 °

ψ (psi) : 0,000 °

Alternatives

G_{ref} : 0,012 kN/mm²

E_{oed} : 0,075 kN/mm²

Advanced...

Next OK Cancel

Figure C.6.b Input data of 6Ø spaced nail group (T4)

Pile Properties

Material set

Nail-t4

Comments

Properties

E : 200,000 kN/mm²

γ : 7,810E-09 kN/mm³

Predefined Type

Massive Circular Pile

Diameter : 6,000 mm

User-defined Type

A : 28,274 mm²

I_3 : 63,617 mm⁴

I_2 : 63,617 mm⁴

I_{23} : 0,000 mm⁴

Skin Resistance

Linear

$T_{top, max}$: 1,690 kN/mm

$T_{bot, max}$: 1,690 kN/mm

Multi-linear

Define...

Layer dependent

T_{max} : 2,293E-03 kN/mm

Base Resistance

F_{max} : 0,000 kN

OK Cancel

Figure C.6.c Input data of 6Ø spaced nail group (T4)

Distributed Load (vertical plane)

Work plane at 0,00

Geometry point 1	Geometry point 2
X-Value : -1,000E- kN/mm ²	X-Value : -1,000E- kN/mm ²
Y-Value : 0,000 kN/mm ²	Y-Value : 0,000 kN/mm ²
Z-Value : 0,000 kN/mm ²	Z-Value : 0,000 kN/mm ²

Work plane at -500,00

Geometry point 1	Geometry point 2
X-Value : -1,000E- kN/mm ²	X-Value : -1,000E- kN/mm ²
Y-Value : 0,000 kN/mm ²	Y-Value : 0,000 kN/mm ²
Z-Value : 0,000 kN/mm ²	Z-Value : 0,000 kN/mm ²

OK Cancel

Figure C.6.d Input data of 6Ø spaced nail group (T4)

Plaxis - Finite Element Code for Soil and Rock Analyses

Project description : s-6t4-6	Output Version 2.1.0.308
User name : PLAXIS BETA TESTER	Step : 48
Project filename : s-6t4-6	Date : 11.09.2009
Output : Load Information - Point Load	Page : 1

ID	Node	Workplane	X [mm]	Y [mm]	Z [mm]	F _x [kN]	F _y [kN]	F _z [kN]
1	9264	0,000	0,000	0,000	0,000	0,000	1,000	0,000
2	9383	0,000	36,000	0,000	-18,000	0,000	1,000	0,000
3	9400	0,000	36,000	0,000	18,000	0,000	1,000	0,000
4	9417	0,000	0,000	0,000	-36,000	0,000	1,000	0,000
5	9434	0,000	0,000	0,000	40,000	0,000	1,000	0,000
6	9451	0,000	-36,000	0,000	-18,000	0,000	1,000	0,000
7	9468	0,000	-36,000	0,000	18,000	0,000	1,000	0,000

Figure C.6.e Input data of 6Ø spaced nail group (T4)

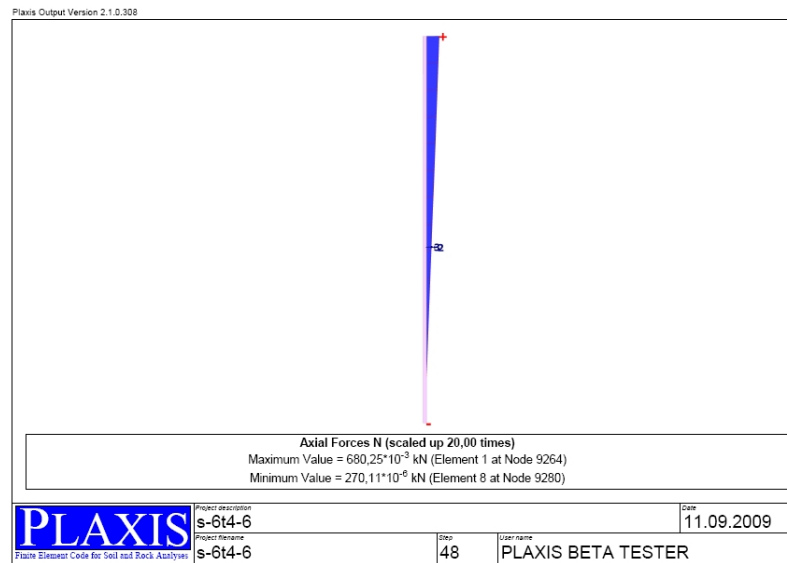


Figure C.6.f Output data of 6Ø spaced nail group (T4)

Mohr-Coulomb - Ankara Clay-t5

General Parameters Interfaces

Material Set

Identification: Ankara Clay-t5

Material model: Mohr-Coulomb

Material type: Drained

General properties

γ_{unsat} : 1,852E-08 kN/mm³

γ_{sat} : 1,852E-08 kN/mm³

Comments

Permeability

k_x : 1,000 m/day

k_y : 1,000 m/day

k_z : 1,000 m/day

Advanced...

Next OK Cancel

Figure C.7.a Input data of 6Ø spaced nail group (T5)

Mohr-Coulomb - Ankara Clay-t5

General Parameters Interfaces

Stiffness

E_{ref} : 0,021 kN/mm²

ν (nu) : 0,437

Strength

c_{ref} : 1,070E-04 kN/mm²

ϕ (phi) : 13,000 °

ψ (psi) : 0,000 °

Alternatives

G_{ref} : 7,307E-03 kN/mm²

E_{oed} : 0,065 kN/mm²

Advanced...

Next OK Cancel

Figure C.7.b Input data of 6Ø spaced nail group (T5)

Pile Properties

Material set

Nail-t5

Comments

Properties

E : 200,000 kN/mm²

γ : 7,810E-09 kN/mm³

Predefined Type

Massive Circular Pile

Diameter : 6,000 mm

User-defined Type

A : 28,274 mm²

I_3 : 63,617 mm⁴

I_2 : 63,617 mm⁴

I_{23} : 0,000 mm⁴

Skin Resistance

Linear

$T_{top, max}$: 1,690 kN/mm

$T_{bot, max}$: 1,690 kN/mm

Multi-linear Define...

Layer dependent

T_{max} : 2,293E-03 kN/mm

Base Resistance

F_{max} : 0,000 kN

OK Cancel

Figure C.7.c Input data of 6Ø spaced nail group (T5)

Figure C.7.d Input data of 6Ø spaced nail group (T5)

Plaxis - Finite Element Code for Soil and Rock Analyses

Project description	: s-6t5-6	Output Version 2.1.0.308
User name	: PLAXIS BETA TESTER	Step : 53
Project filename	: s-6t5-6	Date : 11.09.2009
Output	: Load Information - Point Load	Page : 1

ID	Node	Workplane	X [mm]	Y [mm]	Z [mm]	F _x [kN]	F _y [kN]	F _z [kN]
1	9264	0,000	0,000	0,000	0,000	0,000	1,000	0,000
2	9383	0,000	36,000	0,000	-18,000	0,000	1,000	0,000
3	9400	0,000	36,000	0,000	18,000	0,000	1,000	0,000
4	9417	0,000	0,000	0,000	-36,000	0,000	1,000	0,000
5	9434	0,000	0,000	0,000	40,000	0,000	1,000	0,000
6	9451	0,000	-36,000	0,000	-18,000	0,000	1,000	0,000
7	9468	0,000	-36,000	0,000	18,000	0,000	1,000	0,000

Figure C.7.e Input data of 6Ø spaced nail group (T5)

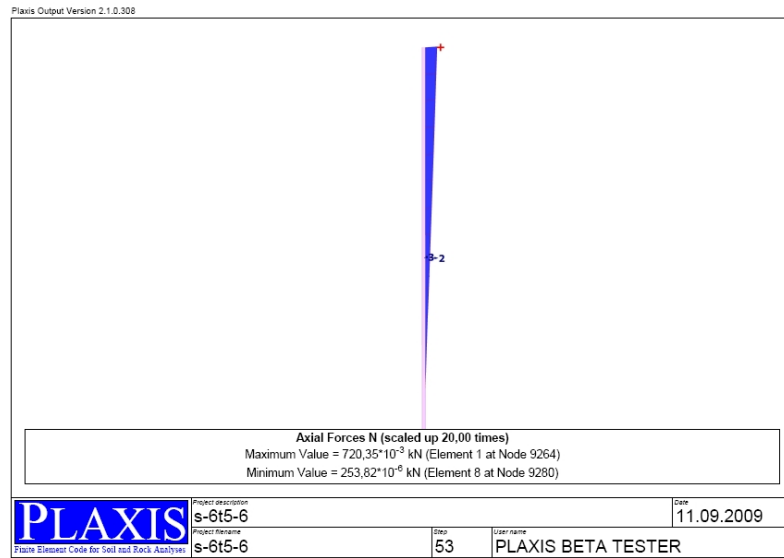


Figure C.7.f Input data of 6Ø spaced nail group (T5)

Mohr-Coulomb - Ankara Clay-t8

General Parameters Interfaces

Material Set

Identification:

Material model:

Material type:

General properties

γ_{unsat} : kN/mm³

γ_{sat} : kN/mm³

Comments

Permeability

k_x : m/day

k_y : m/day

k_z : m/day

Advanced...

Next OK Cancel

Figure C.8.a Input data of 6Ø spaced nail group (T8)

Mohr-Coulomb - Ankara Clay-t8

General Parameters Interfaces

Stiffness

E_{ref} : 0,035 kN/mm²

ν (nu) : 0,414

Strength

c_{ref} : 1,210E-04 kN/mm²

ϕ (phi) : 17,000 °

ψ (psi) : 0,000 °

Alternatives

G_{ref} : 0,012 kN/mm²

E_{oed} : 0,084 kN/mm²

Advanced...

Next OK Cancel

Figure C.8.b Input data of 6Ø spaced nail group (T8)

Pile Properties

Material set: Nail-t8

Comments:

Properties

E : 200,000 kN/mm²

γ : 7,810E-09 kN/mm³

Predefined Type

Massive Circular Pile

Diameter : 6,000 mm

User-defined Type

A : 28,274 mm²

I_3 : 63,617 mm⁴

I_2 : 63,617 mm⁴

I_{23} : 0,000 mm⁴

Skin Resistance

Linear

$T_{top, max}$: 1,690 kN/mm

$T_{bot, max}$: 1,690 kN/mm

Multi-linear Define...

Layer dependent

T_{max} : 2,647E-03 kN/mm

Base Resistance

F_{max} : 0,000 kN

OK Cancel

Figure C.8.c Input data of 6Ø spaced nail group (T8)

Plaxis - Finite Element Code for Soil and Rock Analyses

Project description : s-6t8-6	Output Version 2.1.0.308
User name : PLAXIS BETA TESTER	Step : 46
Project filename : s-6t8-6	Date : 11.09.2009
Output : Load Information - Point Load	Page : 1

ID	Node	Workplane	X [mm]	Y [mm]	Z [mm]	F _x [kN]	F _y [kN]	F _z [kN]
1	9264	0,000	0,000	0,000	0,000	0,000	1,000	0,000
2	9383	0,000	36,000	0,000	-18,000	0,000	1,000	0,000
3	9400	0,000	36,000	0,000	18,000	0,000	1,000	0,000
4	9417	0,000	0,000	0,000	-36,000	0,000	1,000	0,000
5	9434	0,000	0,000	0,000	40,000	0,000	1,000	0,000
6	9451	0,000	-36,000	0,000	-18,000	0,000	1,000	0,000
7	9468	0,000	-36,000	0,000	18,000	0,000	1,000	0,000

Figure C.8.d Input data of 6Ø spaced nail group (T8)

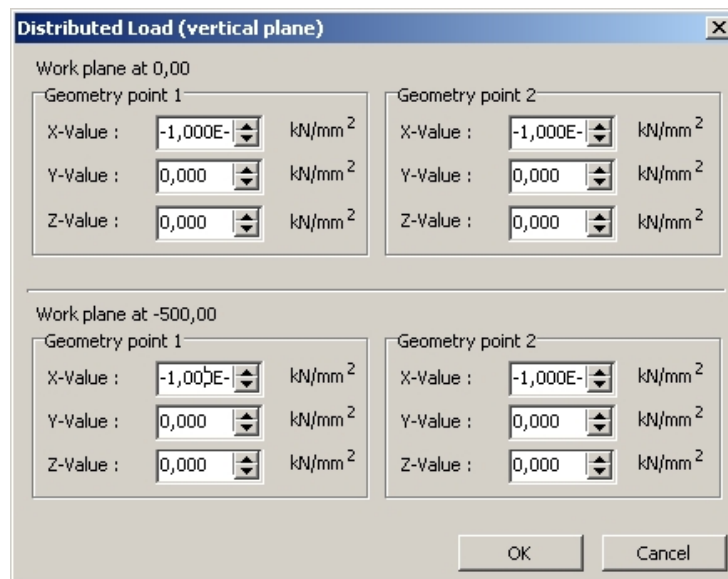


Figure C.8.e Input data of 6Ø spaced nail group (T8)

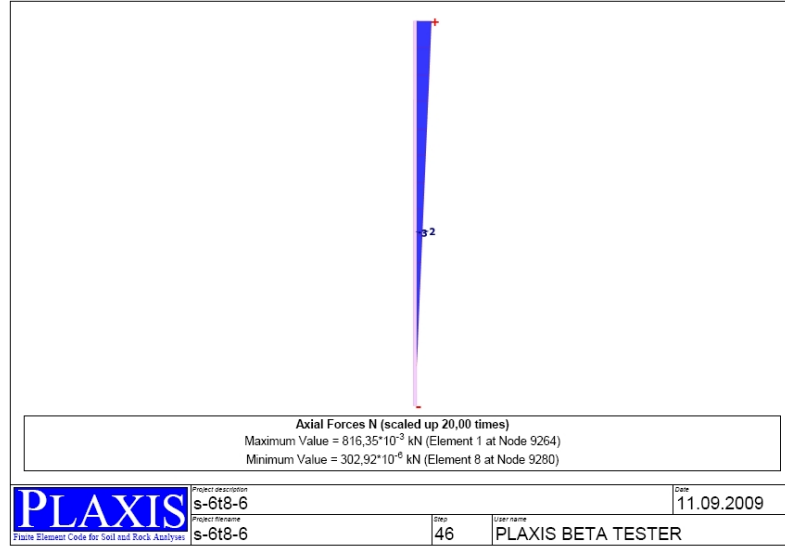


Figure C.8.f Output data of 6Ø spaced nail group (T8)

CURRICULUM VITAE

PERSONAL INFORMATION

Surname,Name: Akış, Ebru

Nationality: Turkish (TC)

Date and Place of Birth: 14.12.1973, İzmir

Marital Status: Married

Phone:+90 312 415 85 52

email:ebruakis@gmail.com

EDUCATION

Degree	Institution	Year of Graduation
MS	METU, Dept. of Civil Engineering	2002
BS	METU, Dept. of Civil Engineering	1995
High School	İzmir Türk College	1990

WORK EXPERIENCE

Year	Place	Enrollement
2008- Present	Technical Research Department of General Directorate of Highways, Ankara	Rock Mechanics Chief
2001-2008	Technical Research Department of General Directorate of Highways, Ankara	Tunnel Engineer
1998-2001	Agricultural Bank, Ankara	Civil Engineer
1996-1998	Temelsu Eng. Co., Ankara	Tunnel Engineer
1995-1996	Entes Co.,İstanbul	Civil Engineer

PUBLICATIONS

Akiş E., Etkesen Z., Solak T., Mucukgil R., Durukan E., Ünver M., “Redesign and Monitoring of a Portal Structure in Built-Up Area”, Proceedings of the Underground Space the 4th Dimension of Metropolises, Prague, 827-832 (2007).

Solak T., Akiş E., Russo M., “Detailed Seismic Analyses for Bolu Tunnel”, Proceedings of the 2nd Symposium on Underground Excavations for Transportation, İstanbul, 283-289, (2007).

Bakır, B.S., Akiş E., “Analysis of a Highway Embankment Failure Associated with the 1999 Düzce, Turkey Earthquake”, Soil Dynamics and Earthquake Engineering, 25, 251-260, (2005).

Atasaral M., Akçelik N., Solak T., Etkesen Z., Akiş E., “Rehabilitation Planning of Old Road Tunnels in Turkey”, Proceedings of the International Conference/Workshop and Exhibition on Tunelling and Underground Space Use, İstanbul, 219-228, (2002).

Akçelik N., Solak T., Akiş E., “Rehabilitation of Dorukhan Tunnel”, Proceedings of the International Conference/Workshop and Exhibition on Tunelling and Underground Space Use, İstanbul, 219-228, (2002).

HOBBIES

Swimming, Scuba, Gourmet.